TO: 5/91
Shannon
with compliments
Mike

KINESTATIC CONTROL: A NOVEL THEORY FOR SIMULTANEOUSLY REGULATING FORCE AND DISPLACEMENT

BY

MICHAEL WILLIAM GRIFFIS

A DISSERTATION PRESENTED TO THE GRADUATE SCHOOL
OF THE UNIVERSITY OF FLORIDA IN PARTIAL FULFILLMENT
OF THE REQUIREMENTS FOR THE DEGREE OF
DOCTOR OF PHILOSOPHY

UNIVERSITY OF FLORIDA

1991

ACKNOWLEDGEMENT

The author wishes to acknowledge the support of the National Science Foundation, Grant No. MSM – 8810017, for research on the subject of kinestatic control.

TABLE OF CONTENTS

Abstract of Dissertation Presented to the Graduate School
of the University of Florida in Partial Fulfillment of the
Requirements for the Degree of Doctor of Philosophy

KINESTATIC CONTROL: A NOVEL THEORY FOR SIMULTANEOUSLY REGULATING FORCE AND DISPLACEMENT

By

Michael William Griffis

May 1991

Chairman: Dr. Joseph Duffy
Major Department: Mechanical Engineering

A new theory for the simultaneous control of force and displacement for a partially constrained end-effector is established based upon the general spatial stiffness of the robotic manipulator. In general, the spatial stiffness of a compliant coupling that connects a pair of rigid bodies is used to map a small twist between the bodies into the corresponding interactive wrench. This mapping is based upon a firm geometrical foundation and establishes a positive-definite inner product (elliptic metric) that decomposes a general twist into a twist of freedom and a twist of compliance.

While controlling the general twist of the end-effector of an experimental robot apparatus (which included compliance in the end-effector and a force/torque sensor), the constraint wrenches and the twist freedoms of the partially constrained gripper were simultaneously controlled, and this was accomplished by using the inner product established for twists. This implementation as well as new analytical results indicate that the stiffness mapping and the induced inner product will be asymmetric.

CHAPTER 1
INTRODUCTION TO THE THEORY OF KINESTATIC CONTROL

A knowledge of the mapping of spatial stiffness is an essential ingredient in establishing the control of both the force and the displacement of a partially constrained rigid body. Spatial stiffness transforms a relative twist (a small rotation on a screw) between two rigid bodies into the change in a wrench that interacts between the bodies through a compliant coupling. In the proposed robotic application, a soft spatial spring is introduced to connect a gripper/workpiece with the end link of its manipulator. This inherently allows the end link to possess six degrees-of-freedom, no matter how the gripper/workpiece is constrained. "Kinestatic Control" exploits this knowledge of the spatial stiffness between the end link and the gripper/workpiece in a task-independent effort of simultaneously controlling the force and the displacement of the gripper/workpiece while solely controlling the displacement of the end link.

The spatial stiffness between two rigid bodies connected together by a compliant coupling, which is essentially a six-dimensional spring, is modeled by the spatial stiffness of a passive parallel mechanism. The simplest model for a "spatial spring" is a parallel mechanism that consists of six linear springs which act in-parallel connecting two platforms together. One platform is considered to be embedded in each of the rigid bodies. (See Figure 1.1.) The model thereby obtained is the most general in the sense that it can be used to quantify the spatial stiffness between any two rigid bodies, regardless of how complex is the coupling

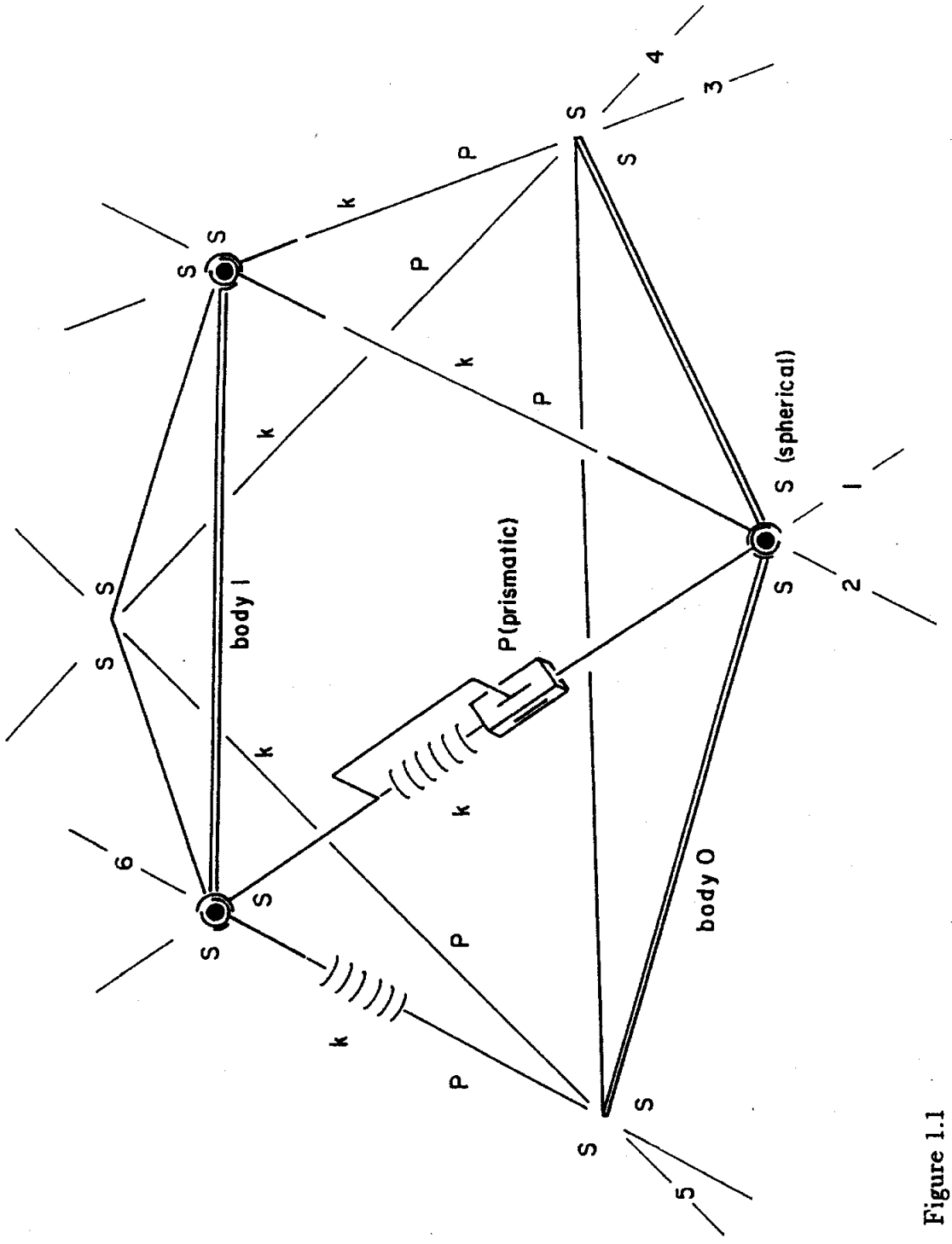
S
S
S
S
S
S
S
S
S
S
S
S
S
S
S
S
S
S
k
k
k
k
k
k
k
k
P
P
P
P
P
P
P
P
body I
body O
P(prismatic)
S (spherical)
1
2
3
4
5
6

Figure 1.1

between the two bodies. It supersedes a previous and widely accepted model that is dependent on the existence of a center-of-compliance. (See Salisbury [1980], Mason [1981], Raibert and Craig [1981], Whitney [1982], and Mason [1982].) This is illustrated by Figure 1.2 where three in-parallel TRPT serial chains cointersect at the center-of-compliance.

The proposed parallel mechanism model consists of six in-parallel SPS serial chains. (See Figure 1.1.) A more general parallel mechanism of this form would consist of six distinct connecting points on both platforms. This level of complexity is, however, not required to quantify a symmetric spatial stiffness between two rigid bodies, and the Stewart Platform of simple octahedral geometry can be used. The two platforms can thus be connected together by six legs that meet in a pair-wise fashion, sharing connections at three points on each platform. In practice, the six leg springs of the Stewart Platform can be calibrated so that, over a wide range of motion, the spatial stiffness of the resultant mechanism quantifies the spatial stiffness of the actual coupling (the spatial spring) between the two given rigid bodies.

The new theory of Kinestatic Control adopts this proposed stiffness modeling technique and applies it to the task-independent, simultaneous regulation of the force and the displacement of the gripper/workpiece of a robotic manipulator. The author considers that this new control theory supersedes such theories as "Stiffness Control" and "Hybrid Control," which essentially rely on erroneous task-dependent estimations of robot stiffness that require the existence of a center-of-compliance. These theories inherently depend on the specialized model of stiffness illustrated in Figure 1.2.

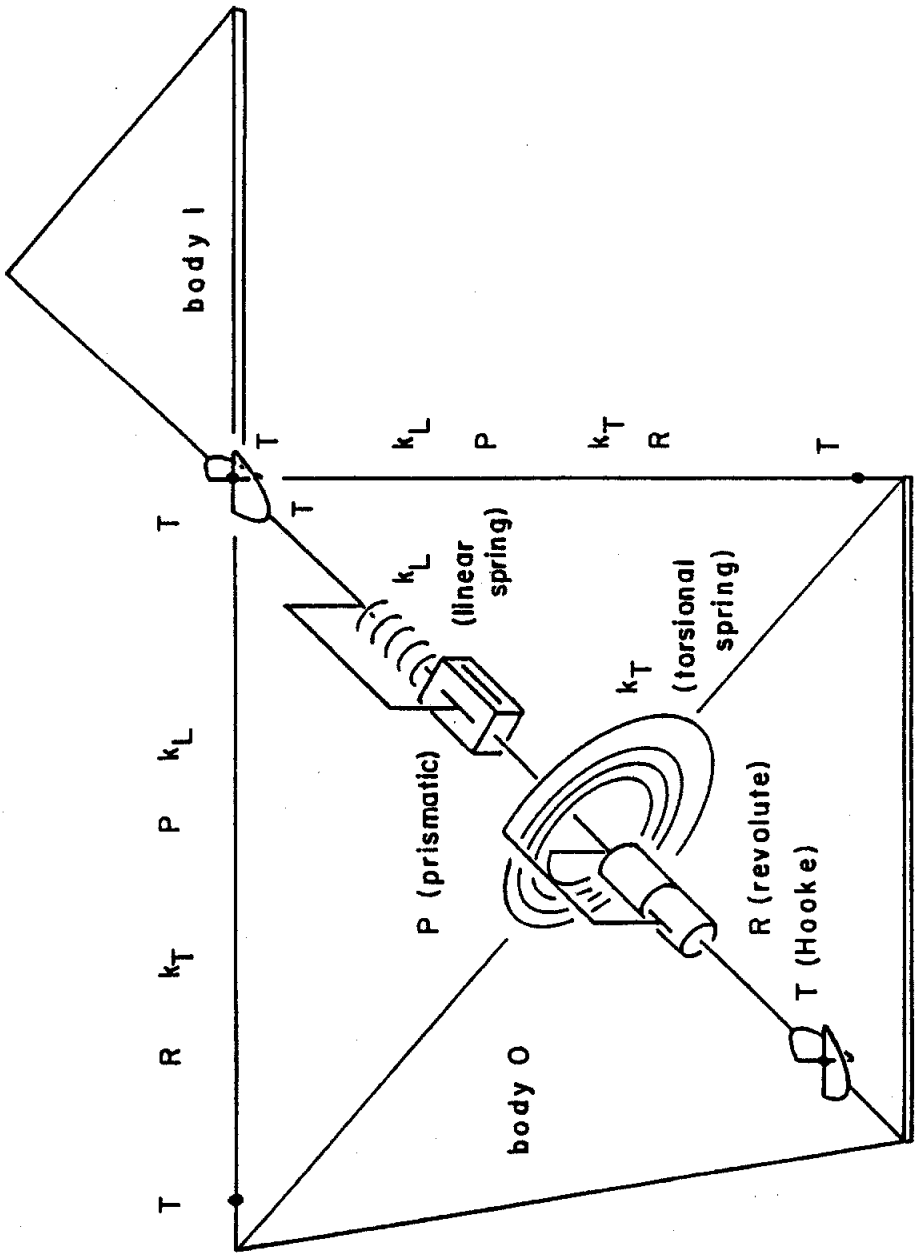
body I
T
T
k_L
P
k_T
R
T
T
k_L
(linear spring)
k_T
(torsional spring)
P (prismatic)
R (revolute)
T (Hooke)
T
R
k_T
P
k_L
T
body O

Figure 1.2

The author believes that an investigation of sparsity in the orthogonal complements associated with Hybrid Control reveals an uncertainty as to the modeled values of the three rotational and three translational spring constants of the mechanism shown in Figure 1.2. Hybrid Control theory thus restricts the center-of-compliance to be a task dependent point, and it does not in any way incorporate the stiffness of the manipulator into the hybrid controller. Special situations where a robot apparently has a center-of-compliance that is concident with a task dependent specification have been reported. (For example, see Raibert and Craig [1981] or An and Hollerbach [1989], where a point on the prismatic joint of a polar (RP) manipulator is aligned with a task, or see Whitney [1982], which discusses the positioning of the center-of-compliance of a Remote-Center-of-Compliance (RCC) device along the axis of a peg.)

Employing the theory of Stiffness Control allows a programmer to choose the location of a center-of-compliance and to adjust the three rotational and three translational spring constants according to a particular task. This mapping of stiffness is then reflected onto the individual joints of the robot. The technique thus essentially represents an adjustable set of gains, which must be synthesized for each given task as well as for each given robot.

Here, a novel theory of Kinestatic Control is proposed, which essentially accepts the stiffness of a robot for what it is and uses it to simultaneously control force and displacement. As a foundation for the new theory, this chapter investigates two representations of the mapping of stiffness, describes the general model of stiffness, and finally, discusses three robotic applications. Throughout this chapter, only positive-definite symmetric mappings of stiffness are considered. However, the remaining chapters employ more general stiffness mappings.

1.1 The General Mapping of Stiffness

Consider a rigid body 1 to be connected to a rigid body 0 by a general but initially unloaded compliant coupling that via its spatial stiffness restricts any relative spatial motion between the bodies. Then, the resulting mapping of stiffness is a one-to-one correspondence that associates a twist describing the relative displacement between the bodies with the corresponding resultant wrench which interacts between them. Figure 1.3 illustrates this compliant-coupling-dependent relationship by suggesting that for a given resultant wrench applied to body 1 of a "small" intensity δf on the screw $\$_1$, the corresponding twist of body 1 relative to body 0 is of a "small" angle $\delta\theta$ on the screw $\$_2$.[1] The term "small" is introduced to convey that the intensity δf of a wrench on the screw $\$_1$ is limited such that it produces a twist of intensity $\delta\theta$ on a screw $\$_2$ via a linear mapping of stiffness.

Consider a spatial spring system consisting of the two bodies and the initially unloaded compliant coupling. Any work input to the system is positive, and from Figure 1.3,

$$\delta f\, \delta\theta \left((h_1 + h_2) \cos \alpha_{12} - a_{12} \sin \alpha_{12} \right) > 0, \tag{1.1}$$

where h_1 and h_2 are the pitches of $\$_1$ and $\$_2$, and where a_{12} and α_{12} are the perpendicular distance and swept angle between the lines of the two screws. The expression in (1.1) is the summation of three products: the work done by the force on the translation $(\delta f\, h_2\, \delta\theta \cos \alpha_{12})$, by the force on the rotation $(-a_{12}\, \delta f\, \delta\theta \sin \alpha_{12})$, and by the couple on the rotation $(h_1\, \delta f\, \delta\theta \cos \alpha_{12})$.

[1] The wrench is illustrated in Figure 1.3 employing a Hunt "wrench applicator", which is a TPHT serial chain. A force δf generated in the P joint applies force δf to body 1 and simultaneously generates a couple $-h_1\, \delta f$ in the H joint, which in turn applies an equal and opposite couple $h_1\, \delta f$ to body 1. In other words, a wrench of intensity δf on screw $\$_1$ is applied to body 1.

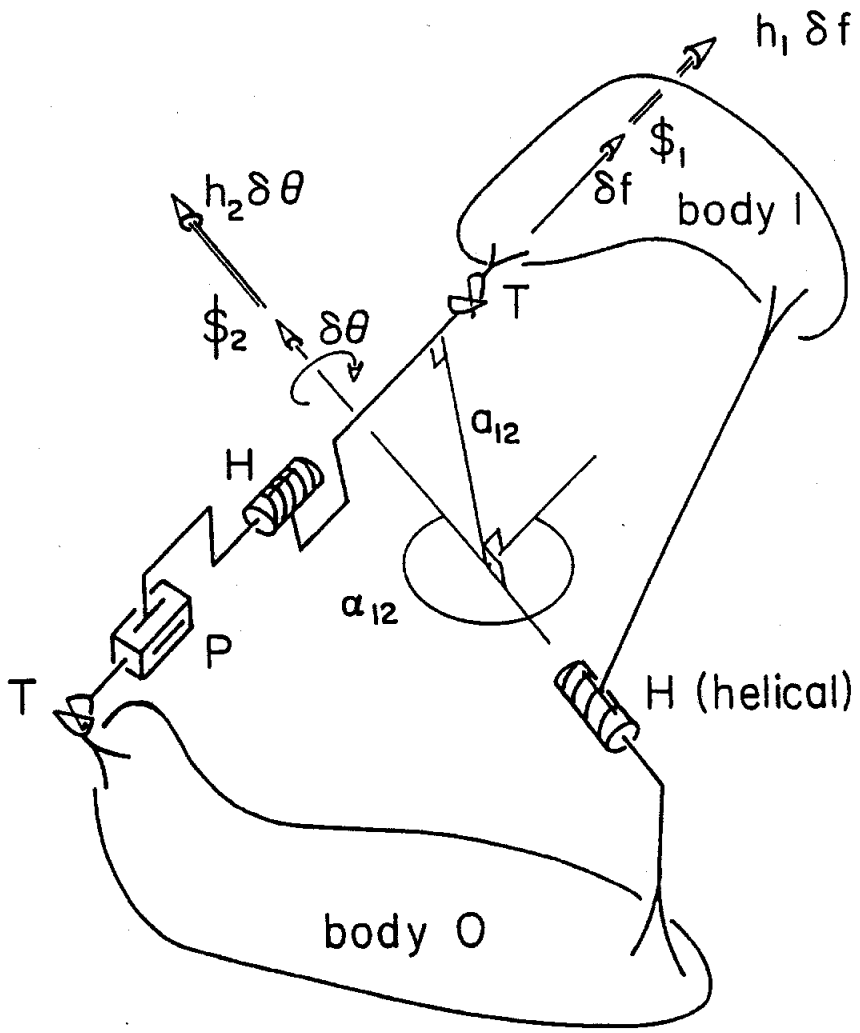
$h_1 \delta f$
$\$_1$
δf
body I
$h_2 \delta \theta$
$\$_2$
$\delta \theta$
T
a_{12}
H
α_{12}
P
T
H (helical)
body O

Figure 1.3

A pair of screws are said to be reciprocal when the expression $\left((h_1+h_2)\cos\alpha_{12}- a_{12}\sin\alpha_{12}\right)$ vanishes. Accordingly, since the work input into the spatial spring system must be positive non-zero, (1.1), then the twist of the coupling cannot be reciprocal to the wrench that produces it.

The transformation of screws illustrated in Figure 1.3 is represented here analytically in two geometrically different ways. Each of the two analytical representations requires the use of a 6x6 stiffness matrix to perform the mapping of stiffness. In comparison, these two stiffness matrices [K] and [k] differ in geometrical foundation: [K] is used to establish a potential energy-based inner product for twists, while [k] defines the "eigen-screws" and "eigenstiffnesses" for the transformation, which are, in other words, the invariant properties of the mapping.

A wrench on a screw will be represented as a general "ray" that is assigned an $\mathbb{R}^6$ vector $\hat{w}=[\vec{f}; \vec{m}_o]$, where $\vec{f}$ is a force vector in the direction of the wrench and $\vec{m}_o$ is a moment vector referenced to the origin. This ordering of screw coordinates is based on Plücker's definition of a ray, which is a line formed from the join of two points. (See Plücker [1865] and [1866].) However, a twist on a screw will be represented using two different formats, one based on the ray, $\hat{d}=[\vec{\theta}; \vec{x}_o]$, and the other based on a general "axis" that is assigned an $\mathbb{R}^6$ vector, $\hat{D}=[\vec{X}_o; \vec{\Theta}]$. Plücker defined the axis to be dual to the ray, and the axis is thus a line dually formed from the meet of two planes.

For a twist, $\vec{\theta}$ and $\vec{\Theta}$ both represent the direction of a finite but "small" rotation, and $\vec{x}_o$ and $\vec{X}_o$ both represent a "small" displacement of the origin. Therefore, the axis and ray representations of the same twist are related by

$$\begin{bmatrix} \vec{\theta} \\ \vec{x}_o \end{bmatrix} = \begin{bmatrix} 0_3 & 1_3 \\ 1_3 & 0_3 \end{bmatrix} \begin{bmatrix} \vec{X}_o \\ \vec{\Theta} \end{bmatrix},$$

which can be more conveniently written as

$$\hat{d} = [\Delta]\ \hat{D}, \tag{1.2}$$

where $[\Delta]$ is the symmetric 6x6 matrix of above. Since $[\Delta]^{-1}=[\Delta]$, a reversal in the ordering of this same transformation yields

$$\hat{D} = [\Delta]\ \hat{d}. \tag{1.3}$$

The transformation described by (1.2) and (1.3) is an example of a more general transformation, defined as a correlation, that maps an axis to a ray (or a ray to an axis). It is important to distinguish this transformation from a collineation, which maps a ray to a ray (or an axis to an axis).

1.2 A Positive-Definite Inner Product for Twists

The first analytical representation [K] of the mapping of stiffness is a general correlation of screws that assumes the form,

$$\hat{w} = [K]\ \hat{D}, \tag{1.4}$$

where axial coordinates $\hat{D}$ are assigned to the twist, where ray coordinates $\hat{w}$ are assigned to the wrench, and where [K] is a symmetric (non-singular) 6x6 matrix. For instance, in Figure 1.3, the screw $\$_2$ with axial coordinates $\hat{D}=[\vec{X}_o;\ \vec{\Theta}]$ is transformed into the screw $\$_1$ with ray coordinates $\hat{w}=[\vec{f};\ \vec{m}_o]$.

The potential energy stored in (or work input into) the spatial spring system can be expressed in terms of the axis coordinates of the twist and the ray coordinates of the wrench, and the same positive-definite expression first given in (1.1) can alternatively be written in the form

$$\vec{X}_o \cdot \vec{f} + \Theta \cdot \vec{m}_o = \hat{D}^T\ \hat{w}\ >\ 0. \tag{1.5}$$

Substituting $\hat{w}$ from (1.4) yields that a given non-singular matrix [K] is not only symmetric but also positive-definite:

$$\hat{D}^T\ \hat{w} = \hat{D}^T\ [K]\ \hat{D}\ >\ 0. \tag{1.6}$$

The expression in (1.6) introduces a quadratic form that can be used to establish a potential-energy-based, positive-definite inner product for the axial coordinates of twists. The symmetric bi-linear form for the axial coordinates $\hat{D}_1$ and $\hat{D}_2$ of a pair of twists is therefore,

$$\langle \hat{D}_1, \hat{D}_2 \rangle = \hat{D}_1^T [K] \hat{D}_2, \tag{1.7}$$

the dimension of which is work. Accordingly, this inner product satisfies three necessary conditions that establish the $\mathbb{R}^6$ used for the axial coordinates of twists as a non-degenerate inner product space:

- $\langle \hat{D}_1, \hat{D}_2 \rangle = \langle \hat{D}_2, \hat{D}_1 \rangle$ (symmetry)
- $\langle \hat{D}_1, \lambda \hat{D}_2 + \mu \hat{D}_3 \rangle = \lambda \langle \hat{D}_1, \hat{D}_2 \rangle + \mu \langle \hat{D}_1, \hat{D}_3 \rangle$ (linear multiples)
- $\langle \hat{D}_1, \hat{D}_1 \rangle \geq 0$, and $\langle \hat{D}_1, \hat{D}_1 \rangle = 0$ if and only if $\hat{D}_1 = \hat{0}$. (positive-definiteness)

Since the inner product given in (1.7) is positive-definite, it cannot establish an invariant Euclidean metric for screws.[2] (See Loncaric [1985], Brockett and Loncaric [1986], and Lipkin and Duffy [1985].) It would in fact induce an elliptic metric because it possesses a positive-definite quadratic form that operates on homogeneous coordinates, i. e. only imaginary $\hat{D}$ would satisfy $\hat{D}^T [K] \hat{D} = 0$. (Coordinates such as $\hat{D}=[0,0,0,0,0,0]^T$ are not considered.) (See Lipkin and Duffy [1985] and [1988].)

Because the mapping of stiffness (and its inner product) does not induce a Euclidean metric, it must undergo a change in representation whenever a change of

[2]For a Euclidean metric to be induced based upon an inner product represented by [K], then [K] must satisfy the relation $[K]=[E]^T[K]\,[E]$, where [E] describes a Euclidean transformation (collineation). (See Duffy [1990].) It will be shown however that the inner product described by [K] does not satisfy this relation. (See Equation (1.12).)

coordinate system is encountered. For a general Euclidean change of coordinate system, the ray coordinates $\hat{w}=[\vec{f};\ \vec{m}_O]$ of a wrench are transformed by the relation

$$\hat{w}=[e]\ \hat{w}', \tag{1.8}$$

where $\hat{w}'=[\vec{f}';\ \vec{m}'_O]$ are ray coordinates of the wrench in the "new" system, and where the 6x6 [e] takes the form,

$$[e]=\begin{bmatrix} R_3 & 0_3 \\ A_3\,R_3 & R_3 \end{bmatrix}.$$

Equation (1.8) represents a Euclidean collineation of screws, and it is specified by R_3 and A_3, which are, respectively, 3x3 rotation and 3x3 skew-symmetric-translation matrices. Under the same change of coordinate system, i.e. the same Euclidean collineation of screws, the axial coordinates $\hat{D}=[\vec{X}_O;\ \vec{\Theta}]$ of a twist are transformed by a similar relation,

$$\hat{D}=[E]\ \hat{D}', \tag{1.9}$$

where $\hat{D}'=[\vec{X}'_O;\ \vec{\Theta}']$ are axial coordinates of the twist expressed in the new coordinate system, and where [E] takes the form,

$$[E]=\begin{bmatrix} R_3 & A_3\,R_3 \\ 0_3 & R_3 \end{bmatrix}.$$

Substituting (1.8) and (1.9) into (1.4) and subsequently inverting [e] yields a new description of the same spatial spring system, viz. $\hat{w}'=[e]^{-1}[K][E]\hat{D}'$, and because $[E]^T=[e]^{-1}$, this can further be expressed in the form

$$\hat{w}' = [E]^T\,[K]\,[E]\,\hat{D}'. \tag{1.10}$$

Therefore, the representation of the mapping of stiffness in the new coordinate system is

$$\hat{w}' = [K'] \hat{D}', \tag{1.11}$$

where from (1.10),

$$[K']=[E]^T[K][E]. \tag{1.12}$$

Equation (1.12) illustrates three important properties of the representation, [K], of the mapping of stiffness that describes a given spatial spring system:

- It is symmetric, regardless of coordinate system.
- It is likewise positive-definite. Equation (1.12) is of the utmost importance because it illustrates that the eigenvalues (and eigenvectors) of a correlation have no invariant geometric meaning for Euclidean collineations, i. e. the equation does not relate similar matrices. Equation (1.12) does, however, relate congruent matrices that in general must have the same invariant signature (π, ν, ζ) which is defined as the number of positive (π), negative (ν), and zero (ζ) eigenvalues. For (1.12), the congruent matrices [K'] and [K] both have six positive eigenvalues (π=6) that are not equal (unless $[E]^T=[E]^{-1}$).
- In general, it is not necessary that [K] be diagonalizable for some [E]. This latter property is also of the utmost importance since it reveals that in general, one must not use a model of stiffness based upon a center-of-compliance. (See Figure 1.2.) In fact, it will be shown later that a proper model for general spatial stiffness is the Stewart Platform device illustrated in Figure 1.1.

It is also important to realize that the inner product $(\hat{D}_1, \hat{D}_2)$ is dependent upon the representation [K] of the mapping of stiffness. (See Equation (1.7).)

Consider now that the inner product is defined in the "new" coordinate system by

$$\langle \hat{D}'_1, \hat{D}'_2 \rangle = (\hat{D}'_1)^T [K'] \hat{D}'_2, \tag{1.13}$$

where $\hat{D}'_1$ and $\hat{D}'_2$ are the axial coordinates of the pair of twists expressed in the new coordinate system. The scalar quantity, work, resulting from the inner product is preserved by substituting (1.12) into (1.13), regrouping, and subsequently substituting (1.9), which yields

$$\begin{aligned} \langle \hat{D}'_1, \hat{D}'_2 \rangle &= (\hat{D}'_1)^T [E]^T [K] [E] \hat{D}'_2 \\ &= \langle [E] \hat{D}'_1, [E] \hat{D}'_2 \rangle \\ &= \langle \hat{D}_1, \hat{D}_2 \rangle. \end{aligned} \tag{1.14}$$

Here, $\hat{D}_1$ and $\hat{D}_2$ are the axial coordinates of the same two twists expressed in the old coordinate system.

In the experimental implementation of this theory (Section 2.3), the inner product established here for twists is used to decompose in a meaningful way a general twist of a partially constrained gripper/workpiece into an allowable twist (twist of freedom) that is consistent with the environment together with a corrective twist (twist of compliance) that nulls an error due to the difference between a command wrench and the actual wrench acting upon the gripper/workpiece.

1.3 The Eigen-Screws of Stiffness

The second analytical representation [k] of the mapping of stiffness is a general collineation of screws that assumes the form,

$$\hat{w} = [k] \hat{d}. \tag{1.15}$$

This form differs from the correlation given by (1.4) because ray coordinates $\hat{d}$ are

now assigned to the twist.[3] For the example in Figure 1.3, the screw $\$_2$ that is now assigned the ray coordinates $\hat{d}=[\vec{\theta};\ \vec{x}_o]$ is transformed into the screw $\$_1$ with ray coordinates $\hat{w}=[\vec{f};\ \vec{m}_o]$.

The characteristics of [k] can be determined by substituting (1.3) into (1.4), which yields

$$\hat{w} = [K][\Delta]\ \hat{d}, \tag{1.16}$$

and comparing with (1.15),

$$[k] = [K][\Delta]. \tag{1.17}$$

This effectively combines two successive correlations of screws, the first, ray to axis and the second, axis to ray. Therefore, the overall transformation is the collineation form of the mapping of stiffness, viz., ray to ray.

Consider now that another twist of an angle $\delta\theta$ on a screw $\$_i$ is chosen to be transformed under the mapping of stiffness, such that the wrench obtained acts upon the same screw $\$_i$ with an intensity δf. (See Figure 1.4.) This screw is accordingly defined as an "eigen-screw of stiffness" and the ratio of intensities of the wrench and the twist is defined as the corresponding "eigenstiffness", κ_i. All six such occurrences of these eigen-screws and their corresponding eigenstiffnesses can be determined from the eigenvectors and eigenvalues of [k].

It is important to recognize that the eigenvectors and eigenvalues of the matrix [k] are <u>always</u> real, and therefore, the eigenscrews and eigenstiffnesses of the mapping of stiffness are also <u>always</u> real. For a symmetric positive-definite $[K]^{-1}$ and a symmetric $[\Delta]$, the solution to the "generalized" eigenvalue problem $\kappa_i\ [K]^{-1}\ \hat{d} = [\Delta]\ \hat{d}$ yields that the product [k]=[K][Δ] possesses real eigenvalues and eigenvectors. (See Korn and Korn [1968].)

[3]Equation (1.15) was in fact the form that Dimentberg [1965] used to describe the mapping of stiffness for two rigid bodies that were connected via a general compliant coupling.

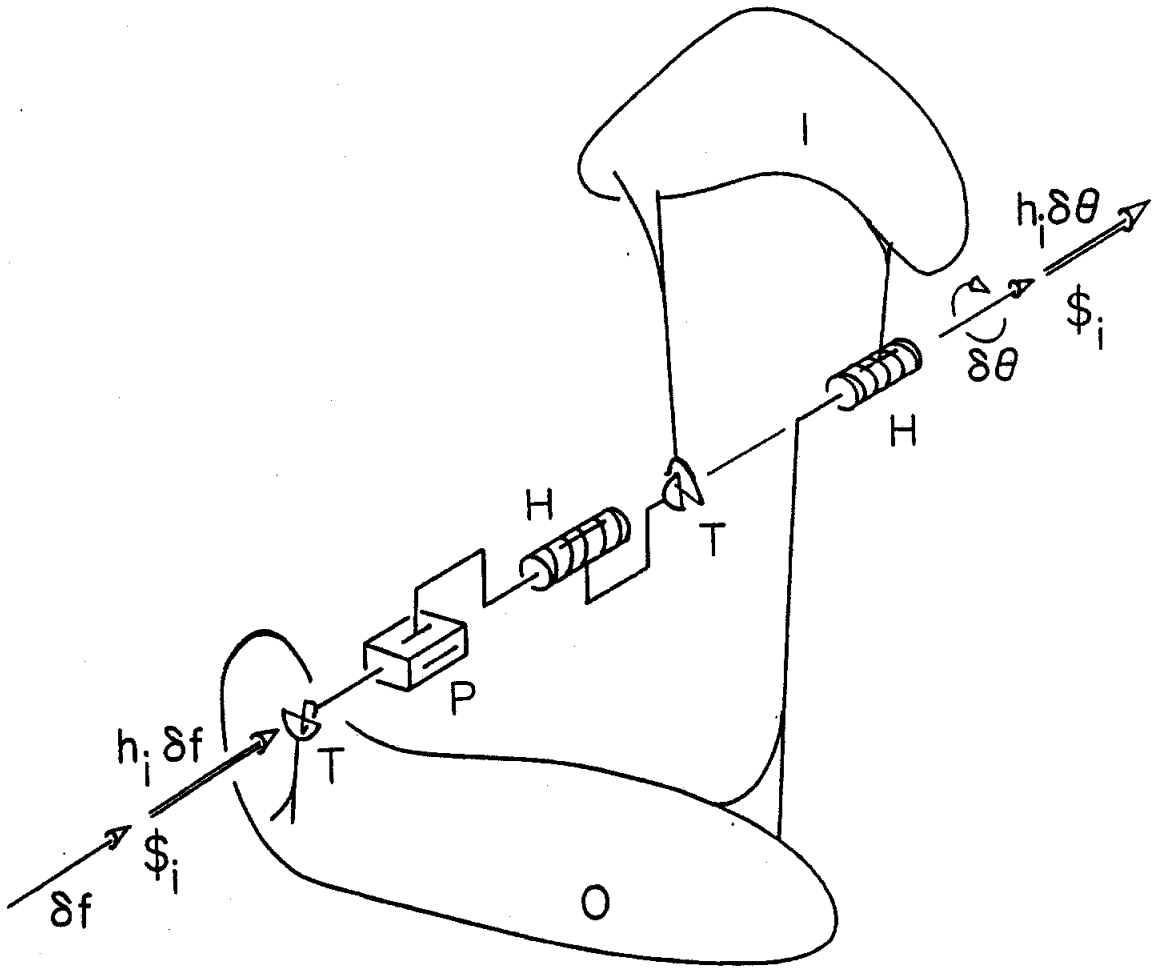

Figure 1.4

Consider that the six eigen-screws $\$_i$, $\$_{ii}$, $\$_{iii}$, $\$_{iv}$, $\$_v$, and $\$_{vi}$, are described by the six eigenvectors of [k], which are the ray coordinates $\hat{d}_i$, $\hat{d}_{ii}$, $\hat{d}_{iii}$, $\hat{d}_{iv}$, $\hat{d}_v$, and $\hat{d}_{vi}$, respectively. (The eigenvectors are not necessarily unitized ray coordinates.) Consider also that the corresponding eigenstiffnesses, κ_i, κ_{ii}, κ_{iii}, κ_{iv}, κ_v, and κ_{vi}, are obtained as the corresponding eigenvalues of [k]. Then, an eigen-screw, such as $\$_i$, transforms according to the relation

$$\kappa_i \, \hat{d}_i = [k] \, \hat{d}_i. \tag{1.18}$$

When comparing (1.15) with (1.18), it should be clear that the dimension of κ_i is force/rad and that κ_i is the ratio of the intensities of the wrench and the twist acting on $\$_i$.

From Figure 1.4, the positive work into the spatial spring system done by a wrench on a twist that is on an eigen-screw is expressed by

$$\delta f \, \delta\theta \left(2 \, h_i\right) > 0. \tag{19}$$

This result can also be deduced from the left side of (1.1), by substituting α_{12}=0 and h_1=h_2=h_i. Finally, substituting the relation δf=$\kappa_i \, \delta\theta$ yields

$$2 \, (\delta\theta)^2 \, \kappa_i \, h_i > 0, \tag{1.20}$$

which shows that the eigenstiffness and the pitch of the eigen-screw must have the same sign and must be non-zero. It should also be clear that the pitch of the eigen-screw is finite, since work cannot be done by a couple on a translation.

Invariance is always the key issue in geometry, and this section reflects this philosophy. With this in mind, consider now that a coordinate system has been changed, by for example (1.8). Then, in an analogy with the development of (1.10)—(1.12), the new representation of the collineation form of the mapping of stiffness can be obtained by substituting [e] $\hat{w}'$ for $\hat{w}$ and [e] $\hat{d}'$ for $\hat{d}$ in Equation (1.15) and subsequently inverting [e], and

$$\hat{w}' = [e]^{-1}\,[k]\,[e]\,\hat{d}', \tag{1.21}$$

which is equivalent to

$$\hat{w}' = [k']\,\hat{d}', \tag{1.22}$$

where the new representation of the collineation form of the mapping of stiffness is

$$[k'] = [e]^{-1}\,[k]\,[e]. \tag{1.23}$$

In contrast with Equation (1.12) which related congruent matrices, Equation (1.23) relates similar matrices. This reflects the fact that the eigenstiffnesses are invariant with a change of coordinate system. Although their representations certainly change, the eigen-screws in both (1.15) and (1.22) are the same, i.e. the eigenvectors of [k'] represent the same six screws as do the eigenvectors of [k], and these six pairs of eigenvectors are ray coordinates related by applications of (1.8).

1.4 The General Model of Spatial Stiffness

It has been established that the mapping of stiffness can be represented in a correlation form (1.4) that uses a symmetric positive-definite 6x6 matrix [K]. For this representation, axial coordinates $\hat{D}$ of a small twist of one body relative to another is transformed into the ray coordinates $\hat{w}$ of the corresponding small change in the wrench that interacts between the two bodies through a real compliant coupling.

This section provides the analytics that are necessary to model any real complicated compliant coupling, whether loaded or unloaded, by the general model of stiffness illustrated in Figure 1.1. The forward displacement analysis of this 3-3 Stewart Platform is known and reducible to an eighth degree polynomial (Griffis and Duffy [1989]).

Consider that referenced to some coordinate system, the unitized ray coordinates, $\hat{m}_i$, i=1, 6, of the six lines illustrated in Figure 1.1 are known and form the columns of a 6x6 matrix [j]. These lines are in fact the lines of action of the six scalar forces, f_i, i=1, 6, of the six linear springs that constrain the motion of the six prismatic joints of the Stewart Platform model.

Firstly, it is necessary to consider a static analysis of the top platform. The ray coordinates $\left(\sum_{i=1}^{6} f_i \hat{m}_i\right)$ of the resultant of forces that the top platform applies to the springs in the legs are equal to the ray coordinates $\hat{w}_o$ of the resultant of the remaining wrenches that are applied to the top platform by other bodies. This can be expressed in the form,

$$\hat{w}_o = [j]\, \underline{f}, \tag{1.24}$$

where $\underline{f}$ is an $\mathbb{R}^6$ vector of the scalar forces (f_i, i=1, 6) applied to the springs by the top platform. The force in a given leg, f_i, is related to the difference between the loaded and unloaded spring lengths, $(l_i - l_{oi})$, by $f_i = k_i(l_i - l_{oi})$, where k_i is the positive spring constant of the i^{th} leg. In the following analysis, it is assumed that eventhough the legs deflect, they do not deflect considerably from their unloaded position, i. e. the ratio l_{oi}/l_i does not deviate far from unity.[4]

In order to obtain a representation of spatial stiffness, [K], this static analysis of the loaded model is now related to small deflections in the legs. A small deviation from a current given operating state of (1.24) can be accommodated by considering small changes in $\hat{w}_o$ and $\underline{f}$ to be respectively $\hat{w}$ and $\delta\underline{f}$. Now, consider that the spring constants of the six legs form a diagonal matrix $[k_i]$ and that $\delta f_i = k_i\, \delta l_i$, where δl_i is a small change in the spring (or leg) length. Repeating for all legs and substituting into (1.24) yields

$$\hat{w} = [j]\, [k_i]\, \delta\underline{l}, \tag{1.25}$$

[4]Chapter 3 relies upon the dimensionless parameters $\rho_i = l_{oi}/l_i$ to illustrate that even the simplest compliant couplings become asymmetric as they deviate from their respective unloaded configurations.

where $\delta \underline{l}$ is an $\mathbb{R}^6$ vector of scalar leg deflections. The entries of the diagonal matrix $[k_i]$ are to be determined experimentally such that the Stewart Platform model represents accurately the spatial stiffness of the actual coupling between the two bodies.

Now, the work done by a given leg force is $f_i \ \delta l_i$, and this is equal to $(f_i \ \hat{m}_i)^T \ \hat{D}$, where $\hat{D}$ is the twist of the top platform relative to the base. Equating these two expressions for work, dividing both sides by f_i, and repeating for all legs yields the matrix expression

$$\delta \underline{l} = [j]^T \ \hat{D}, \tag{1.26}$$

which is the reverse kinematic solution.

Substituting (1.26) into (1.25) gives the correlation form representation of the mapping of stiffness for the resultant model,

$$\hat{w} = [j] \ [k_i] \ [j]^T \ \hat{D}. \tag{1.27}$$

Comparing (1.27) with (1.4) yields

$$[K] = [j] \ [k_i] \ [j]^T. \tag{1.28}$$

The matrix [K] contains twenty-one independent parameters (due to symmetry), whereas $[k_i]$ and [j] respectively contain six and eighteen independent parameters. Each column of [j] consists of the six ray coordinates of a line (four independent parameters) that joins a point in the base to a point in the top platform. Hence, the six columns of [j] contain separately a total of twenty-four independent parameters. However, the six lines meet pair-wise at six points, which imposes six conditions and reduces [j] to containing a total of eighteen independent parameters, and these together with the six parameters of $[k_i]$ result in a total of twenty-four parameters for $[k_i]$ and [j]. Therefore, given a general [K] of twenty-one independent parameters, it is necessary to specify three further conditions (i. e.

to solve for $[k_i]$ and [j]). These additional free choices can ideally result in a virtually unchanged [j] for a wide range of relative motion between the two rigid bodies. In other words, the model should be designed such that changes in actual spatial stiffness ([K]), resulting from finite changes in relative position and orientation between the two rigid bodies, are accommodated as far as possible by changes solely in $[k_i]$.

1.5 Parallel and Serial Arrangements

Consider two bodies to be connected in-parallel by a pair of Stewart Platform models, represented in the correlation forms $[K_1]$ and $[K_2]$. (See Figure 1.5a.) It is required to determine the equivalent mapping of stiffness for an equivalent model, represented by $[K_e]$. This can be accomplished by considering that

$$\hat{w}_e = \hat{w}_1 + \hat{w}_2, \tag{1.29}$$

where $\hat{w}_e$, $\hat{w}_1$, and $\hat{w}_2$ are ray coordinates of the resultant wrenches due to models $[K_e]$, $[K_1]$, and $[K_2]$, respectively. Substituting (1.4) for each of the models yields

$$[K_e]\ \hat{D}_e = [K_1]\ \hat{D}_e + [K_2]\ \hat{D}_e, \tag{1.30}$$

where $\hat{D}_e$ are the axial coordinates of the twist that is the same for each of the three models. This result yields

$$[K_e]\ = [K_1] + [K_2], \tag{1.31}$$

which is the spatial equivalent of two single degree-of-freedom springs connected in-parallel.

Consider now that two models are connected in series. (See Figure 1.5b.) Then, the base of the model $[K_2]$ is the top platform for the model $[K_1]$. It is required to determine the equivalent mapping of stiffness for an equivalent model,

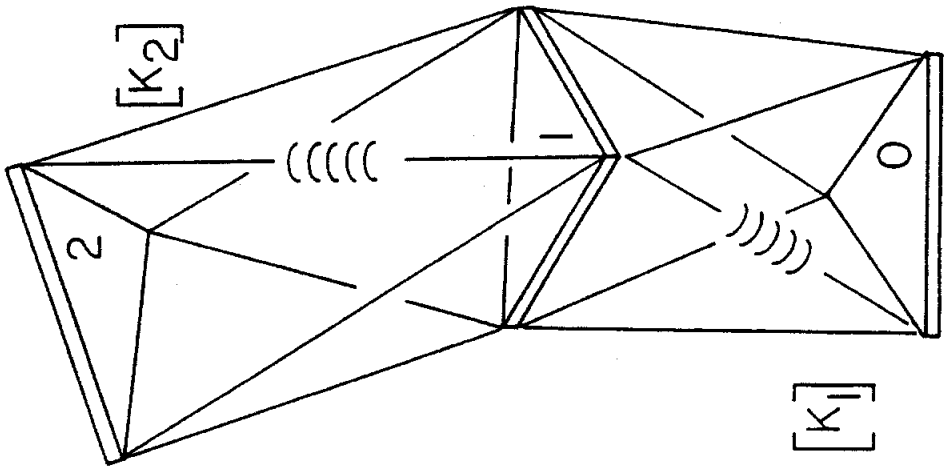

(b)

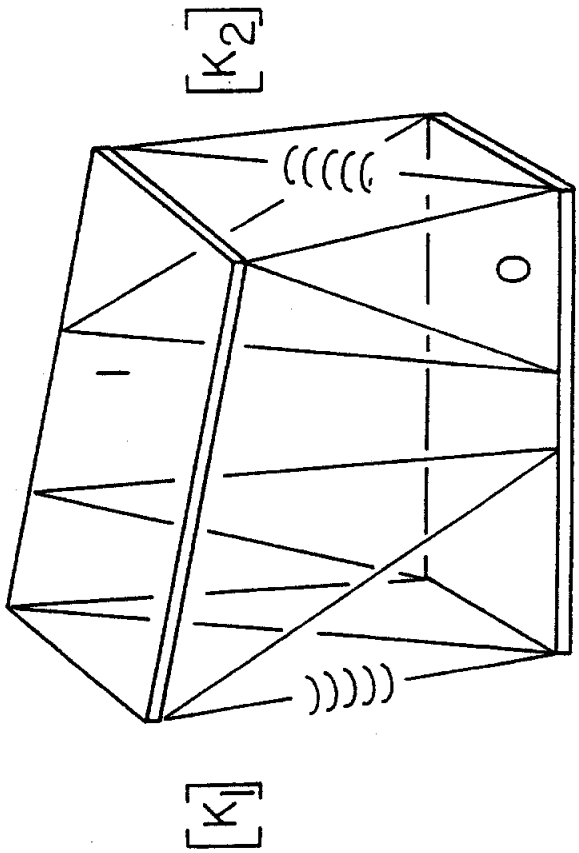

(a)

Figure 1.5

$[K_e]$, whose base is attached to the base of $[K_1]$ and whose top platform is attached to the top platform of $[K_2]$. This can be accomplished by analogously considering that

$$\hat{D}_e = \hat{D}_1 + \hat{D}_2, \tag{1.32}$$

where $\hat{D}_e$ are the axial coordinates of the effective twist relating the relative motion between bodies 2 and 0, and $\hat{D}_1$ and $\hat{D}_2$ are the axial coordinates of the two intermediate twists, which relate the relative motions of bodies 1 and 0 and bodies 2 and 1, respectively. Substituting the inverse of (1.4) for each of the models yields

$$[K_e]^{-1}\,\hat{w}_e = [K_1]^{-1}\,\hat{w}_e + [K_2]^{-1}\,\hat{w}_e, \tag{1.33}$$

where $\hat{w}_e$ are the ray coordinates of the resultant wrench that is the same for each of the three models. Therefore, the effective mapping of stiffness for two models that are connected in series is obtained from the sum of the two spatial compliances:

$$[K_e]^{-1} = [K_1]^{-1} + [K_2]^{-1}\,, \tag{1.34}$$

where the term "spatial compliance" is used to denote the inverse of spatial stiffness. Equation (1.34) is the spatial analogy of a pair of single degree-of-freedom springs connected in series.

1.6 Robotic Applications

This representation of stiffness provides a novel and attractive way of properly utilizing spatial displacements to control general systems of forces/torques acting in combinations upon a body. When the rigid body is the gripper/workpiece of a general, six degree-of-freedom robotic manipulator, then, based on the guidelines set forth in this work, a new algorithm emerges for the simultaneous control of an allowable twist and a constraint wrench.

The end-effector is considered to consist of two rigid bodies, one the gripper/workpiece and the other, the end link of the manipulator. In order to implement the new algorithm, the end link and the gripper/workpiece must be connected together by some compliant connection such as, for example, an (instrumented) Remote-Center-of-Compliance (iRCC) device.[5] (A force/torque sensor is also needed in the connection.) The spatial stiffness of the iRCC can be easily quantified by an octahedral Stewart Platform model. This model of the iRCC is more attractive than the center-of-compliance model, since it is not necessary to operate the iRCC within bounded regions which were designed to contain a center-of-compliance.

When unconstrained, the gripper/workpiece is considered to be connected to ground by two spatial springs connected in series. (Figure 1.5b also illustrates this when the gripper/workpiece is considered to be body 2, the end link considered to be body 1, and ground considered to be body 0.) One of the spatial springs is the manipulator itself, which connects the end link to ground, and its spatial stiffness can be modeled by a Stewart Platform and represented by $[K_1]$. The other spatial spring is the iRCC that connects the gripper/workpiece to the end link of the manipulator. The mapping of stiffness of the second spatial spring can be analogously represented by $[K_2]$. From (1.34), it is clear that the effective spatial stiffness relating the unconstrained gripper/workpiece to ground, $[K_e]$, is obtained from the sum of the inverses of $[K_1]$ and $[K_2]$. When the effects of the inverse of $[K_1]$ is minimal in comparison with the inverse of $[K_2]$, i. e. the iRCC is far more compliant than the manipulator, then the compliance of the manipulator can be neglected. In other words, $[K_e] \approx [K_2]$ when the manipulator is much stiffer than the end-effector's wrist (iRCC).

[5]The Charles Stark Draper Laboratory, Cambridge, MA.

Consider now that the gripper/workpiece is fully constrained with respect to ground and that the iRCC is initially unloaded. Although the gripper/workpiece is fully constrained, the end link still possesses six degrees-of-freedom due to the compliance in the iRCC. Since there can be no twist of the gripper/workpiece relative to ground, then the twists of the gripper/workpiece relative to the end link and of the end link relative to ground must be on the same general screw \$, but their rotations, $\delta\theta_2$ and $\delta\theta_1$, must be in opposing directions. (See Figure 1.6.) This means that $\hat{D}_1 = -\hat{D}_2$, where $\hat{D}_1$ and $\hat{D}_2$ are the axial coordinates of the twists of the end link relative to ground and of the gripper/workpiece relative to the end link. Therefore, based upon a twist of the end link relative to ground, the iRCC is subsequently loaded with a wrench whose ray coordinates are $\hat{w} = [K_2]\ \hat{D}_2$. Substituting $\hat{D}_2 = -\hat{D}_1$ and neglecting a gravity wrench yields the small wrench that is applied to the gripper/workpiece by ground due to the twist of the end link,

$$\hat{w} = -\ [K_2]\ \hat{D}_1. \tag{1.35}$$

Consider further that there is a general wrench with ray coordinates $\hat{w}_r$ reacting between the gripper/workpiece and ground which is to be controlled. In order to begin to null an error between the desired wrench and a known (sensed) actual wrench with ray coordinates $\hat{w}_s$, a small corrective twist of the end link relative to ground is needed. The axial coordinates, $\hat{D}_c = \hat{D}_1$, of the proper corrective twist can be obtained by inverting (1.35), and expressing it in the form,

$$\hat{D}_c = -\ G\ [K_2]^{-1}\ \hat{w}_e, \tag{1.36}$$

where G is a single dimensionless scalar gain that is used to limit $\delta\theta_c = \delta\theta_1$ of the corrective twist command, and where $\hat{w}_e = \hat{w}_r - \hat{w}_s$. This corrective twist is to be supplied by commanding the six joint motors of the manipulator. Therefore, the control of the twist of the end link relative to ground regulates the reaction wrench between the gripper/workpiece and ground.

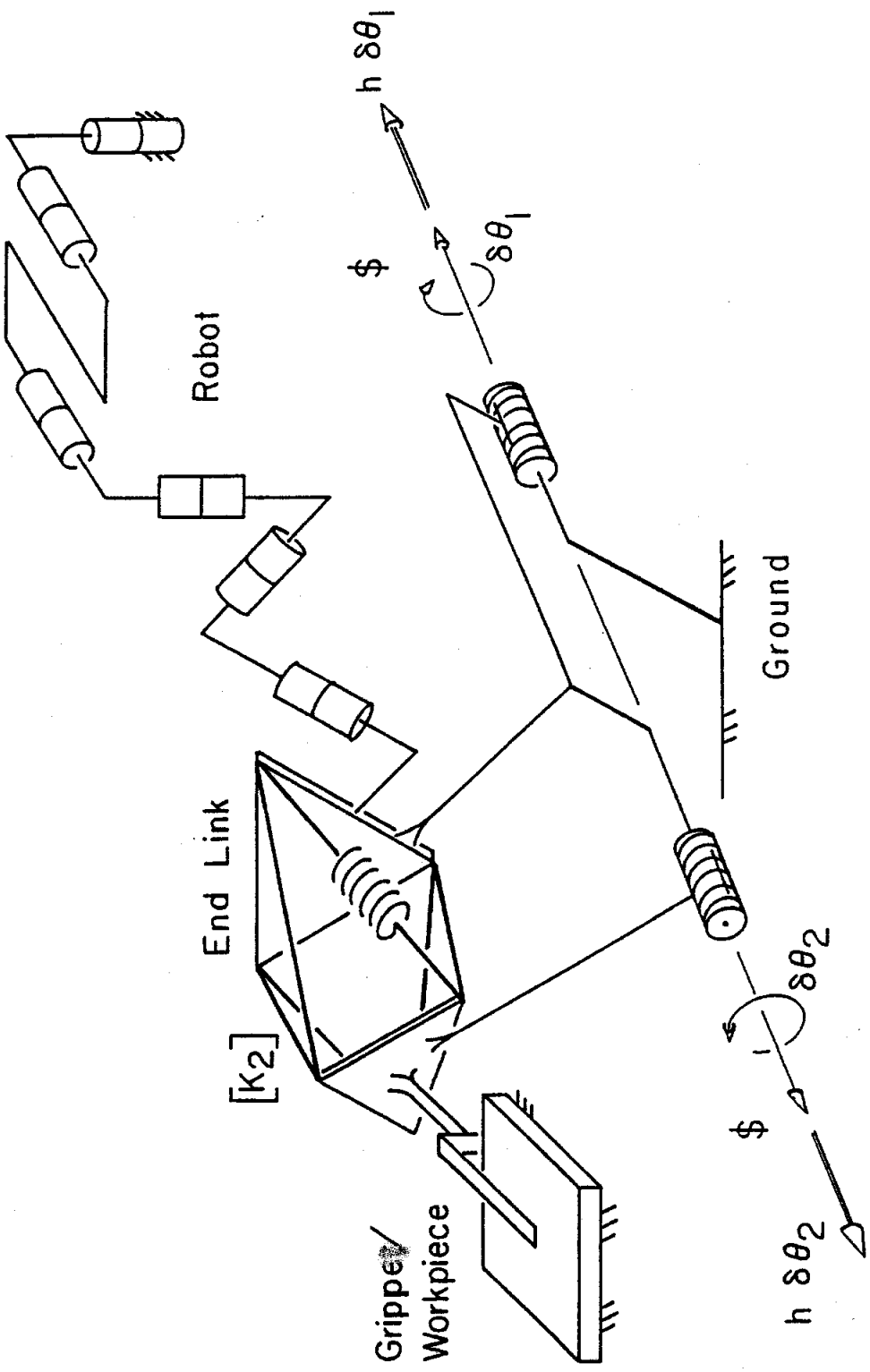
h δθ1
$
δθ1
Robot
End Link
[K2]
Ground
δθ2
$
Gripper/
Workpiece
h δθ2

Figure 1.6

Finally, consider the situation where the gripper/workpiece is only partially constrained with respect to ground via a stiff connection. Figure 1.7 illustrates an example of line contact between the gripper/workpiece and ground. Here, the possible screw of a reaction wrench must be an element of a 2-system of screws, viz. the possible reaction wrench must be a force on a line parallel to and in the same plane as the lines $\$_1$ and $\$_2$.[6] This system of wrenches is accordingly defined as the "wrenches of constraint" that constrain the motion of the gripper/workpiece relative to ground, and the ray coordinates $\hat{w}_r$ of such a wrench are obtained via the linear combination

$$\hat{w}_r = \lambda_1 \hat{w}_1 + \lambda_2 \hat{w}_2, \tag{1.37}$$

where $\hat{w}_1$ and $\hat{w}_2$ are ray coordinates of $\$_1$ and $\$_2$.

The gripper/workpiece has four degrees-of-freedom, and it can be considered to be initially motionless relative to ground. An error wrench due to the difference between the desired wrench and the actual wrench is nulled by a small corrective twist of the end link relative to ground, the axial coordinates of which, $\hat{D}_c$, can be obtained from (1.36). This is because this corrective twist cannot move the gripper/workpiece, since the corresponding wrench that is induced to null the error in the iRCC is fully supported as a wrench of constraint between the gripper/workpiece and ground.

Because the desired and actual wrenches of constraint can be written as linear combinations (1.37), it is clear that the error wrench can also be written as a linear combination,

$$\hat{w}_e = \mu_1 \hat{w}_1 + \mu_2 \hat{w}_2, \tag{1.38}$$

where $\hat{w}_e = \hat{w}_r - \hat{w}_s$ are ray coordinates of the error wrench. It can be concluded from (1.36) and (1.38) that the corrective twist must also be an element of a 2-

[6]The fact that the points of contact can only take compression is neglected.

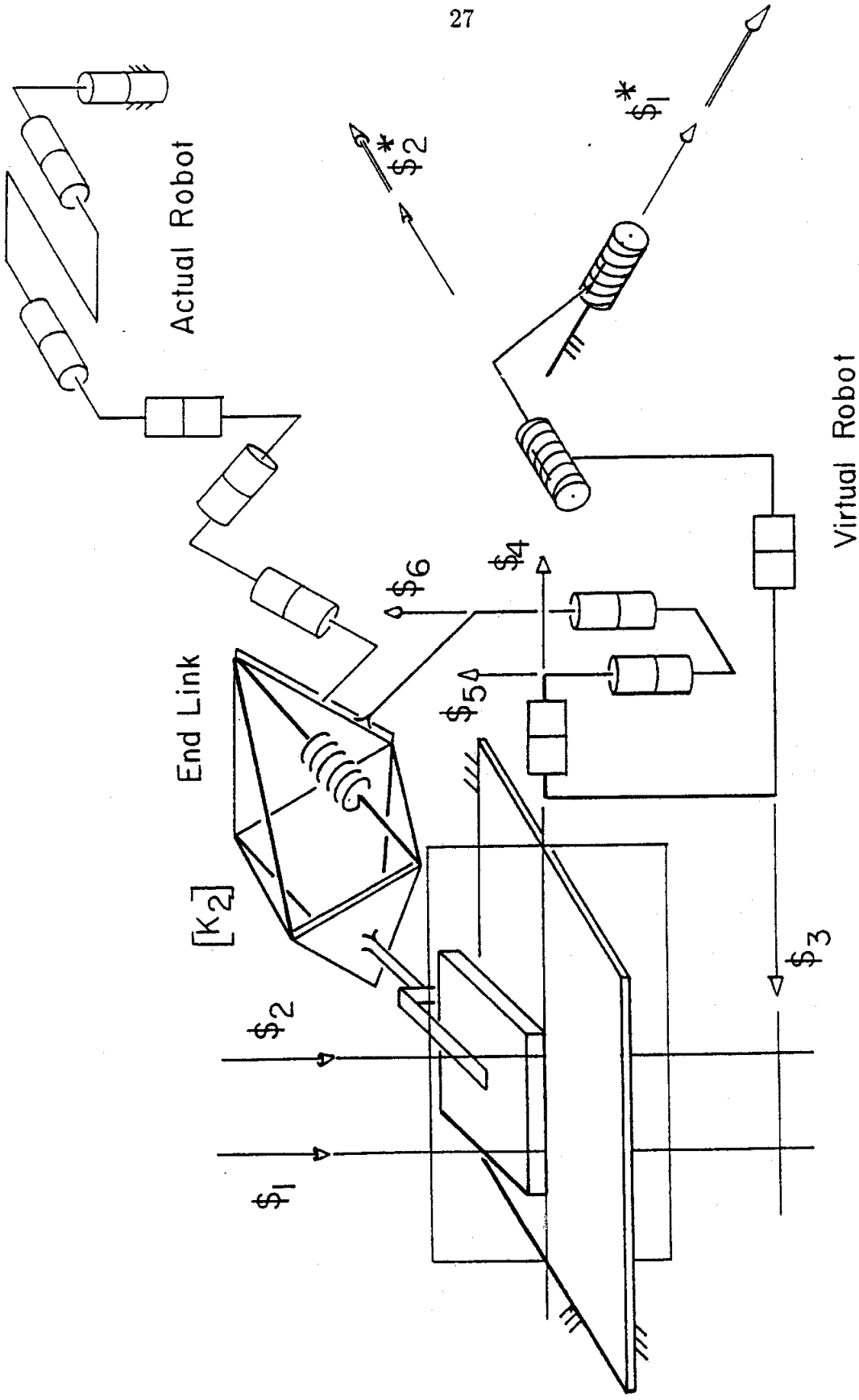

Figure 1.7

system, and this system is defined as the "twists of compliance". Then, the axial coordinates $\hat{D}_c$ of the corrective twist are obtained from the linear combination

$$\hat{D}_c = \alpha_1 \hat{D}_1^* + \alpha_2 \hat{D}_2^*, \tag{1.39}$$

where $\hat{D}_1^*$ and $\hat{D}_2^*$ are axial coordinates of $\$_1^*$ and $\$_2^*$, which are the screws that correspond under the mapping of stiffness with the lines of force $\$_1$ and $\$_2$. (See Figure 1.7.) The axial coordinates of the the two twists of compliance can therefore be obtained by the relations,

$$\hat{D}_1^* = [K_2]^{-1} \hat{w}_1 \text{ and } \hat{D}_2^* = [K_2]^{-1} \hat{w}_2. \tag{1.40}$$

From (1.1), it follows that the two screws $\$_1^*$ and $\$_2^*$ are <u>not</u> reciprocal to the screws $\$_1$ and $\$_2$, which span the wrenches of constraint, and from (1.6),

$$(\hat{D}_1^*)^T \hat{w}_1 \neq 0 \text{ and } (\hat{D}_2^*)^T \hat{w}_2 \neq 0. \tag{1.41}$$

Thus, it is clear that the screws spanning the twists of compliance are <u>not</u> elements of the 4-system of screws which is reciprocal to the wrenches of constraint. Four screws that are each reciprocal to the two lines which span the wrenches of constraint do in fact quantify the twists of freedom of the gripper/workpiece relative to ground. These twists of freedom constitute all allowable twists that are consistent with the environment, and Figure 1.7 illustrates four such screws of zero pitch, namely the lines of rotation $\$_3$, $\$_4$, $\$_5$, and $\$_6$. Assigning the axial coordinates $\hat{D}_i$, i=3, 6, to these four twists and introducing them into the axial-ray coordinate form of reciprocity yields

$$\hat{D}_i^T \hat{w}_1 = 0 \text{ and } \hat{D}_i^T \hat{w}_2 = 0, \tag{1.42}$$

for i=3, 6.

The twists of freedom are thus linearly independent from the twists of compliance. In fact, the two systems are orthogonal complements with respect to $[K_2]$. This can be shown by firstly considering that the axial coordinates $\hat{D}_b$ of a

given twist of freedom of the gripper/workpiece relative to ground can be expressed by the linear combination,

$$\hat{D}_b = \gamma_1 \hat{D}_3 + \gamma_2 \hat{D}_4 + \gamma_3 \hat{D}_5 + \gamma_4 \hat{D}_6. \tag{1.43}$$

From (1.37), (1.42), and (1.43), it can be deduced that any twist of freedom is reciprocal to any wrench of constraint and that it can be expressed by

$$\hat{D}_b^T \hat{w} = 0, \tag{1.44}$$

where $\hat{w}=(\hat{w}_r=\hat{w}_e)$ are the ray coordinates of any wrench of constraint. Now, for each wrench of constraint, there is a unique twist of compliance, i. e. $\hat{w}=[K_2]\ \hat{D}_c$, and therefore substituting into (1.44) yields

$$\hat{D}_b^T [K_2]\ \hat{D}_c = 0. \tag{1.45}$$

This expresses the condition of orthogonality between twists of freedom and twists of compliance with respect to the potential-energy-based inner product, and from (1.7),

$$\langle \hat{D}_b, \hat{D}_c \rangle = \hat{D}_b^T [K_2]\ \hat{D}_c = 0. \tag{1.46}$$

Therefore, in a direct sum of orthogonal complements $[B] \oplus [C]=\mathbb{R}^6$, where the matrix labels are used to denote the vector subspaces. The consequence of this direct sum is that a general $\hat{D} \in \mathbb{R}^6$ can be written is a unique combination of a $\hat{D}_b \in [B]$ and a $\hat{D}_c \in [C]$, so that $\hat{D}=\hat{D}_b+\hat{D}_c$.

It is important to realize that the twists of freedom and the wrenches of constraint are determined solely by the nature of the contact between the gripper/workpiece and ground. The twists of compliance are, however, dependent on the mapping of stiffness of the robot, shown here to be represented by $[K_2]$, together with the wrenches of constraint. It is important to further recognize that the screws $\$_1^*$ and $\$_2^*$ are not dependent on the choice of origin, and that these same two screws will always be obtained given a properly represented mapping of

stiffness. The sole requirement of this mapping of stiffness is that it be positive-definite. A center-of-compliance is not necessary, and a compliant coupling (such as the iRCC) need not be positioned and oriented in some special way to perform a given partially constrained task.

Figure 1.7 essentially illustrates a virtual robot manipulator consisting of six serially connected screws, $\$_1^*$, $\$_2^*$, $\$_3$, $\$_4$, $\$_5$, and $\$_6$. This virtual robot operates in-parallel with the actual robot that controls the 6 d.o.f. displacement of the end link. In order to better visualize the decomposition, it is useful to consider that when the six virtual joints displace, the axial coordinates of the resultant twists producing ($\$_1^*$, $\$_2^*$) and ($\$_3$, $\$_4$, $\$_5$, $\$_6$) are respectively, $\hat{D}_c$ and $\hat{D}_b$. Finally, it can be concluded by superposition that these two twists, which together produce a general twist of the end link, provide a means to control the reaction wrench between the gripper/workpiece and ground, while simultaneously controlling the displacement of the gripper/workpiece relative to ground. This novel control strategy is defined as "Kinestatic Control."

CHAPTER 2
IMPLEMENTING KINESTATIC CONTROL: USING DISPLACEMENTS TO NULL FORCES

2.1 Introduction

Which way does a robot move itself in order to null the external contact forces that act on its gripper? In general, the contact forces that interact between the gripper and its environment are not nulled or even altered when the robot moves the partially constrained gripper in the unrestricted direction of a remaining freedom. Consequently, the efforts here are to document the investigations and implementations of other robot motions that though restricted do correctly null (or change) these contact forces.

While addressing this question, this work establishes the property of robot stiffness to be the key and central issue. Robot stiffness is after all a property that is independent of the task required of the gripper. Succinctly, the robot is considered here to be a spatially deflecting spring that connects two rigid bodies together, viz. the gripper to ground.

In the previous chapter, the author analyzed the geometrical properties of spatial stiffness and presented two analytical representations, one that defined a positive-definite, potential-energy-based inner product and another that established the properties of spatial stiffness which are invariant for Euclidean motions. (See Chapter 1.) This work further used the positive-definite inner product to facilitate a decomposition of the vector space of all twists[1]. A robotic example was given

[1] "Twist" is used here as a generic word to denote the infinitesimal displacement/rotation of one rigid body relative to another, while "wrench" is a similar generic word for the forces/torques that interact between two rigid bodies.

where a gripper (with workpiece) was in straight line contact with its environment, resulting uniquely in two degrees-of-constraint (characterized by the wrenches of constraint) and four degrees-of-freedom (characterized by the twists of freedom). Using the positive-definite inner product, an orthogonal complementary twist space was reasoned to exist. This complementary twist space was defined as the "twists of compliance," and each twist contained therein possessed a working relationship with its own unique wrench of constraint. *Accordingly, the twists of compliance are the restricted (non-allowable) twists that are reserved for nulling and/or correcting the contact forces which interact between the gripper and its environment.*

2.1.1 The Non-Euclidean Geometry of Stiffness

While analyzing the geometrical properties of the inner product defined by spatial stiffness, it was concluded that it must be non-Euclidean, because it is positive-definite and operates on twist coordinates.[2] (See Section 1.2.) The use of a positive-definite (non-Euclidean) inner product is clearly a necessity in the general case for determining a twist space that is an orthogonal complement to the twists of freedom (or a wrench space that is an orthogonal complement to the wrenches of constraint).

---

[2]Suppose [K] to be a positive-definite 6x6 symmetric stiffness matrix. Then, the only twists that satisfy the quadratic form $\hat{D}^T[K]\,\hat{D}=0$ are imaginary, where six not-all-zero homogeneous twist coordinates are given by $\hat{D}=[\delta\vec{x}^T;\ \delta\vec{\phi}^T]^T$. In other words, for a non-degenerate coupling, there is no real twist about which no work is done. (An inner product that operates on homogeneous coordinates is considered to be non-Euclidean, specifically elliptic (Lipkin and Duffy [1985]) or virtual (Sommerville [1929]), when only imaginary elements satisfy the vanishing of its quadratic form. As far as a Euclidean inner product is concerned, mathematicians have demonstrated that one which operates on homogeneous coordinates is either positive semi-definite or indefinite. See (Semple and Kneebone [1979] and Porteous [1981].)

The degree of freedom afforded to a gripper (its twists of freedom) is a purely geometrical notion, as well as its degree of constraint (its wrenches of constraint). In other words, the freedoms and constraints of the gripper are determinable through pure Euclidean geometry. Therefore, it cannot be meaningful to establish a non-Euclidean (positive-definite) inner product based solely upon the nature of the freedoms and constraints acting between the gripper and its environment. In certain instances, using a "selection matrix" introduces a fallacy, as does defining a point where a "compliant frame" is to be located and subsequently used to perform decomposition. (See Duffy [1990].) *The result of such an operation yields an orthogonal complementary twist space that is not necessarily the best twist space for nulling errors in the contact forces which interact between the gripper and its environment.* In other words, it will not yield the correct twists of compliance.

2.1.2 An Example

To further investigate this important statement, consider the planar two-dimensional example illustrated in Figure 2.1. A wheel is connected to a platform via two translational springs, which are capable of compression as well as tension. The platform is then subsequently connected to ground via two actuated prismatic (slider) joints that are tuned for fine-position control. The wheel is to maintain contact with a rigid environment. The center point of the wheel thus has a single freedom, which is a displacement p_t in the direction of $\vec{u}_t$. Based on the constraint imposed upon the wheel, a normal contact force, f_n acting through the center point along $\vec{u}_n$, may interact between the wheel and the environment.

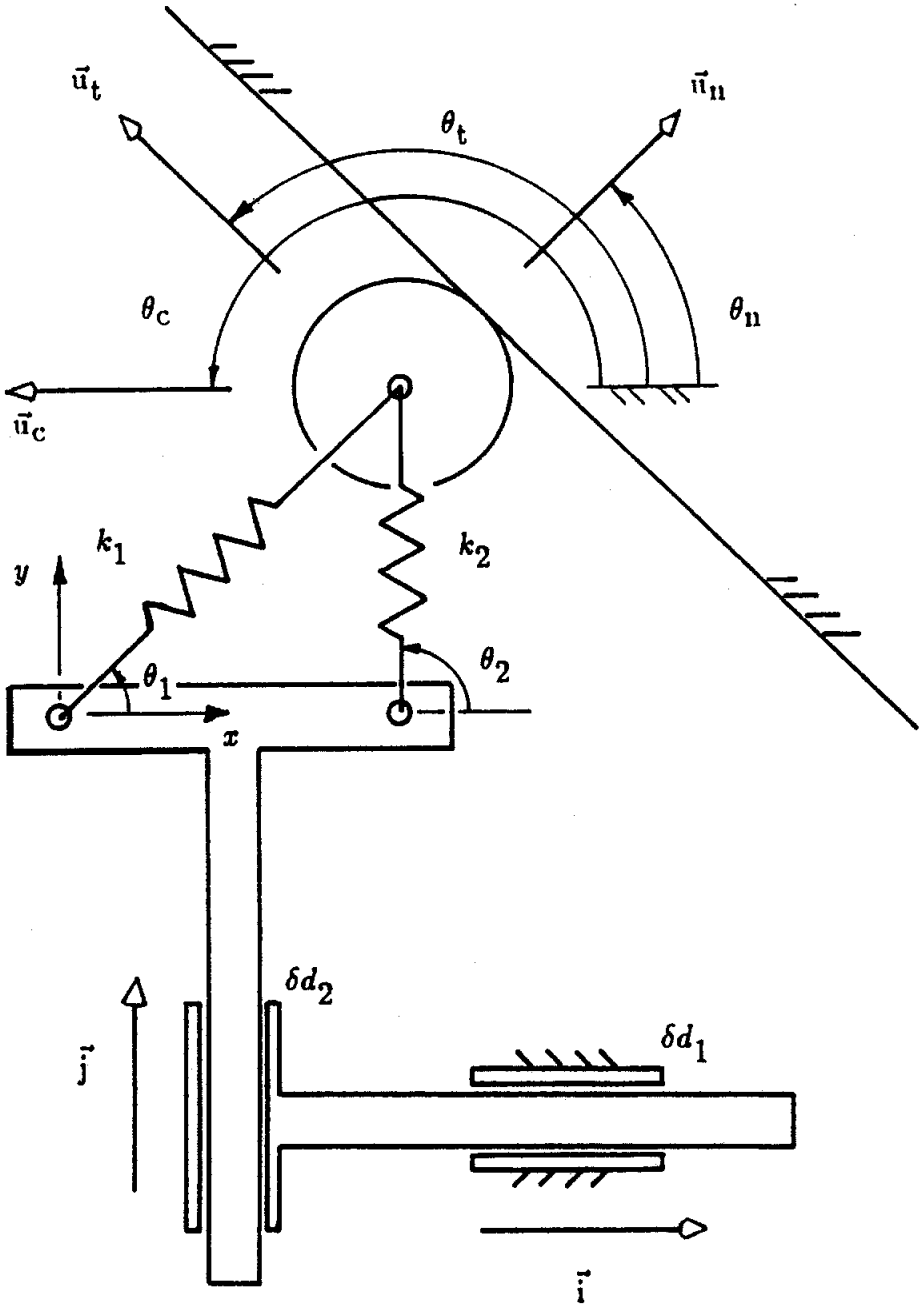
$\vec{u}_t$
$\vec{u}_n$
θ_t
θ_c
θ_n
$\vec{u}_c$
k_1
k_2
y
θ_1
θ_2
x
δd_2
δd_1
$\vec{j}$
$\vec{i}$

Figure 2.1

It will be shown that the control of f_n along $\vec{u}_n$ and p_t along $\vec{u}_t$ is accomplished by judicious choices of slider displacements δd_1 and δd_2, which together combine to move the platform in some direction. Intuitively, one may at the outset consider that the *best* motion for nulling errors in the force f_n would be a displacement of the platform in the $\vec{u}_n$ direction, i. e. parallel to the normal force. However, this is not the case, and in general, the best displacement is in some other direction, $\vec{u}_c$, which is canted to $\vec{u}_t$ at an angle not equal to 90°. *The best displacement is one that changes the force error in a desired way without affecting the control of the wheel's displacement in the* $\vec{u}_t$ *direction.* For example, displacing the platform in the $\vec{u}_c$ direction would not move an at-rest wheel, but it would change the normal force.

For this simple example, a positive-definite Euclidean inner product mandates that a displacement along $\vec{u}_n = \cos(\theta_n)\,\vec{i} + \sin(\theta_n)\,\vec{j}$ is Euclidean-orthogonal to a displacement along $\vec{u}_t = \cos(\theta_t)\,\vec{i} + \sin(\theta_t)\,\vec{j}$. However, these vectors are elements of a Euclidean vector space, which uses two *non*-homogeneous coordinates to locate ∞^2 elements.[3] (See Ryan [1989].) Even though there exists a purely geometrical positive-definite inner product here in this simple case, it is not the best one with which to perform twist decomposition.

It is proposed here that stiffness can be used to define a proper inner product with which to obtain the *best* f_n-error-nulling direction: the twist of compliance, $\vec{u}_c = \cos(\theta_c)\,\vec{i} + \sin(\theta_c)\,\vec{j}$. In other words, for coordinates

[3] A Euclidean vector space does not possess the power of locating infinite elements with finite coordinates. Once a rotational coordinate is incorporated with the two translational ones (general planar rigid body motion), then a rotation about a point at infinity yields a pure translation, and accordingly, three finite homogeneous coordinates are used to describe general planar motion. Because the resulting homogeneous twist coordinates would no longer belong to a Euclidean vector space, a positive-definite inner product acting on them must be non-Euclidean. (See the previous footnote.)

$\vec{u}_t = \begin{bmatrix} \cos(\theta_t) \\ \sin(\theta_t) \end{bmatrix}$ and $\vec{u}_c = \begin{bmatrix} \cos(\theta_c) \\ \sin(\theta_c) \end{bmatrix}$, $\vec{u}_t^T\,[K]\,\vec{u}_c = 0$, where the 2x2 matrix [K] is symmetric, and its three elements have the dimension F/L. This matrix quantifies the stiffness of the mechanism consisting of a wheel connected to ground by two translational springs, a platform, and two actuated sliders. (It does not quantify its task, which is the surface to be tracked by the wheel). It is assumed that the actuated sliders are stiff (they are tuned for fine-position control), and since they act in series with the more compliant translational springs, their compliances can be neglected, and the stiffness of the overall mechanism is thus solely due to the translational springs.

In order to obtain a mechanism stiffness mapping relating the small displacement of the wheel relative to the platform with the incremental change in external force acting on the wheel, it is necessary to express the force, $\vec{f} = f_x\,\vec{i} + f_y\,\vec{j}$, that the wheel applies to the springs:

$$\begin{bmatrix} f_x \\ f_y \end{bmatrix} = \begin{bmatrix} c_1 & c_2 \\ s_1 & s_2 \end{bmatrix} \begin{bmatrix} k_1\,(l_1 - l_{o1}) \\ k_2\,(l_2 - l_{o2}) \end{bmatrix}, \tag{2.1}$$

where $c_i = \cos(\theta_i)$ and $s_i = \sin(\theta_i)$, and where k_i and $(l_i - l_{oi})$ are respectively the positive non-zero spring constant and difference between the current and free lengths of the i^{th} spring. When the wheel is in quasi-static equilibrium, then $\vec{f}$ is the force that the the environment applies to the wheel plus any other externally applied forces (gravity, for instance).

Consider now that the two springs do not deviate too far from their free lengths. Then, from (2.1), for a small deviation,

$$\begin{bmatrix} \delta f_x \\ \delta f_y \end{bmatrix} = \begin{bmatrix} c_1 & c_2 \\ s_1 & s_2 \end{bmatrix} \begin{bmatrix} k_1\,\delta l_1 \\ k_2\,\delta l_2 \end{bmatrix}, \tag{2.2}$$

where δf_x and δf_y are deviations away from f_x and f_y and where δl_i is a deviation of the i^{th} spring away from its current length. Substituting into the right-hand side of (2.2) the inverse kinematic transformation,

$$\begin{bmatrix} \delta l_1 \\ \delta l_2 \end{bmatrix} = \begin{bmatrix} c_1 & s_1 \\ c_2 & s_2 \end{bmatrix} \begin{bmatrix} \delta x \\ \delta y \end{bmatrix}, \tag{2.3}$$

(obtained from a projection) establishes the stiffness relationship,

$$\begin{bmatrix} \delta f_x \\ \delta f_y \end{bmatrix} = [K] \begin{bmatrix} \delta x \\ \delta y \end{bmatrix}, \tag{2.4}$$

where δx and δy are deviations of the center position of the wheel away from its current position measured relative to the platform, and where the stiffness matrix [K] is given by

$$[K] = \begin{bmatrix} c_1 & c_2 \\ s_1 & s_2 \end{bmatrix} \begin{bmatrix} k_1 & 0 \\ 0 & k_2 \end{bmatrix} \begin{bmatrix} c_1 & s_1 \\ c_2 & s_2 \end{bmatrix}. \tag{2.5}$$

Consider a numerical example of $\theta_1 = 45°$, $\theta_2 = 90°$, and $k_1 = k_2 = 10$ kg/cm. Then, from (2.5), the stiffness matrix assumes the form, $[K] = \begin{bmatrix} 5. & 5. \\ 5. & 15. \end{bmatrix}$ kg/cm. Now it remains to vary the task required of the wheel in order to demonstrate the concepts here that are new and of interest. (They are easily extendible to higher dimensions. Section 2.2 illustrates the extension to planar three-dimensional and spatial six-dimensional cases.)

Prior to analyzing the specific task illustrated in Figure 2.1, consider first that the wheel center point is fully constrained. This means that any force,

$\vec{f} = f_x \vec{i} + f_y \vec{j}$, acting through the center point may be applied to the wheel by the environment. It is clear that any small displacement of the platform due to slider displacements δd_1 and δd_2, $\delta \vec{d} = \delta d_1 \vec{i} + \delta d_2 \vec{j}$, will cause via stiffness a small change in this force. Specifically, the change will be

$$\begin{bmatrix} \delta f_x \\ \delta f_y \end{bmatrix} = -\begin{bmatrix} 5. & 5. \\ 5. & 15. \end{bmatrix} \begin{bmatrix} \delta d_1 \\ \delta d_2 \end{bmatrix}. \tag{2.6}$$

The negative sign accounts for the kinematic inversion of specifying the displacement of the platform relative to the wheel. In other words, $\begin{bmatrix} \delta d_1 \\ \delta d_2 \end{bmatrix} = -\begin{bmatrix} \delta x \\ \delta y \end{bmatrix}$.

Conversely consider that certain desired changes in f_x and f_y are known and are denoted by δf_x and δf_y. The proper direction, $\delta \vec{d}_c = \delta d_{c1} \vec{i} + \delta d_{c2} \vec{j}$, to move the platform to accomplish this change can be obtained by inverting the spring matrix in (2.6), which yields

$$\begin{bmatrix} \delta d_{c1} \\ \delta d_{c2} \end{bmatrix} = -\begin{bmatrix} 0.3 & -0.1 \\ -0.1 & 0.1 \end{bmatrix} \begin{bmatrix} \delta f_x \\ \delta f_y \end{bmatrix}. \tag{2.7}$$

Equation (2.7) can be used to control a time-varying general force, $\vec{f} = f_x \vec{i} + f_y \vec{j}$, that interacts between the fully constrained wheel and its environment. At each instant, a force error is given, and (2.7) specifies the proper force-error-reducing displacement $\delta \vec{d}_c$.

Consider now that the wheel is at rest but is loaded with an excessive normal force. (See Figure 2.1.) By application of (2.7), this force can be reduced in a desired way without moving the wheel as long as the change in force, $\begin{bmatrix} \delta f_x \\ \delta f_y \end{bmatrix}$, is supported by the lone constraint imposed by the environment. Therefore, based on the figure, $\begin{bmatrix} \delta f_x \\ \delta f_y \end{bmatrix} = \delta f_n \begin{bmatrix} 0.707 \\ 0.707 \end{bmatrix}$, where δf_n is the desired change in the normal

force, f_n. Substituting into (2.7) yields the correct direction (with a magnitude) to move the platform: $\begin{bmatrix}\delta d_{c1}\\ \delta d_{c2}\end{bmatrix} = \delta f_n \begin{bmatrix}-0.1414 \text{ cm/kg}\\ 0.0\end{bmatrix}$. This demonstrates that for this example a displacement of the platform in the negative x direction (positive δf_n) reduces the compressive normal force that acts on the wheel at an angle of 45°. (The force f_n is referenced negative for compression, and therefore, a positive δf_n reduces an excessively compressive force.) Because the wheel does not move when the platform displaces in this direction, this is inherently the *best* direction for correcting a normal force error, and consequently, it is the twist of compliance, $\vec{u}_c$.

The control of the normal force has been accomplished without displacing the wheel. It is important to recognize this since now, by superposition, a desired allowable displacement of the wheel,

$$\delta\vec{d}_t = \delta d_{t1}\,\vec{i} + \delta d_{t2}\,\vec{j} = \delta p_t(-0.707\,\vec{i} + 0.707\,\vec{j}),$$

can be accomplished by simply adding it to the force-error correcting displacement, $\delta\vec{d}_c$. (Because $\delta\vec{d}_t$ is an allowable displacement, adding it to $\delta\vec{d}_c$ does not affect the control of normal force.) Therefore, the following small slider displacements can be computed to control the normal force and the tangential displacement simultaneously:

$$\begin{bmatrix}\delta d_1\\ \delta d_2\end{bmatrix} = G_t\,\delta p_t \begin{bmatrix}-0.707\\ 0.707\end{bmatrix} + G_c\,\delta f_n \begin{bmatrix}-0.1414 \text{ cm/kg}\\ 0.0\end{bmatrix}. \tag{2.8}$$

In (2.8), G_t and G_c are dimensionless scalar gains, and δp_t and δf_n are errors in wheel position and normal force. Successive applications of (2.8) based on updated errors in δp_t and δf_n provides the means for controlling both the tangential wheel position and the normal force.

2.1.3 The Justification for Stiffness to be the Inner Product

The desired control algorithm has thus been formulated. A highlight of the example demonstrates precisely where the theory depends upon geometry and precisely where it is enhanced by the *non*-geometrical physical properties of the spring stiffnesses, k_i. This establishes that stiffness can be used to define a physically meaningful inner product with which to perform twist decomposition.

The constraint force, f_n, does no work, as it acts in the direction $\vec{u}_n$ canted at an angle θ_n to the horizontal. The condition that the constraint force does no work may be written:

$$(\delta p_t \, \vec{u}_t) \cdot (f_n \, \vec{u}_n) = 0, \tag{2.9}$$

where δp_t denotes a small displacement of the wheel in an allowable direction, $\vec{u}_t$. As the wheel moves to accommodate the no-work condition (2.9), the center point of the wheel is restricted to a displacement δp_t in the direction $\vec{u}_t$. Therefore, from (2.9), $\vec{u}_t$ is perpendicular to $\vec{u}_n$ ($\vec{u}_n \cdot \vec{u}_t = 0$). Consequently, $\theta_t - \theta_n = \pm 90°$. (See Figure 2.1.)

While this reaffirms the statement that the relationship between constraint and freedom is one of geometry, it often also conjures up the erroneous notion that an inner product for displacements has been established. The condition that the virtual work of a constraint force must vanish has been introduced solely for the purpose of obtaining the unrestricted freedom based on the constraint. (In Section 2.2, it becomes ever more apparent that (2.9) is not an inner product for displacements, and that in general, it is not an inner product at all, but rather, for example, a condition that a point lies on a line.)

With the lone freedom established, it remains to determine the necessary complementary normal-force-correcting displacement. Via stiffness, displacements

are related to forces via a one-to-one mapping. Therefore, for

$$\delta f_n \, \vec{u}_n = \delta f_n \begin{bmatrix} \cos(\theta_n) \\ \sin(\theta_n) \end{bmatrix},$$

there exists the one correcting displacement,

$$\delta p_c \, \vec{u}_c = \delta p_c \begin{bmatrix} \cos(\theta_c) \\ \sin(\theta_c) \end{bmatrix},$$

and this relationship can be written, $\delta f_n \, \vec{u}_n = [K] \, \delta p_c \, \vec{u}_c$. Substituting into (2.9) and dividing by the non-zero magnitudes δp_t and δp_c yields that the directions $\vec{u}_t$ and $\vec{u}_c$ are "[K]–orthogonal":

$$\vec{u}_t^T \, [K] \, \vec{u}_c = \begin{bmatrix} \cos(\theta_t) \\ \sin(\theta_t) \end{bmatrix}^T [K] \begin{bmatrix} \cos(\theta_c) \\ \sin(\theta_c) \end{bmatrix} = \langle \, \vec{u}_t, \, \vec{u}_c \, \rangle = 0. \tag{2.10}$$

Since the normal force must do work on a displacement in the $\vec{u}_c$ direction, $\vec{u}_c$ cannot be perpendicular to $\vec{u}_n$. Therefore, it is not possible for $\vec{u}_c$ to be equal to $\vec{u}_t$, and consequently, $\vec{u}_c$ must be independent of $\vec{u}_t$. Equation (2.10) provides an orthogonal decomposition that allows for any displacement to be written as a linear combination of $\vec{u}_t$ and $\vec{u}_c$. (For example, $\vec{u}_n = \lambda_1 \vec{u}_t + \lambda_2 \vec{u}_c$.)

For the example illustrated in Figure 2.1, $\theta_t = 135^\circ$ which from (2.10) yields that $\theta_c = 180^\circ$. It is interesting to examine how θ_c varies as the task of the wheel varies, viz. θ_n and θ_t vary. Figure 2.2 illustrates θ_c as a function of θ_t, for the same mechanism with task-independent stiffness $[K] = \begin{bmatrix} 5. & 5. \\ 5. & 15. \end{bmatrix}$ kg/cm.

This solution for the twists of compliance (the best directions to move to null force errors) is by no means intuitive. The author submits the reason for this to be the non-Euclidean properties of stiffness.[4] Simply considering all of the

[4]Variations in k_1 and k_2 cause θ_c to vary, even when all (other) geometry is held fixed. This clearly illustrates that the solution of θ_c is not fully dependent on geometry, which is another way of saying that the positive-definite inner product (2.10) is non-Euclidean. The example given in Chapter 1 also explained that the complementary twists of compliance vary as the non-geometrical stiffness properties vary, even though the robot, gripper, workpiece, and environment are not moved.

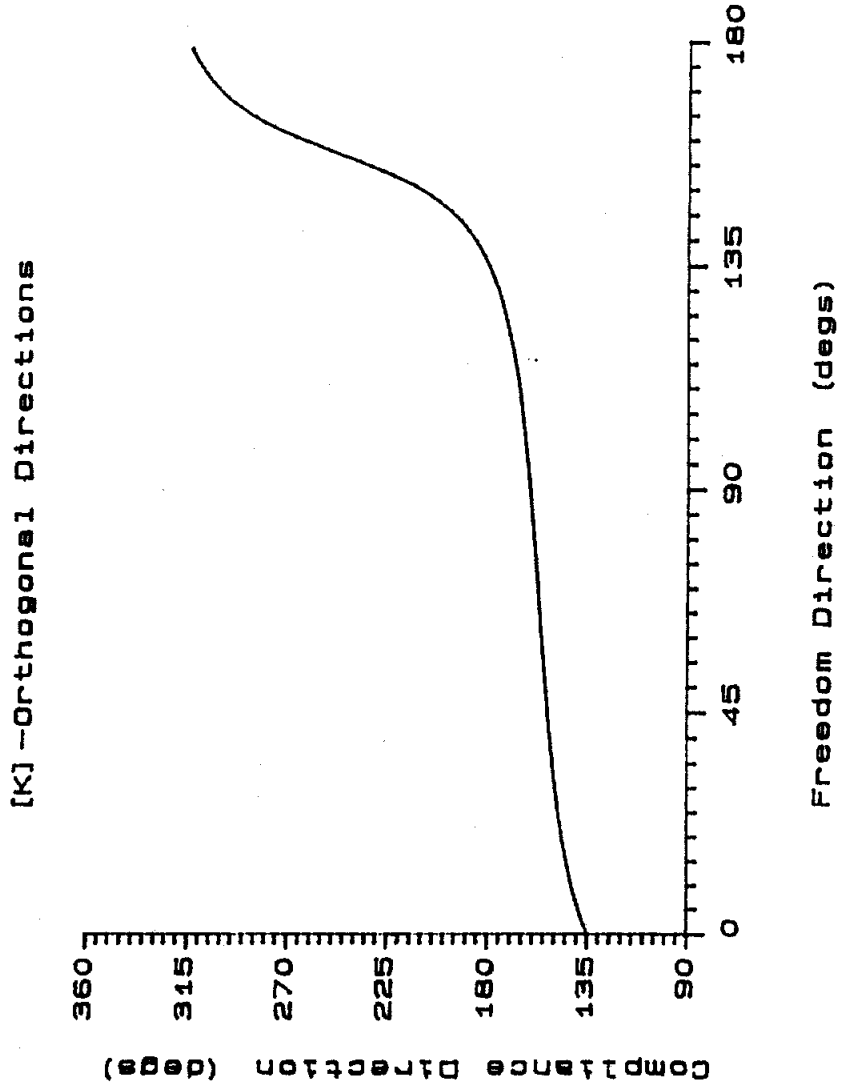
[K]-Orthogonal Directions
Compliance Direction (degs)
360
315
270
225
180
135
90
0
45
90
135
180
Freedom Direction (degs)

Figure 2.2

available motions of the wheel does not immediately produce the correct force-error-nulling displacement direction. In order to make the solution intuitive, the engineer must incorporate into the thought process the appropriate mechanism properties, which at the very minimum must include its stiffness properties. In other words, "if I move the platform in this direction that is dependent on stiffness and the constraint, then there will be no displacement of the at-rest wheel."

While it has been recognized here that the use of a positive-definite (and hence, a non-Euclidean) inner product is necessary, it only remains to justify the use of a chosen non-Euclidean inner product. Clearly, a more thorough examination includes properties affecting the dynamic (higher frequency) characteristics of the mechanism. Griffis [1988] investigated the use of a positive-definite inner product defined by the kinetic energy of a rigid body. From a practical point of view, however, a meaningful algorithm to control force and displacement does not result from it.

The author considers that most robots do not accelerate significantly and do not respond to inputs of higher frequency. (The position control loop for the robot used in this work had a 1 Hz. bandwidth, and for example, the robot responded to only 20% of a 2 Hz. sinusoidal input.) Therefore, it must be clear that the force vs. displacement (and wrench vs. twist) relations are inherently dominated by mechanism stiffness. Consequently, it has been the thrust of this work to examine the stiffness properties of the robot, and to use its knowledge to simultaneously regulate the force and the displacement of its end-effector. (Section 2.3 describes in detail the initial implementation of this theory, beginning with an empirical determination of robot stiffness and ending with proof-of-principle control examples.)

2.1.4 Relation to Previous Work

In general, force/position control laws given in the literature depend upon the synthesis of matrices of control gains that effectively create commands of actuator torque (or force) increments.[5] Figure 2.3 illustrates a general force/torque control loop. The author considers that this figure adapts itself in some form or fashion to all force control loops cited in the literature. For this loop, it remains to synthesize the control matrices $[K_f]$ and $[K_p]$. The vast majority of the literature on this subject supports, I believe erroneously, that the matrix $[K_f]$ is the designer's or programmer's choice and often relegates its synthesis to being dependent on robot task (for instance, making $[K_f]$ diagonal for the $\vec{u}_t$ and $\vec{u}_n$ directions in Figure 2.1). When robot stiffness is ignored, the author considers that the task-dependent synthesis of $[K_f]$ (and $[K_p]$) is necessary for these control laws to work, so that compatible force-error and position-error corrections can be combined.

Excellent, insightful, and thorough investigations of one-dimensional force control have been given in the literature, e. g. An et al. [1988], Chapter 8. Haefner, et al. [1986] effected two-dimensional force control by employing a pair of one-dimensional controllers acting in-parallel (which does not offer much geometrical insight). The extension of Haefner, et al. is valid, but the extension of many other one-dimensional applications to multi-dimensional ones has not been a natural one. It is common place for one to read that a robot is desired to have a "stiffness 'k_x' in the 'x' direction." To coerce the close-loop robot system to exhibit this task-dependent characteristic clearly requires the task-dependent synthesis of $[K_f]$ and

[5]See Whitney [1987] for a survey of other force/position control laws, such as Hybrid Control (Raibert and Craig [1981]), Stiffness Control (Salisbury [1980], Kazerooni, et al. [1986]) and Impedance Control (Hogan [1985]). This survey is an excellent overview, and therefore, the control laws need not be repeated here. As far as torque control is concerned, see An, et al. [1988], which documented experimentation on a unique prototype direct drive serial robot that was specifically designed to facilitate the control of joint torques.

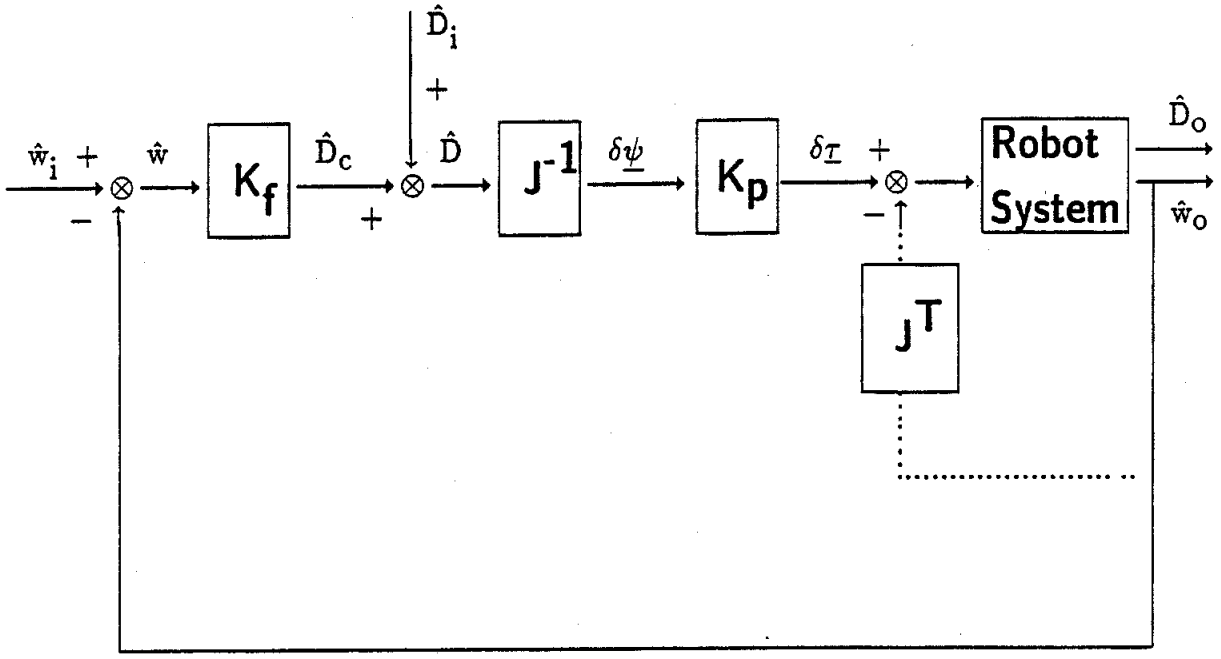

Nomenclature

$\hat{w}_i$ – desired wrench
$\hat{w}_o$ – actual wrench of constraint
$\hat{w}$ – wrench error
} constraints ($\hat{w}_a \in [a]$)

$\hat{D}_c$ – twist of compliance (wrench-error correction)

$\hat{D}_i$ – desired twist of freedom
$\hat{D}_o$ – actual twist of freedom
} freedoms ($\hat{D}_b \in [B]$)

$[K_f]$ – wrench gain matrix

$\hat{D}$ – general command twist to robot

$\delta\underline{\psi}$ – actuator displacement

$\delta\underline{\tau}$ – actuator torque increment

$[K_p]$ – actuator gain matrix

$[J]$ – kinematic Jacobian relating $\delta\underline{\psi}$ to $\hat{D}$

[Robot System] – robot actuators, permanently attached compliant devices and sensors, reacting against a rigid environment.

Figure 2.3

$[K_p]$, as well as possibly others. Some researchers deem the synthesis of the 36 elements in each of these 6x6 matrices necessary due to the robot system complexity, but it seems that this widespread synthesis itself introduces a complexity which is an order of magnitude greater than it needs to be, especially in a research lab where a graduate student likes to see the effects of initially implementing one scalar proportional gain, even if it is to control a six-dimensional system.

Kinestatic Control establishes $[K_p]$ and $[K_f]$ whenever the back-drivable effects are minimal (shown with a dotted line in Figure 2.3), i. e., wrenches acting on the gripper do not affect the response of the actuators. For this case, the matrix $[K_p]$ represents itself as no more than fine-position control gains, which are easily synthesized for a given robot while it is unconstrained. While the commands to the actuators are displacement-based, the matrix $[K_f]$ must map a force/torque (wrench) error into a displacement/orientation (twist) correction, and consequently, $[K_f]$ is a scalar times the inverse of stiffness (compliance).

Under the provisions of Kinestatic Control, general six-dimensional simultaneous regulation of both force and position is accomplished via the synthesis and subsequent actions of only two single dimensionless scalar gains: one for force (wrench of constraint) and one for position (twist of freedom). (This is a generalization of (2.8).) The force gain essentially magnifies how far to move the end-effector along a wrench-corrective twist of compliance, while the position gain magnifies how far to twist along a desired twist of freedom. Consequently, this control methodology depends on the knowledge of the open-loop stiffness of the robot, which enables the actual control law to be simple yet responsive.

2.2 Twist Space Decomposition

2.2.1 Planar Twists

Figure 2.4 illustrates a planar three revolute (3R) serial robot with a compliant device connecting its gripper to its end-effector (platform). The workpiece held fixed in the gripper touches the rigid environment in a single point, P. At the instant in this example, the environment has imposed one constraint on the gripper, which leaves it with two freedoms. In fact, a constraint force may be generated to act on the gripper along the line $\$_a$. (The point contact is considered to be a bi-lateral constraint here in the discussion, even though it is really a uni-lateral one at the times of contact and withdrawal.)

The revolute joints of the robot are actuated ($\delta\psi_1$, $\delta\psi_2$, and $\delta\psi_3$) and considered to be tuned for fine-position control so that the robot is non-back-drivable while servoing. The compliant device considered here is a parallel mechanism consisting of three extendible legs whose displacements are restricted via translational springs of known stiffnesses. The compliance of the stiff robot is neglected, and the stiffness of the robot system connecting gripper to ground is defined by the stiffness of the compliant device.

For this planar example, force coordinates are initially defined, so that they can be used to determine the forces that the gripper applies to the springs. Obtaining a variational form of this is followed in turn with the definition of twist coordinates for the plane. This section continues by developing the mapping of stiffness for the compliant device (and hence, the robot system). It is shown that this mapping of stiffness relates a general point (of rotation) with a unique line (of force). This is finally used to obtain a twist of compliance that is necessary to complement the two freedoms of the gripper to effect kinestatic control.

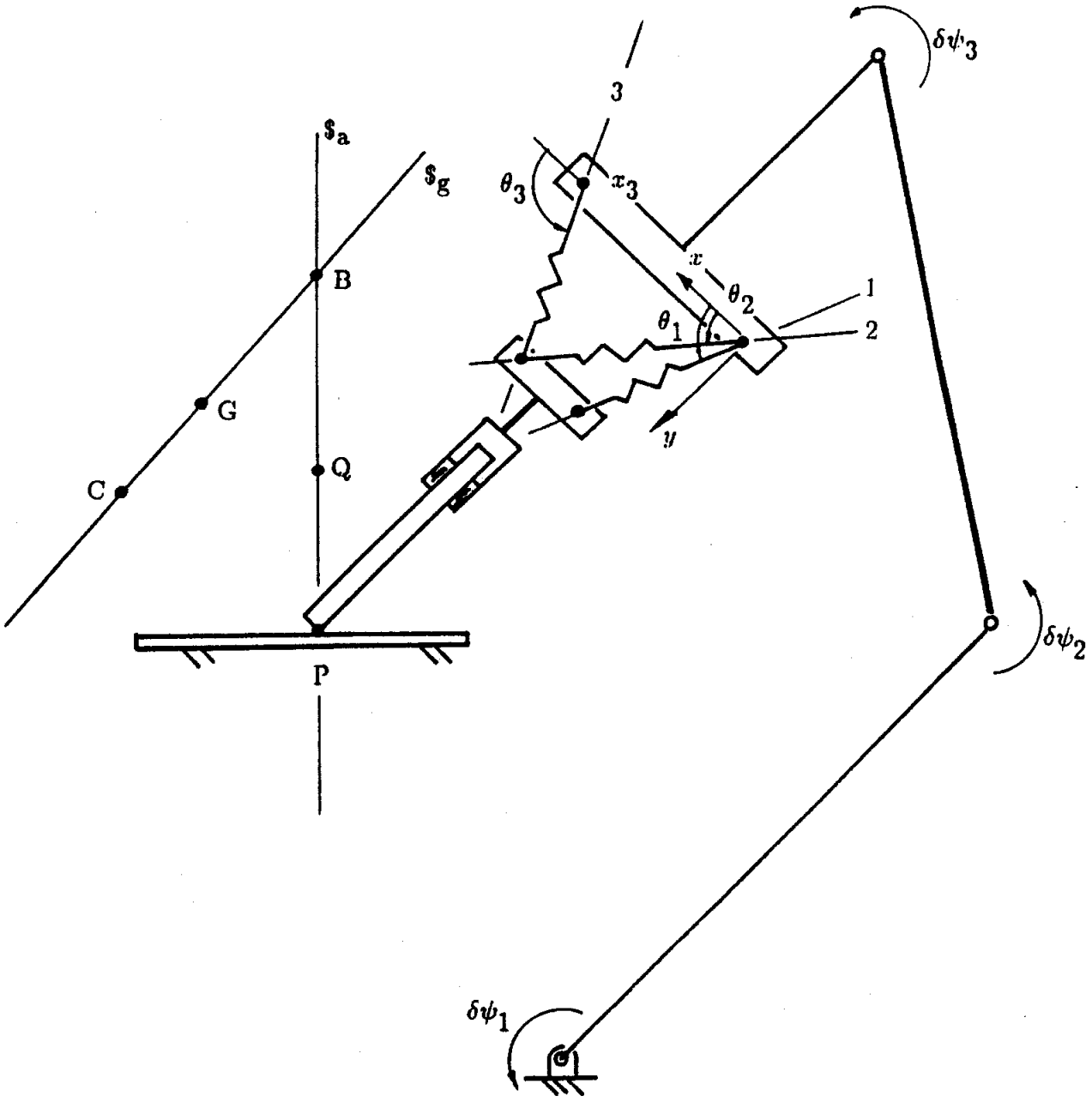
$\delta\psi_3$
3
$\$_a$
$\$_g$
θ_3
x_3
x
θ_2
1
2
θ_1
B
G
C
Q
y
P
$\delta\psi_2$
$\delta\psi_1$

Figure 2.4

Lines of forces in the plane may be located with three homogeneous coordinates that are normalized, $\hat{s}=[c, s; r]^T$, where c and s are direction cosines and r the signed perpendicular distance of the line from the origin. A scalar multiple, f, of these coordinates varies the force acting along the line, and this can be represented by the three homogeneous coordinates $\hat{w}=f\,\hat{s}=[f_x, f_y; m_o]^T$. The force acting along a general line can be decomposed into a force acting along a parallel line through the origin together with a couple. The coordinates $[f_x, f_y; 0]^T$ denote a force acting through the origin, while the coordinates $[0, 0; m_o]^T$ denote a couple (an infinitesimal force on the line at infinity whose homogeneous coordinates are $[0, 0; 1]^T$). Adding the two sets of coordinates together reproduces the coordinates of the force.

The homogeneous coordinates $[f_x, f_y; m_o]^T$ of the force that the gripper applies to the springs can be written in the matrix form,

$$\begin{bmatrix} f_x \\ f_y \\ m_o \end{bmatrix} = \begin{bmatrix} c_1 & c_2 & c_3 \\ s_1 & s_2 & s_3 \\ 0 & 0 & x_3\, s_3 \end{bmatrix} \begin{bmatrix} k_1\,(l_1 - l_{o1}) \\ k_2\,(l_2 - l_{o2}) \\ k_3\,(l_3 - l_{o3}) \end{bmatrix}, \tag{2.11}$$

where the columns of the matrix contain the normalized homogeneous line coordinates ($\hat{s}_1$, $\hat{s}_2$, and $\hat{s}_3$) of the lines (1, 2, and 3) of the three extensible legs shown in the figure, and where $k_i\,(l_i - l_{oi})$ is the leg force due to the extension of the i^{th} spring. All coordinates are referenced to the coordinate system located on the platform at the intersection of the first two legs (hence the moment entries for those legs are zero). A variational form of (2.11) can be written as

$$\begin{bmatrix} \delta f_x \\ \delta f_y \\ \delta m_o \end{bmatrix} = \begin{bmatrix} c_1 & c_2 & c_3 \\ s_1 & s_2 & s_3 \\ 0 & 0 & x_3\, s_3 \end{bmatrix} \begin{bmatrix} k_1\,\delta l_1 \\ k_2\,\delta l_2 \\ k_3\,\delta l_3 \end{bmatrix}, \tag{2.12}$$

provided the legs do not deviate too far from their unloaded positions. Equation (2.12) can be expressed in the compact form:

$$\hat{w} = [j][k_l]\delta\underline{l}, \tag{2.13}$$

where $\hat{w} = [\delta f_x, \delta f_y; \delta m_o]^T$, where [j] replaces the 3x3 matrix of normalized line coordinates, and where $[k_l]$ is a 3x3 diagonal matrix of positive non-zero spring stiffnesses. The three elements of $\delta\underline{l}$ are the small displacements of the legs, which are referenced positive for extension.

Prior to defining an inverse kinematic transformation so that its incorporation into (2.13) will define the overall stiffness mapping, it is necessary to first define twist coordinates. A twist is a rotation about any point in the plane of motion.[6] It can also be thought of as a pure translation, together with a rotation about the origin. The twist coordinates $[\delta x, \delta y; 0]^T$ denote the pure translation, while the coordinates $[0, 0; \delta\phi]^T$ denote the rotation about the origin. Adding these two sets of coordinates together produce the homogeneous coordinates of the general planar twist. These coordinates can also be written in the forms,

$$\hat{D} = [\delta x, \delta y; \delta\phi]^T = [\delta\phi\ y, -\delta\phi\ x; \delta\phi]^T = \delta\phi[\ y, -x; 1]^T = \delta\phi\ \hat{S}, \tag{2.14}$$

where x, y are the Cartesian coordinates of the point of rotation.

The three coordinates $\hat{S} = [y, -x; 1]^T$ are essentially a form of homogeneous point coordinates that are normalized. The twist coordinates $\hat{D} = \delta\phi\ \hat{S}$ are accordingly a form of homogeneous point coordinates, the point being that about which one body rotates $\delta\phi$ relative to another. As such, a point that is infinitely distant, such as one with homogeneous coordinates $[c, s; 0]^T$ for instance, defines a pure translation.

[6] It is really a rotation about a line normal to the plane of motion, but for brevity, the point of intersection of this line and the plane is used in discussion.

While defining an inverse kinematic transformation for the compliant device, consider that the gripper twists relative to the platform. In general, this is a rotation of an amount $\delta\phi$ about the point whose Cartesian coordinates are x, y. Then, it is straightforward to express, for example, the signed perpendicular distance, d_3, between the point of rotation and the line of action of the third leg spring force as

$$d_3 = \hat{\mathrm{s}}_3^{\mathrm{T}}\,\hat{\mathrm{S}} = c_3 y - s_3 x + x_3 s_3, \tag{2.15}$$

where $\hat{\mathrm{S}} = [y,\ -x;\ 1]^{\mathrm{T}}$ are the normalized homogeneous coordinates of the point of rotation. While considering only those points of the gripper that instantaneously lie on the line of the third leg, one sees that, as they move tangent to their respective concentric circles, they all share the same component ($\delta\phi\ d_3$) directed along the line. This component consequently defines the displacement of the third spring, and therefore, $\delta l_3 = \delta\phi\ d_3$. Multiplying (2.15) by $\delta\phi$ and substituting (2.14) yields $\delta l_3 = \hat{\mathrm{s}}_3^{\mathrm{T}}\,\hat{\mathrm{D}}$. Repeating for the other two legs yields the inverse kinematic solution for the compliant device:

$$\delta\underline{l} = [\mathrm{j}]^{\mathrm{T}}\,\hat{\mathrm{D}}. \tag{2.16}$$

Substituting into (2.13) yields the overall mapping of stiffness, which is expressed here in the form,

$$\hat{\mathrm{w}} = [\mathrm{K}]\,\hat{\mathrm{D}}, \tag{2.17}$$

where $[\mathrm{K}] = [\mathrm{j}][k_{\mathrm{i}}][\mathrm{j}]^{\mathrm{T}}$.

The stiffness mapping [K] now represents a linear geometric transformation that relates points with lines (specifically, a projective correlation). Equation (2.17) clearly shows that for a fixed [K], there is a one-to-one correspondence between a point of rotation and a line of force: the point of rotation being that point in the platform about which the gripper turns an amount $\delta\phi$ and the line of

force being that line along which a small force δf acts to change the nominal force which the environment applies to the gripper. For the mechanism in Figure 2.4, the stiffness matrix [K] is considered known. (It is determined by [j] and $[k_i]$.)

The columns of [K] are scalar multiples of the coordinates of the forces necessary to cause twists respectively corresponding to a translation in the x-direction, a translation in the y-direction, and a rotation about the origin. Considering the columns further as scalar multiplies of line coordinates, one sees that the intersection of the first two columns defines a unique point through which a force must act to cause a translation of the gripper relative to the platform. (If a force does not act through that point, then the gripper must rotate $\delta\phi$ about some point in the platform.)

Prior to analyzing the specific task illustrated in Figure 2.4, consider first that the gripper is fully constrained relative to ground (bolted down, for example). This means that any nominal force whose coordinates are $\hat{w}_O = [f_X, f_Y; m_O]^T$ is applied to the gripper by ground at a given instant with the robot in a stationary configuration. Clearly, any twist of the platform relative to ground (with coordinates $\hat{D}_C$) will effect a change in this nominal force, and analytically, this can be expressed in the form,

$$\hat{w} = -[K]\,\hat{D}_C, \tag{2.18}$$

where a sign change has been installed in (2.17) because of the kinematic inversion of now specifying the twist of the platform relative to the grounded gripper. Because of (2.18), the force acting on the gripper changes to

$$\hat{w}_O + \hat{w} = [f_X + \delta f_X, f_Y + \delta f_Y; m_O + \delta m_O]^T.$$

Alternatively, suppose that the desired change $\hat{w}$ is known, then $\hat{D}_C$ is computed by

inverting (2.18):

$$\hat{D}_C = -[K]^{-1}\,\hat{w}. \tag{2.19}$$

Equation (2.19) can be used to control a time-varying general force $\hat{w}_O = [f_x, f_y; m_O]^T$, that interacts between the fully constrained gripper and its environment, because it specifies at each instant the best force-error-nulling point C about which to rotate the platform an amount $\delta\phi$.

It is interesting to consider the columns of $[K]^{-1}$ using superposition. They represent themselves as scalar multiples of the coordinates of twists that are necessary to change a nominal force by adding to it respectively a force along the x-axis, a force along the y-axis, and the couple normal to the plane. Considering the columns further as scalar multiples of point coordinates, one sees that the last column locates the only point for which a twist of the gripper relative to the platform generates a couple. (A twist of the gripper relative to the platform about any other point generates a force acting along some line.)

Returning to the task at hand, namely that illustrated in Figure 2.4, it is clear that we must interest ourselves in specifically what point is related via (2.17) with the line of action $\$_a$ of the constraint force. For it is about this point that the platform of the compliant device should rotate in order to null (or control) the constraint force. In other words, the point C that is sought is the twist of compliance, and from (2.19), its homogeneous coordinates are

$$\hat{D}_C = -[K]^{-1}\,\hat{w}_a, \tag{2.20}$$

where $\hat{w}_a = f_a\,[c_a, s_a; r_a]^T$ are homogeneous coordinates of a force on the line $\$_a$. Figure 2.4 illustrates C, the precise location[7] of which is only known after establishing $[k_i]$ and the geometry, i. e. [K] of the compliant device.

[7]The twist of compliance will usually not be the intuitive pure translation of the platform in the direction of the line $\$_a$. This would put point C at infinity to the left, which is only valid when (2.20) yields the homogeneous coordinates $\hat{D}_C = [c_a, s_a; 0]^T$.

A rotation of the platform about point C cannot move the gripper, because the force, or change in force, applied to it is fully supported along $\$_a$. In other words, from (2.17),

$$\hat{w}_a = -[K]\,\hat{D}_c. \tag{2.21}$$

Here, point C represents the *best* point to use to control force, because its use does not affect the control of the displacement of the workpiece (under ideal situations, e. g. no friction and a good stiffness model). A rotation of the platform about any other point does cause or affect the motion of the gripper. To visualize this, consider that because of $\delta\psi_1$, $\delta\psi_2$, and $\delta\psi_3$, the platform rotates relative to ground about a general point G. This twist decomposes itself into an unrestricted rotation of the gripper about point B together with a rotation about C, which causes a change in the contact force acting along $\$_a$. (Analytically, $\hat{D}_g = \hat{D}_b + \hat{D}_c$. Synthetically, the line $\$_g$ containing G and C intersects $\$_a$ in precisely point B.) It is the platform that twists $\hat{D}_g$ relative to ground, while the gripper twists $\hat{D}_b = \hat{D}_g - \hat{D}_c$ relative to ground.

Imagining point G to place itself anywhere in the plane furthers the concept of decomposition of twist. Moving G, and hence $\$_g$, moves the point of intersection of $\$_g$ and $\$_a$, causing B to slide up and down $\$_a$. That B lies on $\$_a$ is in fact the condition that it is a twist of freedom. In other words, the linear restriction (or single constraint) on coordinates $\hat{D}_b$ is the vanishing of the virtual work of a constraint force:

$$\hat{D}_b^T\,\hat{w}_{oa} = \delta x_b\, f_x + \delta y_b\, f_y + \delta\phi_b\, m_o = 0, \tag{2.22}$$

where $\hat{w}_{oa}$ are coordinates of a nominal wrench acting on the gripper along $\$_a$. While it is clear that (2.22) is the point equation of the line $\$_a$, it should also be clear that it is valid for any scalar force acting along it. Supposing the magnitude

to be small, $\hat{w}_{oa} = \hat{w}_a$, then substituting (2.21) into the left-hand side of (2.22) and multiplying throughout by a minus sign gives the [K]-orthogonal relationship between the twist of compliance and the twist of freedom,

$$\hat{D}_b^T [K] \hat{D}_c = \langle \hat{D}_b, \hat{D}_c \rangle = 0, \tag{2.23}$$

which, after dividing throughout by non-zero rotation angles, $\delta\phi_b$ and $\delta\phi_c$, states clearly that the two points B and C are [K]-orthogonal:

$$\hat{S}_b^T [K] \hat{S}_c = \langle \hat{S}_b, \hat{S}_c \rangle = 0. \tag{2.24}$$

The concept of twist decomposition is extended by considering point B to be an element of the linear span of two points P and Q that lie on $\$_a$. In other words, analytically, the twist coordinates of B can be written as the linear combination,

$$\hat{D}_b = \delta\phi_b \hat{S}_b = \delta\phi_p \hat{S}_p + \delta\phi_q \hat{S}_q, \tag{2.25}$$

where $\hat{S}_p$ and $\hat{S}_q$ are normalized coordinates of P and Q. Substituting (2.25) into (2.23) yields that, for general rotations $\delta\phi_p$ and $\delta\phi_q$, both points P and Q are [K]-orthogonal to C. It can be said then that P and Q define a system of points, whose [K]-orthogonal complement is C.

Because C is the [K]-orthogonal complement of P and Q and because it shares a working relationship with a constraint force acting along $\$_a$, it cannot lie on $\$_a$. This fulfills the concept of twist decomposition, since now the twist coordinates $\hat{D}_g$ of a general point G may be written,

$$\hat{D}_g = \delta\phi_g \hat{S}_g = \delta\phi_p \hat{S}_p + \delta\phi_q \hat{S}_q + \delta\phi_c \hat{S}_c, \tag{2.26}$$

where the three linearly independent points P, Q, and C are used to span all points in the plane and represent all possible motions of the platform. Via the [K]-orthogonal decomposition, the general platform twist is decomposed into a gripper twist ($\hat{D}_b = \delta\phi_p \hat{S}_p + \delta\phi_q \hat{S}_q$) and a constraint-force-error twist correction ($\hat{D}_c = \delta\phi_c \hat{S}_c$), and this is illustrated in Figure 2.4 with the line $\$_g$.

Kinestatic Control of the mechanism in Figure 2.4 is accomplished by an extension of Equation (2.8). It follows that the control law may take one of the following forms:

$$\hat{D}_g = G_b\,\hat{D}_b + G_c\,\hat{D}_c,$$

$$\hat{D}_g = G_b\,\hat{D}_b - G_c\,[K]^{-1}\,\hat{w}_a, \text{ or}$$

$$\hat{D}_g = G_b\,(\delta\phi_p\,\hat{S}_p + \delta\phi_q\,\hat{S}_q) - G_c\,\delta f_a\,[K]^{-1}\,\hat{s}_a, \tag{2.27}$$

where [K] depends on the robot, $\hat{S}_p$, $\hat{S}_q$, and $\hat{s}_a$ on its task, and where G_b and G_c are dimensionless gains for position and force errors. The scalars $\delta\phi_p$ and $\delta\phi_q$ are errors in the rotations of the gripper about points P and Q, while the scalar δf_a is an error in the constraint force. Comparing (2.27) with Figure 2.3 shows that $[K_f] = -G_c\,[K]^{-1}$. (See Hennessey [1986] for an alternative planar algorithm that controls the displacement of the gripper in addition to the compliance levels of an iRCC which is attached to a PUMA robot.)

Clearly, there are other ways of constraining the gripper of Figure 2.4, whether by just moving $\$_a$ or by changing the kind of constraint altogether. An example of a different kind of constraint sees the incorporation of another point of contact and, hence, a second normal line of contact, $\$_z$. (See Figure 2.5.) This example leaves the gripper with a single freedom relative to ground, which is a rotation about the point of intersection (B) of the two lines $\$_a$ and $\$_z$. Complementing this single twist of freedom must now be a pair of points (C_1 and C_2) denoting the twists of compliance. The pair corresponds (via [K]) with the lines $\$_a$ and $\$_z$. The pair of points C_1 and C_2 themselves define another line, whose ∞ of points share a one-to-one correspondence with the ∞ of lines that pass through B. It is this one-to-one relationship defined by [K] that is used to control the constraint force passing through B. In summary, similar to (2.26), the

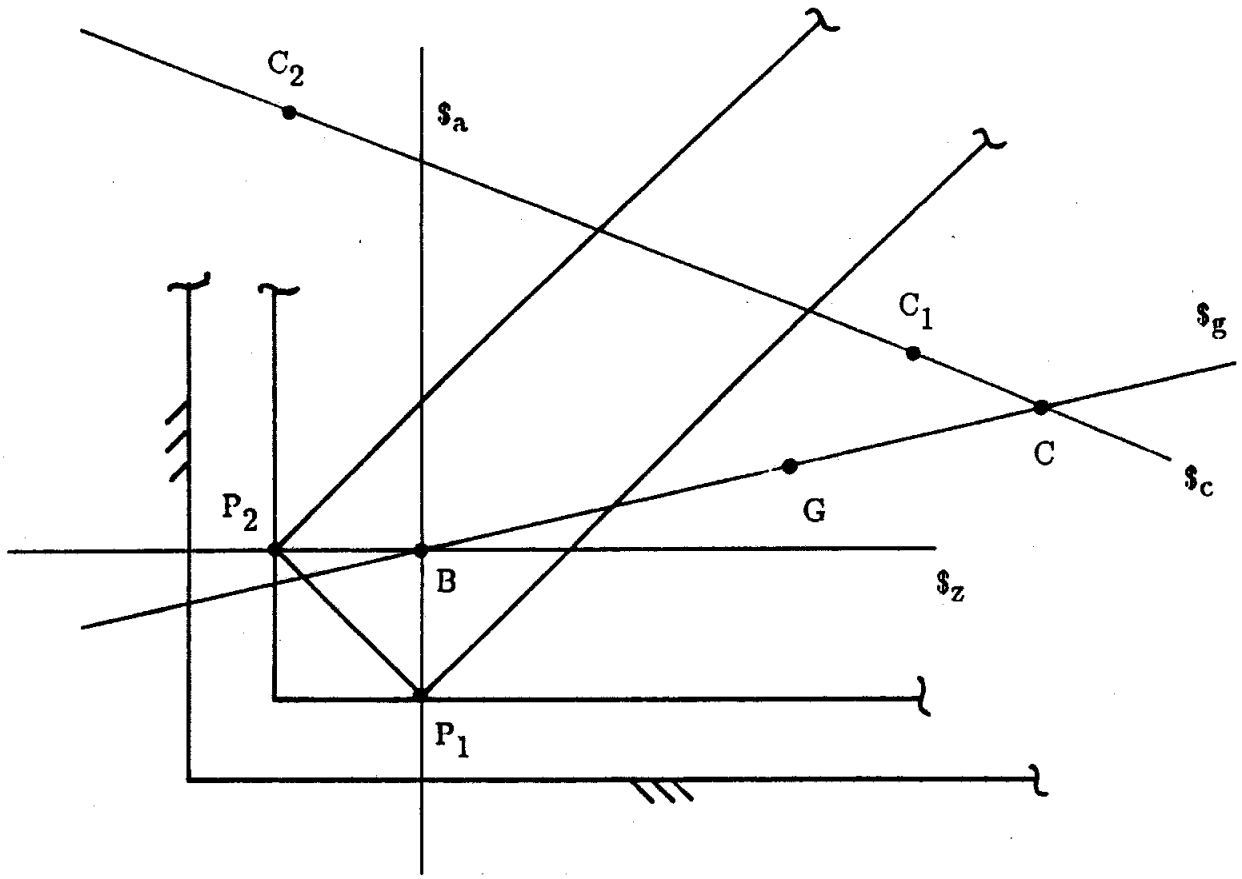

Figure 2.5

coordinates of the general twist may be written as a linear combination of the normalized coordinates of the points B, C_1, and C_2.

2.2.2 Spatial Twists

The purpose of this section is to establish twist decomposition for spatial applications involving a robot with six independent actuators. This is accomplished by

i) defining twists and wrenches for six-dimensional spatial applications,

ii) recognizing a task-independent mapping of stiffness [K] for the robot,

iii) investigating the task-dependent freedoms and constraints of the gripper relative to ground, which defines the twists of freedom and the wrenches of constraints,

iv) determining the twists of compliance from the wrenches of constraints (via the inverse of [K]), and

v) establishing that the twists of compliance and the twists of freedom are [K]-orthogonal complements.

In the spatial case, a twist is a rotation about a general unique line together with a translation in the same direction. It can also be thought of as a rotation about a line through the origin together with a general translation. Its homogeneous coordinates in either case are given by $\hat{D}=[\delta\vec{x}_O^T; \delta\vec{\phi}^T]^T$, where $\delta\vec{x}_O$ is an infinitesimal displacement, and $\delta\vec{\phi}$ is an infinitesimal rotation. (These coordinates are more conveniently expressed as $\hat{D} = [\delta\vec{x}_O; \delta\vec{\phi}]$, where the transposes are understood.) Its normalized coordinates, on the other hand, are given by

$\hat{S} = [\vec{s}_O^T; \vec{s}^T]^T (= [\vec{s}_O; \vec{s}])$, where $\| \vec{s} \| = 1$. The magnitude $\delta\phi$ of a twist is that scalar which scales all six normalized coordinates $\hat{S}$ to reproduce the homogeneous coordinates $\hat{D}$ of the twist ($\hat{D} = \delta\phi\ \hat{S}$).

Exactly three kinds of twists exist. One body may move relative to another by a general twist, which is a rotation about a line together with a translation in the same direction. Analytically, this case is true when $\delta\vec{x}_O \cdot \delta\vec{\phi} \neq 0$, where the pitch of the twist is given by $h = \vec{s} \cdot \vec{s}_O$. A pure rotation is the case whenever $\delta\vec{x}_O \cdot \delta\vec{\phi} = 0$ and $\| \delta\vec{\phi} \| \neq 0$. Finally, a pure translation is the case whenever $\| \delta\vec{\phi} \| = 0$, for which twist coordinates may not be normalized (because $\| \vec{s} \| = 0$). Accordingly, twist coordinates for translations are normalized differently, $\hat{S} = [\vec{s}_O; \vec{0}]$, where now $\| \vec{s}_O \| = 1$.

Similarly in the spatial case, a wrench is a force acting along a general unique line together with a couple in the same direction. It can also be thought of as a force acting along a line through the origin together with a general couple. Its homogeneous coordinates in either case are given by $\hat{w} = [\vec{f}^T; \vec{m}_O^T]^T$, where $\vec{f}$ is the force and $\vec{m}_O$ is the moment. (This can also be more conveniently expressed as $\hat{w} = [\vec{f}; \vec{m}_O]$, where the transposes are understood.) Its normalized coordinates, on the other hand, are given by $\hat{s} = [\vec{s}^T; \vec{s}_O^T]^T (= [\vec{s}; \vec{s}_O])$, where $\| \vec{s} \| = 1$. The wrench magnitude, f, is that scalar which scales all six normalized coordinates $\hat{s}$ to reproduce the coordinates of the wrench $\hat{w}$ ($\hat{w} = f\ \hat{s}$). A wrench increment (or a small change in a wrench) is defined by a wrench of small magnitude, e. g. δf, which means $\hat{w} = [\delta\vec{f}; \delta\vec{m}_O]$.

Exactly three kinds of wrenches exist. The resultant of the forces that one body applies to another may be a general wrench, which is a force acting along a line together with a couple in the same direction. Analytically, this case is true

when $\vec{f} \cdot \vec{m}_o \neq 0$, where the pitch of the wrench is given by $h = \vec{s} \cdot \vec{s}_o$. A force is the case whenever $\vec{f} \cdot \vec{m}_o = 0$ and $\| \vec{f} \| \neq 0$. Finally, a couple is the case whenever $\| \vec{f} \| = 0$, for which wrench coordinates may not be normalized (because $\| \vec{s} \| = 0$). Accordingly, wrench coordinates for couples are normalized differently, $\hat{s} = [\vec{0};\ \vec{s}_o]$, where now $\| \vec{s}_o \| = 1$.

With twists and wrenches established for spatial applications, consider now that the spatial stiffness of the robot is known and that it provides a task-independent relationship between twist and wrench,

$$\hat{w} = [K]\ \hat{D}, \tag{2.28}$$

where the magnitude of $\hat{w}$ is small, and where now [K] is a 6x6 positive-definite matrix denoting the spatial spring. Equation (2.28) relates the twist of the gripper (relative to the base of the spatial spring) to the change in wrench that the environment applies to the gripper. Equation (2.28) is considered to be a natural extension of (2.4) and (2.17). (See Chapter 1 and Equation (1.4).)

Natural six-dimensional extensions of (2.9) and (2.22) provide the means to establish the general relationship between freedoms and constraints existing between a gripper and its environment:

$$\hat{D}_b^T\, \hat{w}_a = \delta \vec{x}_{ob} \cdot \vec{f}_a + \delta \vec{\theta}_b \cdot \vec{m}_{oa} = 0, \tag{2.29}$$

where $\hat{D}_b = [\delta \vec{x}_{ob};\ \delta \vec{\theta}_b]^T$ are coordinates of a twist of freedom and where $\hat{w}_a = [\vec{f}_a;\ \vec{m}_{oa}]^T$ are coordinates of a constraint wrench. Now, (2.22) is geometrically an incidence relation, specifying that a point lies on a line or a line contains a point. By analogy, (2.29) specifies, for example, that a line of a rotation must intersect a line of a force. In general, (2.29) states that a constraint wrench does no work. Clearly, (2.29) is valid regardless of the magnitude of the constraint wrench, and it may be finite (f) or incremental (δf).

It is important to recognize that the sum of the number of freedoms and the number of constraints for the gripper relative to ground is six in a spatial application. (It may be recalled that this sum was two for the example in Figure 2.1 and three for the examples in Figures 2.4 and 2.5.) This means that when, for instance, four independent constraints are active, then two freedoms remain. In such a case, four sets of normalized coordinates $\hat{s}_i$, $i = 1,\ldots,4$, are used to denote the wrenches of constraints, while two sets of normalized coordinates $\hat{S}_j$, $j = 1,2$, are used to denote the twists of freedom. All linear combinations of these two bases in conjunction with (2.29) mandate that $\hat{S}_j^T \hat{s}_i = 0$, for any i taken with either j. This essentially establishes vector spaces for both the twists of freedom and the wrenches of constraint.

Recognizing that via (2.28) there exists for every wrench of constraint a unique twist essentially proves the existence of the twists of compliance. This can be expressed as

$$\hat{w}_a = [K]\ \hat{D}_c, \tag{2.30}$$

which to a sign change is an extension of (2.21). Because [K] has been specified as positive definite, which mandates that the constraint wrench with coordinates $\hat{w}_a$ share a working relationship with the twist having coordinates $\hat{D}_c$, it can be categorically stated that such a twist is a non-freedom. Consequently, the twists of compliance vector space, whose normalized coordinates $\hat{S}_i$, $i = 1,\ldots,4$, are obtained via an inverse mapping of (2.28),

$$\Lambda_i\ \hat{S}_i = [K]^{-1}\ \hat{s}_i, \tag{2.31}$$

for $i = 1,\ldots,4$, where Λ_i is a scalar having dimensions L/F. (Refer to the example in Figure 2.1 where $1/\delta f_n \begin{bmatrix} \delta d_{c1} \\ \delta d_{c2} \end{bmatrix} = \begin{bmatrix} -0.1414 \text{ cm/kg} \\ 0.0 \end{bmatrix}$.) Linear combinations of the six linearly independent sets of twist coordinates, $\hat{S}_j$, $j = 1, 2$ and $\hat{S}_i$, $i = 1, \ldots, 4$, span the coordinates of all twists.

Substituting (2.30) into (2.29) yields the [K]-orthogonal relationship between a twist of freedom and a twist of compliance. Succinctly, an extension of (2.10) and (2.23) is

$$\hat{D}_b^T [K] \hat{D}_c = \langle \hat{D}_b, \hat{D}_c \rangle = 0, \tag{2.32}$$

which is valid for all $\hat{D}_c$ taken with any $\hat{D}_b$. Note that twists of freedom are on the left, while twists of compliance are on the right. This bookkeeping allows for asymmetric [K]s and is necessary for the general case of Kinestatic Control. Reconsider (2.30), where it was desired to obtain the twist of compliance ($\hat{D}_c$) that was the only restricted twist capable of properly changing a given wrench of constraint ($\hat{w}_a$). *Obtaining* $\hat{D}_c$ *from* (2.30) *is not contingent on* [K] *being symmetric but rather only on its symmetric part* $([K]+[K]^T)/2$ *being positive-definite.* (That no real twist of freedom can be self [K]-orthogonal, viz. $\hat{D}_b^T [K] \hat{D}_b = 0$, ensures that no intersection exists between the two twist systems.) Examples thus far have been limited to symmetric stiffness matrices. In the next section, the theory is implemented employing a real empirically determined stiffness matrix that is not symmetric.

2.3 Implementing Kinestatic Control

This section documents the six-dimensional implementation of this theory on a robot system comprising a modified General Electric P60 robot, two 386PC computers, three Creonics[8] motion controller cards, a Lord ATI Corp. model 15/50 force/torque sensor, and a homemade un-instrumented compliant device. (See Figure 2.6.) Essentially, one of the computers (ROBOT) was employed to control the fine-position displacement of the robot, while the other (KINESTATIC) was employed to generate the twist commands of the end-effector platform.

[8]Creonics Inc., Lebanon, NH, and Lord ATI Corp., Inc, Raleigh, NC.

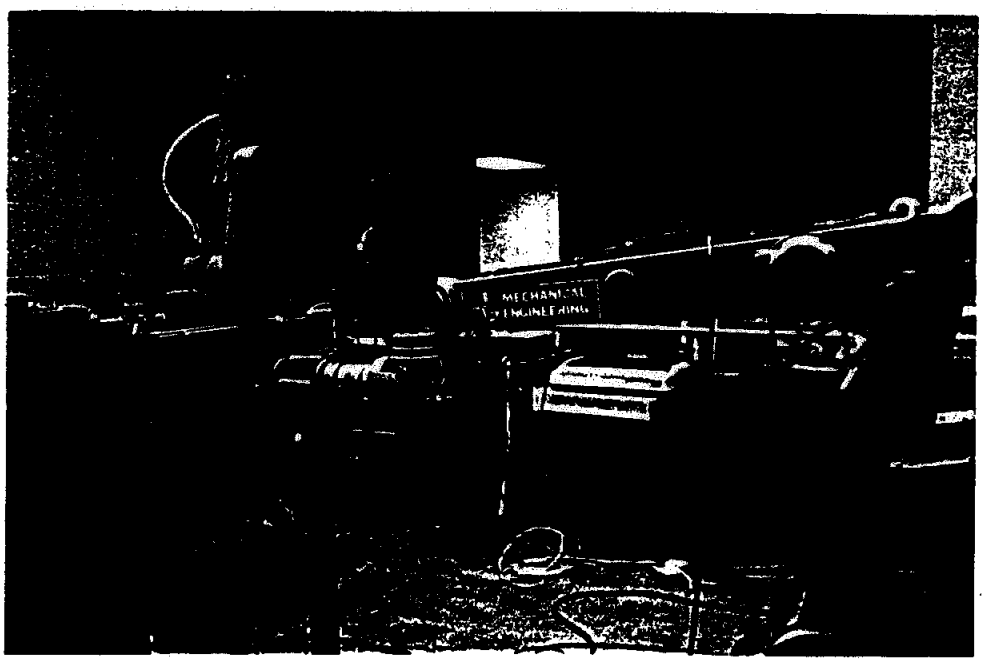

Figure 2.6

(Communications between the two asynchronously operating PCs was over Ethernet and consisted of a end-effector platform twist command sent one way and an actual position and orientation of the end-effector sent the other.) The end result of this assemblage of hardware and software provided a convenient test bed upon which to verify the theory.

A liberal amount of compliance was introduced into the end-effector of the robot by the compliant device.[9] Figure 2.6 illustrates this and the force/torque sensor that constitutes the last link of the robot. The arrangement – robot-force/torque sensor-compliant device-gripper – is essentially a six-dimensional experimental extension of the slider actuators-platform-springs-wheel arrangement shown in Figure 2.1 and the robot-platform-compliant device-gripper arrangement shown in Figure 2.4. Therefore, with the force/torque sensor constituting the "platform" that was connected to ground by six non-back-drivable actuators, it remained to twist it relative to ground (with six degrees-of-freedom) in order to simultaneously control the constraint wrenches and twist freedoms of the gripper. For the implementation, the "gripper" was a three inch long bar of aluminum square stock, drilled and tapped. (See Figure 2.6 which shows the gripper bolted to a large immovable table.)

2.3.1 Empirical Determination of [K]

Prior to simultaneously controlling force and displacement, it was necessary to first measure the mapping of stiffness for the robot, which established the relationship given by (2.28). This was done while the robot was in the

[9]Other researchers have installed compliance into their end-effectors: Whitney [1982], parts assembling aid, experimentally verified; Roberts, et al. [1985], fast responding one degree-of-freedom, experimentally verified; Xu and Paul [1988], for reasons of stability; Goswami, et al. [1990], programmable, task-dependent stiffness and damping.

configuration shown in Figure 2.6, where the gripper was bolted to the table. During the measurement the force/torque sensor was used to record the data on the forces/torques (wrenches) applied to the end-effector by the table. The six actuator encoders were used, and their sum total effect was representative of the twist of the force/torque sensor relative to ground, and hence of the grounded gripper relative to the force/torque sensor. From (2.28), it was clear that a minimum of six of these twists were necessary to measure [K], provided they were independent. Because the compliance of the servoing robot was considered very low compared to that of the compliant device connected in series, the deflections of the robot were not measured during the determination of [K]. The four factors that were considered to have influenced the measurement of robot stiffness are given by the following:

i) force/torque sensor (wrench measurement) resolution,

ii) encoder (twist measurement) resolution,

iii) linearity, and

iv) robot configuration.

Not only was the resolution in the individual coordinates considered, (f_x for instance was 0.02 kg, and m_{ox} was 0.02 kg-cm), but it was also necessary to consider the resolution in obtaining direction and location information from the measured wrench and twist coordinates. Therefore, one must displace the robot (command it to move) significantly enough to obtain a measurable (and more accurate) $\hat{D}$, viz. it is necessary to accurately locate the twist together with its direction, pitch, and magnitude. This commanded twist must provide, through a reasonable amount of compliance, an accurate measure of wrench increment ($\hat{w}$), viz. an accurate determination of its location, direction, pitch, and magnitude.

It is important to note that the robot was not given too large a displacement (twist) for which the matrix [K] would lose its linearity. Such a set of six independent large twists taken together with their corresponding six wrench increments would yield a matrix [K] that would not map correctly a linear combination of the original six twists.

In order to convince the investigator that the compliance of the robot was negligible, the robot configuration was changed, and measurements for [K] were repeated. A stiffness matrix [K] for each of two different robot configurations is presented here.

Initially, a Remote Center-of-Compliance (Lord ATI Corp. RCC) device was installed. However, this device was too stiff for axial displacements and cocking rotations.[10] In other words, because the force/torque sensor tended to saturate, the robot could not be displaced far enough in these directions to obtain an accurate and repeatable measure of $\hat{D}$. A second effort resulted in a spatial spring that was far too compliant, which meant that sufficient forces/torques could not be applied to the spring. A third and final assemblage (three compression springs each clamped at both ends) is shown in Figure 2.6. This yielded the repeatable and manageable stiffness matrix:

$$[K] = \begin{bmatrix} 3.140 & -0.168 & -0.344 & -1.051 & 34.898 & -0.083 \\ 0.197 & 3.439 & 0.052 & -31.914 & -0.783 & 0.057 \\ -0.295 & 0.366 & 11.194 & 5.049 & -1.159 & -0.093 \\ -1.381 & -28.511 & -2.082 & 394.018 & -5.979 & 2.235 \\ 25.660 & -1.342 & -2.008 & 2.243 & 377.047 & 5.944 \\ 0.959 & 0.087 & 0.073 & -8.484 & 8.377 & 76.698 \end{bmatrix}.$$

[10]The RCC was not designed for force control, but rather it was designed to avoid it.

The upper-left 3x3 has units of kg/cm, the lower-right 3x3 has units of kg-cm, and the other two 3x3s have units of kg. It should be noted that [K] is asymmetric and that its symmetric part $([K] + [K]^T)/2$ is positive-definite.

The coordinate system used to express [K] was located at the center of the force/torque sensor. The z-axis was coaxial with the sixth joint of the robot, and the x-axis defined the reference for the last joint of the robot. (This coordinate system is referenced by the label $\mathbb{F}$.) This choice of representation proved to be the most convenient, but another one could have just as well been used to establish a different representation, $[K']$, where $[K'] = [E]^T[K][E]$, and the 6x6 matrix [E] represents the transformation of twist coordinates. (In other words, the same twist needs a pair of twist coordinates $\hat{D}$ and $\hat{D}'$, one set for each coordinate system. Then, $\hat{D} = [E]\ \hat{D}'$.)

While the gripper was grounded and the compliant device was in an unloaded configuration, the matrix [K] was measured by sequentially moving the six individual actuators of the robot, and recording the changes in the forces and torques (wrench increment) applied to the end-effector. In other words, the six independent twists chosen were the individual actuator displacements themselves. (This choice ensured the directions and locations of the respective twists, while at the same time it enabled easy monitoring of twist magnitude.) Twists were referenced so to describe the gripper's motion relative to the platform (force/torque sensor). The following steps were taken to find [K] in terms of $\mathbb{F}$:

i) While holding the last five actuators fixed, the first actuator was moved 133 encoder edges, which corresponded to 0.25° degrees of the first

joint. The twist and wrench increment were expressed in terms of $\mathbb{F}$ and recorded. The actuator was then returned to its original location, and the same command was given again. This process was performed ten times. The sum of the twist data was stored in $\hat{D}_1$, and the sum of the wrench data was stored in $\hat{w}_1$.

ii) Step (i) was repeated for joints 2 through 6 in turn, and this generated the twist data $\hat{D}_i$ and wrench data $\hat{w}_i$, $(i = 2, \ldots, 6)$. The following summarizes the displacements commanded to the actuators:

Actuator	Command	Corresponding Joint Command
1	133 4X encoder edges	0.25°
2	230	0.25
3	139	0.15
4	277	0.5
5	185	0.5
6	150	0.5

iii) The wrench data, $\hat{w}_1, \ldots, \hat{w}_6$ was assembled as columns in a 6x6 matrix [W], and the twist data, $\hat{D}_1, \ldots, \hat{D}_6$ was likewise assembled as the columns of a 6x6 matrix [D]. From (2.28), these matrices are related [W] = [K] [D], and therefore [K] was determined by inverting [D].

iv) In order to check for linearity, twists that were not used to determine [K] were commanded, and the actual measured wrench increments were compared to those computed using [K]. The twists commanded were in fact the six cardinal twists of $\mathbb{F}$. The end-effector

(force/torque sensor) was successively given small displacements in the x, y, and z directions, and then successive small rotations about the x, y, and z axes. These twists effected six wrench increments that corresponded respectively to scalar multiples of the six columns of [K].

v) In order to investigate the dependence of robot configuration on [K], the last joint was rotated 90°, and steps (i) – (iii) were repeated.

This represented a significant change in the robot configuration as seen from the force/torque sensor and spatial spring, since the first five joints all moved relative to them. A stiffness matrix that was measured in the second robot configuration was

$$[K] = \begin{bmatrix} 3.708 & -0.175 & -0.282 & -0.653 & 28.950 & 0.000 \\ 0.094 & 3.167 & -0.190 & -35.810 & 3.678 & -0.129 \\ -0.310 & -0.095 & 11.298 & -2.568 & 4.686 & -0.001 \\ -1.841 & -26.456 & -0.373 & 385.484 & -2.320 & 8.246 \\ 30.373 & -1.016 & -0.751 & -2.486 & 352.869 & 9.167 \\ 0.791 & 0.181 & 0.046 & -0.949 & 13.464 & 76.315 \end{bmatrix},$$

where the units are the same as before.

Finally, the following quantifies the repeatability of [K] (in terms of its 3x3 sub-matrices) by listing the average differences between all empirically determined [K]s. The first measure quantifies repeatability for [K]s measured while the robot remained in one of the two configurations. The second measure quantifies repeatability for [K]s measured while the robot was in either of the two configurations.

3x3 Sub-Matrix[11]	First Measure	Second Measure
upper-left	1%	8%
lower-left	1%	8%
upper-right	5%	13%
lower-right	4%	7%

2.3.2 Implementation of 6 DOC Wrench Control

Six degree-of-constraint wrench control was implemented on the experimental apparatus illustrated in Figure 2.6. A desired wrench was commanded to the KINESTATIC computer, which generated a corrective twist ($\hat{D}_C = [\delta\vec{x}_{OC};\ \delta\vec{\phi}_C]$) based on the control law,

$$\hat{D}_C = -G\,[K]^{-1}\,\hat{w}, \tag{2.33}$$

where $\hat{w} = [f_X,\ f_Y,\ f_Z;\ m_X,\ m_Y,\ m_Z]^T$ expressed in $\mathbb{F}$ is the difference between the desired and actual wrenches. (The scalar gain G was 0.03.) Equation (2.33) was performed approximately every 100 milliseconds, and each time it generated a new twist command.

Before commanding $\hat{D}_C$, it was necessary to first transform it into $\hat{D} = [\delta\vec{x}_O;\ \delta\vec{\phi}]$, where

$$\delta\vec{x}_O = [R_3]\ \delta\vec{x}_{OC} \quad \text{and} \quad \delta\vec{\phi} = [R_3]\ \delta\vec{\phi}_C, \tag{2.34}$$

and where $[R_3]$ is a 3x3 rotation matrix. The columns of $[R_3]$ are the direction cosines of the coordinate axes of $\mathbb{F}$ expressed in terms of a coordinate system G. The origins of $\mathbb{F}$ and G are the same, but the coordinate axes of G are parallel to

[11]The values given for the upper-left 3x3 matrix are valid for elements in the $3-12$ kg/cm range. The values given for the lower-left and upper-right 3x3 matrices are valid for elements with a magnitude in the $25-40$ kg range, and the values given for the lower-right 3x3 matrix are valid for elements in the $75-400$ kg-cm range.

those of the grounded system located at the shoulder of the GE Robot. (The coordinate system at the shoulder of the robot is labeled as $\mathbb{R}$.)

The result of (2.34) was communicated to the ROBOT computer, which controlled the position and orientation of the end-effector (force/torque sensor). The ROBOT computer performed its reverse and forward displacement kinematics every 20 milliseconds, and each time it communicated the results of the forward displacement analysis to the KINESTATIC computer. Figure 2.7 illustrates the response to a step input of $\hat{\mathrm{w}}_i = [0,\ -1\ \mathrm{kg},\ 4\ \mathrm{kg};\ 3\ \mathrm{kg\text{-}cm},\ 2\ \mathrm{kg\text{-}cm},\ 1\ \mathrm{kg\text{-}cm}]^{\mathrm{T}}$, given in terms of $\mathbb{F}$.

It is interesting to examine the response shown in Figure 2.7. This was a typical response – the largest errors being in m_{X} and m_{Y}. This is because these coordinates measured torques in the x and y directions that, taken together with their corresponding twists, constituted the stiffest twist-wrench combinations. (The coordinates of these twists are respectively the fourth and fifth columns of $[\mathrm{K}]^{-1}$.) Consequently, small errors in these twists were magnified as shown in Figure 2.7.

The investigator realized that placing bounds on these coordinates was necessary. For instance, -8 kg-cm$<m_{\mathrm{X}}<8$ kg-cm, -2 kg$<f_{\mathrm{X}}<2$ kg, and -5 kg$<f_{\mathrm{Z}}<5$ kg. This was necessary because the [K] measured in Section 2.3.1 and used in (2.33) was no longer accurate when the compliant device was under loads outside of these bounds. (These bounds also affected where a controlled force could be located. For example, a 1 kg force in the z-direction could not be accurately controlled if it had more than an 8 cm moment about the x-axis.)

A further examination of Figure 2.7 indicates that the lags were the same for all coordinates. (This was typical in the response plots of other, different

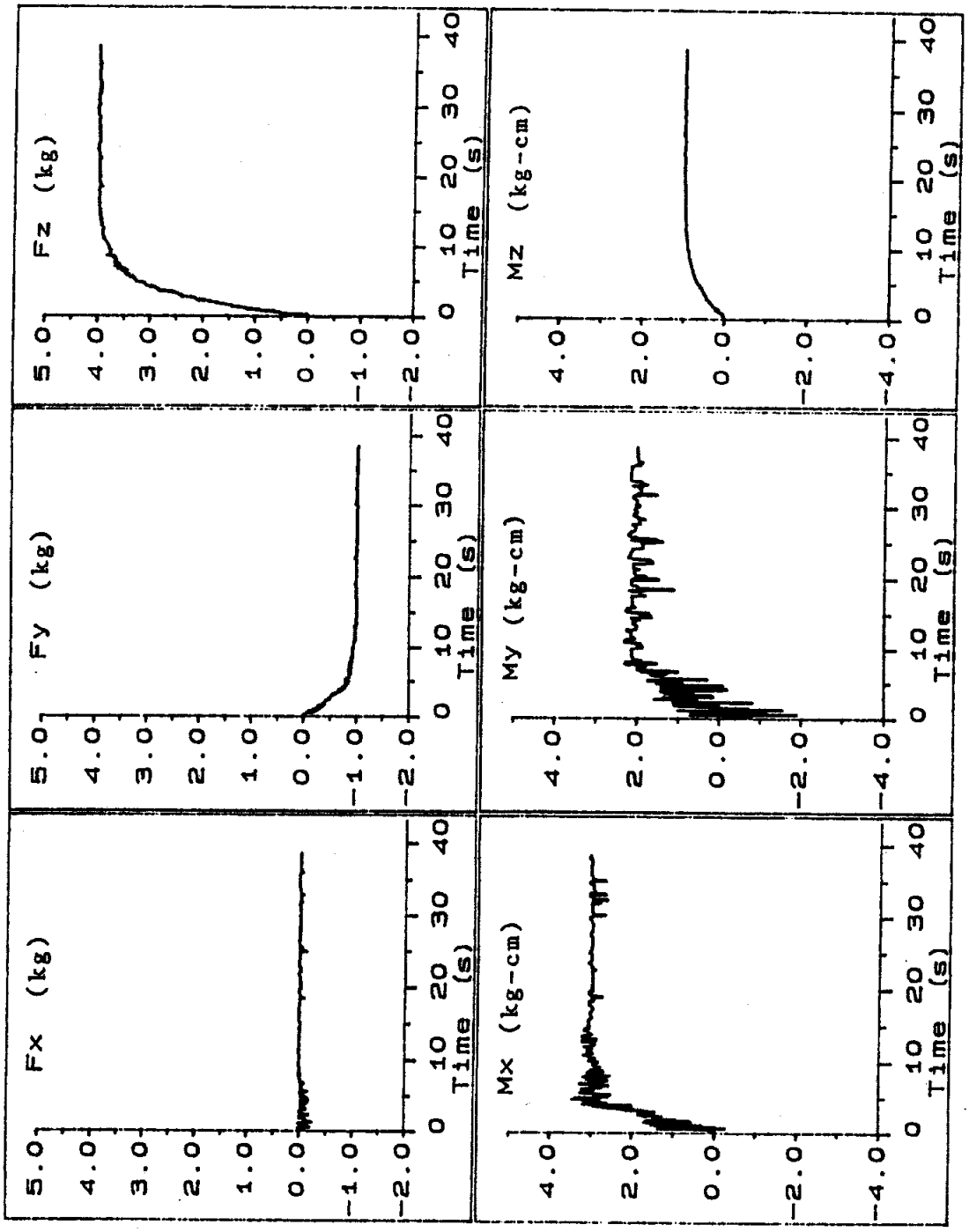
Fx (kg)
Fy (kg)
Fz (kg)
Mx (kg-cm)
My (kg-cm)
Mz (kg-cm)
Time (s)
5.0
4.0
3.0
2.0
1.0
0.0
-1.0
-2.0
-4.0
0
10
20
30
40

Figure 2.7

wrench step changes.) It is important to recognize this, because this proves the principle that at each instant the wrench error is nulled by the best corrective twist. In other words, the wrench error coordinates are nulled at the same pace.

2.3.3 Implementation of 5DOC/1DOF Kinestatic Control

Five degree-of-constraint/one degree-of-freedom kinestatic control was implemented on the experimental apparatus illustrated in Figure 2.8. The gripper was bolted to a slider (prismatic) joint that was in turn bolted to the level table. Relative to the slider, the gripper was positioned and oriented in a general way.

The twist of freedom of the gripper was $\hat{D}_b = [-1, 0, 0; 0, 0, 0]^T$, which was a translation in the negative x-direction of $\mathbb{G}$. (It was also a translation in the negative x-direction of $\mathbb{R}$, the grounded coordinate system located at the shoulder of the robot). The position of the slider was p, where $0<p<8$ cm.

Because of the bounds placed on controllable wrenches (See Section 2.3.2.), judicious choices had to be made regarding which wrenches of constraint to control. Three (m_1, m_2, and m_3) of the five constraints were torques whose directions were those specified by the coordinate axes of $\mathbb{F}$. The other two constraints (f_1 and f_2) were forces along respectively the y and z axes of $\mathbb{G}$. A desired wrench of constraint was conveniently expressed in terms of $\mathbb{F}$ by

$$\hat{w}_i = [a]\, \underline{f}_i, \tag{2.35}$$

where the columns of the 6x5 matrix [a] were the coordinates (in terms of $\mathbb{F}$) of the five constraint wrenches, and where $\underline{f}_i = [f_1, f_2, m_1, m_2, m_3]^T$.

While the five columns of [a] were the coordinates of the wrenches of constraints expressed in terms of $\mathbb{F}$, it was necessary to declare a sixth wrench that was independent of the wrenches of constraint. This was because the force/torque sensor reported a general wrench ($\hat{w}_s$ in terms of $\mathbb{F}$), and it was necessary to filter it

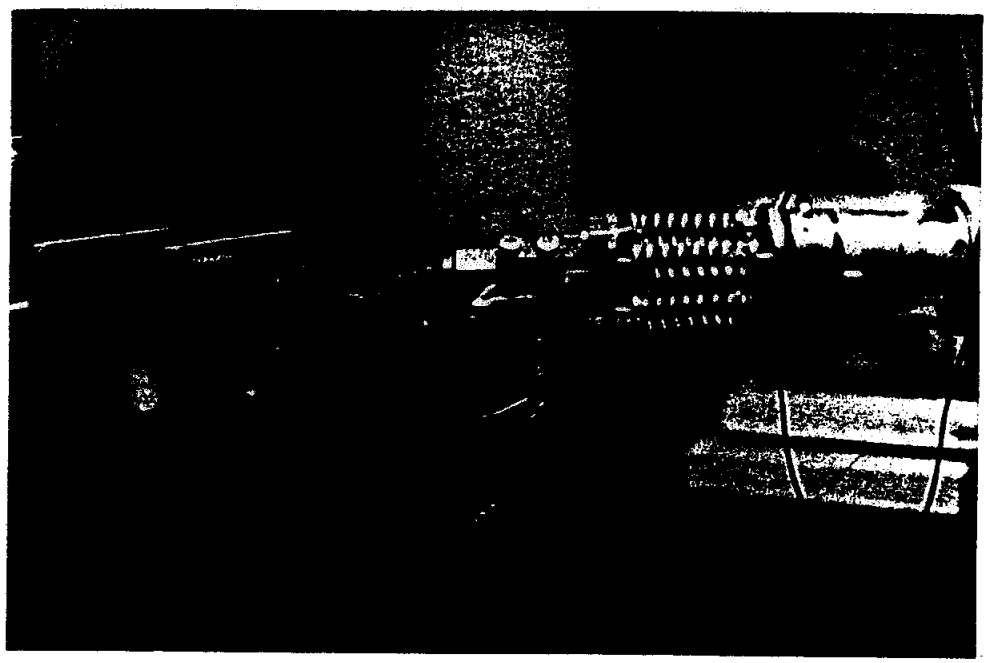

Figure 2.8

into an actual wrench of constraint ($\hat{w}_o$ in terms of $\mathbb{F}$). Accordingly, a sixth wrench was declared whose coordinates constituted first column of the 6x6 matrix [m], and

$$[m] = \begin{bmatrix} [R_3]^T & [0_3] \\ [0_3] & [1_3] \end{bmatrix}, \tag{2.36}$$

where the last five columns correspond to the five columns of [a]. The 3x3 sub-matrix $[R_3]$ was defined in (2.34), $[0_3]$ is a 3x3 zero matrix, and $[1_3]$ is a 3x3 identity matrix. The filtering of the sensed wrench was then accomplished by the relation,

$$\hat{w}_o = [m][i][m]^{-1}\, \hat{w}_s, \tag{2.37}$$

where [i] is a 6x6 identity matrix whose first element is replaced by a zero, and where $[m]^{-1} = [m]^T$. There were no working wrenches (the friction of the slider was considered minimal), and the assumption was made that the actual wrench of constraint ($\hat{w}_o$) was insensitive to which sixth wrench was chosen to be the first column of [m]. In other words, the first element of $[m]^T\, \hat{w}_s$ is small.

A desired set of five constraints (f_1, f_2, m_1, m_2, and m_3) together with a desired position (p) of the slider was commanded to the KINESTATIC computer, which generated a corrective twist ($\hat{D} = [\delta\vec{x}_o;\ \delta\vec{\phi}]$) based on the control law:

$$\hat{D} = G_1 \delta p\, \hat{D}_b + G_2\, \hat{D}_c, \tag{2.38}$$

where $\hat{D}_c$ is the coordinates of the twist of compliance expressed in G, where δp is an error in slider position, and where the twist and wrench gains are G_1 and G_2. The coordinates $\hat{D}'_c$ of the twist of compliance expressed in $\mathbb{F}$ was calculated from

$$\hat{D}'_c = -[K]^{-1}\, (\hat{w}_i - \hat{w}_o), \tag{2.39}$$

where $\hat{w}_i$ is from (2.35) and $\hat{w}_o$ is from (2.37). The coordinates $\hat{D}'_c$ were

transformed into $\hat{D}_c$ by (2.34) where $\hat{D}_c$ is replaced by $\hat{D}'_c$ and where $\hat{D}$ is replaced by $\hat{D}_c$. Equation (2.38) was calculated approximately every 100 milliseconds, and the result was communicated to the ROBOT computer.

Representative response plots of this system are given in Figures $2.9-11$. Figure 2.9 illustrates the nulling of a wrench of constraint for initially loaded gripper. It is important to recognize that for this experiment, the twist gain was set to zero, $G_1 = 0$. $(G_2 = 0.03.)$ This further illustrates that the twist of compliance used to null the wrench of constraint error was the best twist, since it did not move the slider significantly while nulling a wrench of constraint. (Figure 2.9 shows constraint response curves with the same type of lagging that was present in the 6 DOC wrench control, and also, it shows that the displacement of the slider was only minimal with some drift.)

Figure 2.10 illustrates the response of the system that was given a displacement command $p = 5$ cm, and a constraint command, $f_1 = f_2 = m_1 = m_2 = m_3 = 0.0$. The system accomplished the move in 40 seconds, and the constraint forces and torques were suppressed throughout the move. $(G_1 = 0.008)$

Figure 2.11 illustrates the response of the system that was initially given a step command of $p = 4.0$, $f_1 = 0.$, $f_2 = -1$ kg, $m_1 = 4$ kg-cm, $m_2 = -5$ kg-cm, $m_3 = 2$ kg-cm. Midway through the response, the displacement command was changed to $p = 7.0$ cm. The constraint response curves continued to exhibit lags that were similar, which is indicative of the fact that the correct twist of compliance was commanded at every instant.

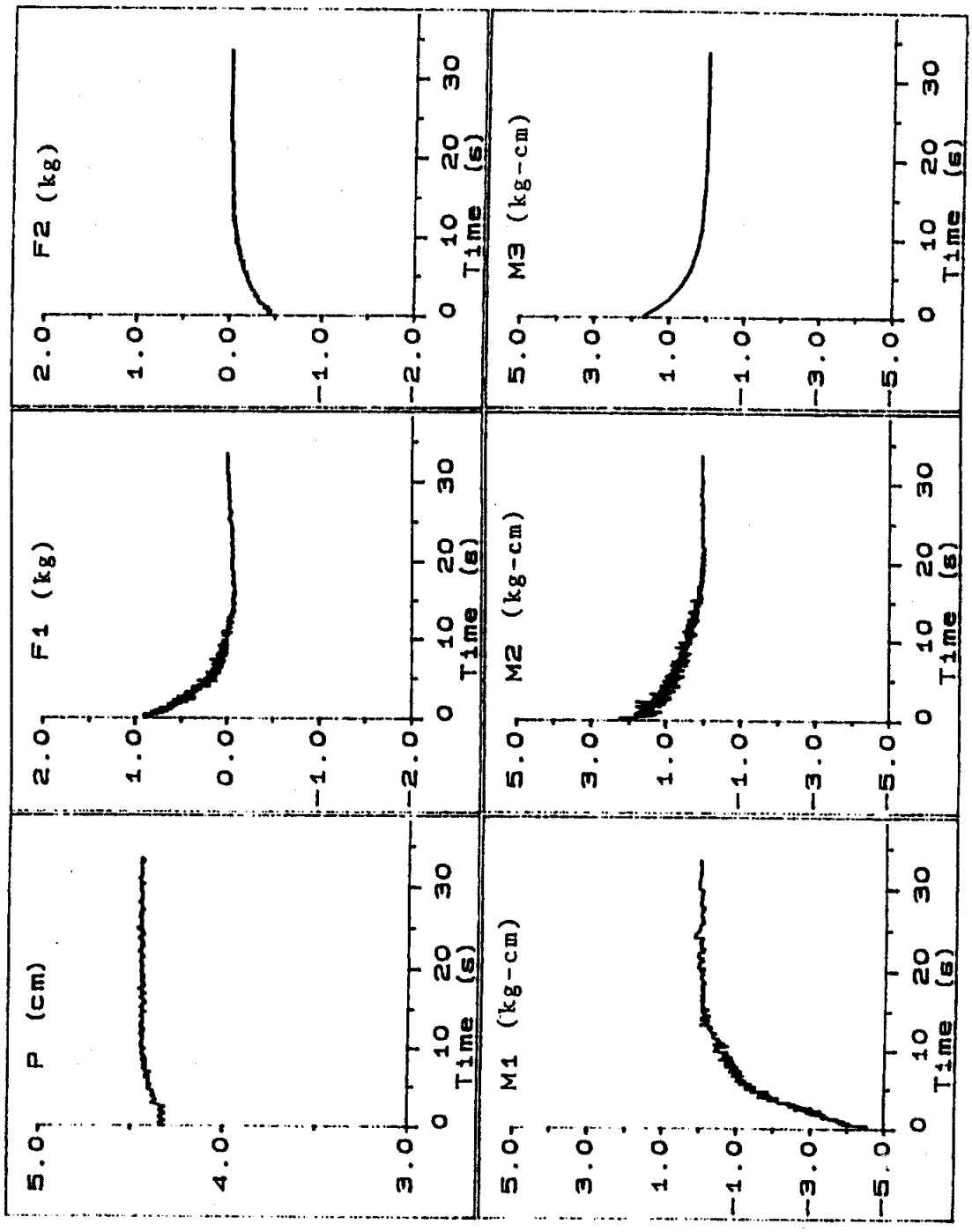

Figure 2.9

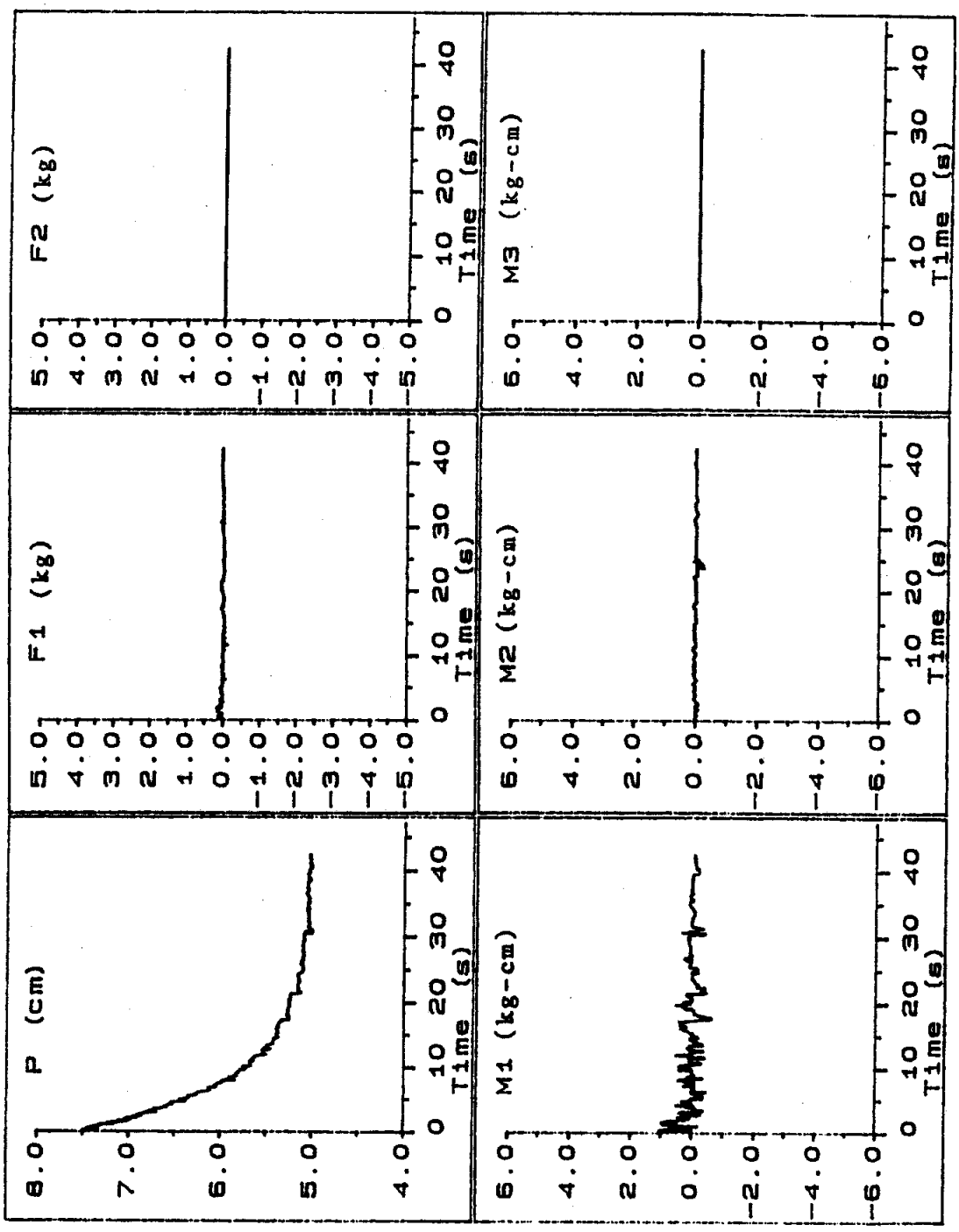

Figure 2.10

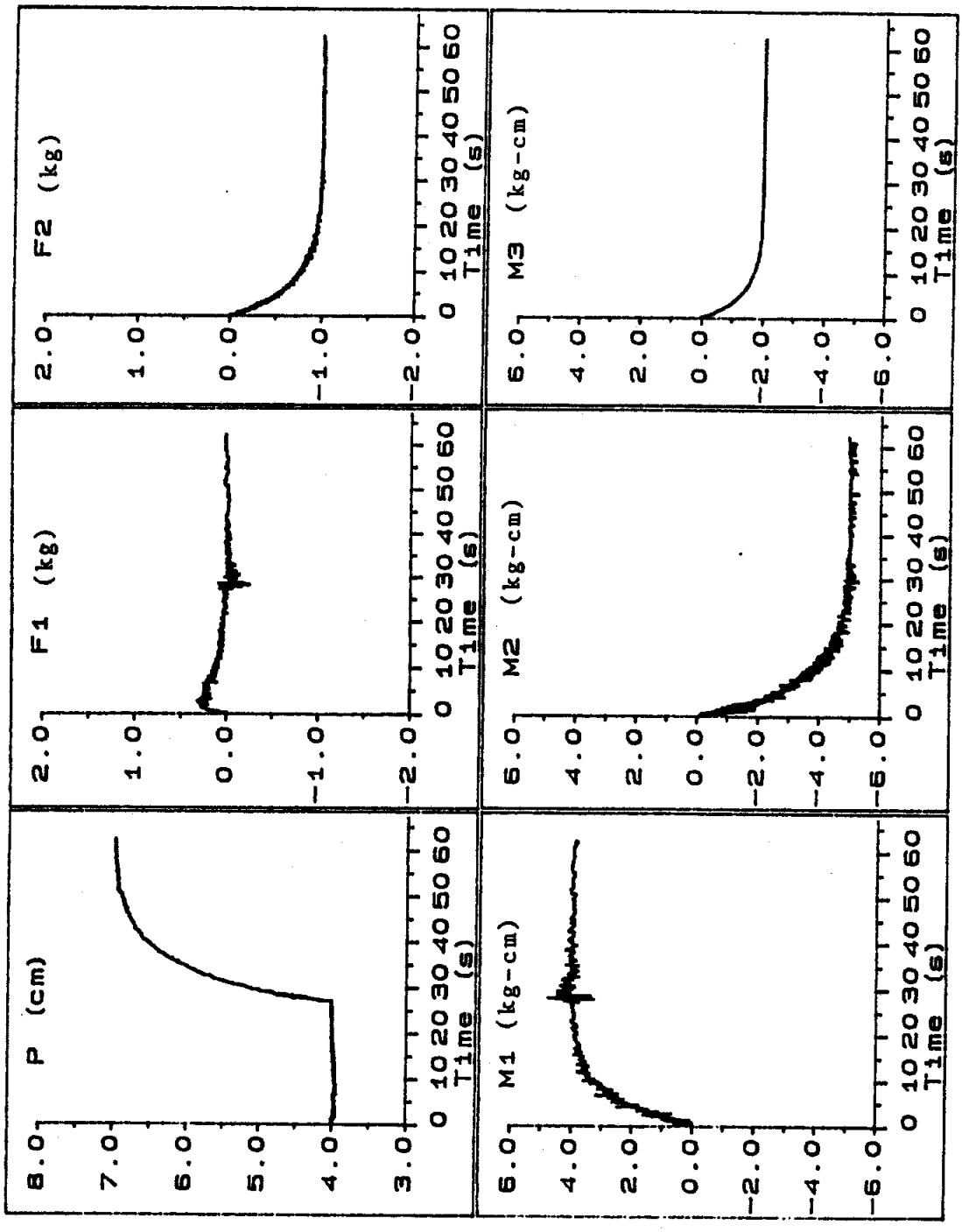

Figure 2.11

CHAPTER 3
GLOBAL STIFFNESS MODELING OF A CLASS OF SIMPLE COMPLIANT COUPLINGS

Stiffness is a geometric mapping, one that transforms a differential displacement (twist) into an incremental change in force (wrench). In order to analyze stiffness, one must first define two rigid bodies and a compliant coupling that connects them. Thus, by the mapping of stiffness, a differential displacement (twist) of one body relative to the other is transformed into an incremental change in the force (wrench) that one body applies to the other through the coupling.

The word "global" is introduced here to denote that the mapping of stiffness changes and that it is a function of the configuration of the compliant coupling. Therefore, a global stiffness model defines the correct mapping of stiffness for a compliant coupling even when it is displaced far from an unloaded configuration. This new concept in modeling supersedes a previously accepted and widely accepted modeling technique that requires a compliant coupling to remain near an unloaded configuration. (Such a restriction was specified in Chapter 1.) The work of Dimentberg [1965] remains the standard for the stiffness modeling of a compliant coupling that stays near its unloaded configuration. His model results in a mapping of stiffness that is represented by a constant and symmetric stiffness matrix.

In this chapter, the exact position-and-orientation-dependent stiffness mapping is derived for a simple compliant coupling that is made up of a number of translational springs acting in-parallel. A "simple compliant coupling" is defined in

the general case as a frictionless and massless mechanism having prismatic joints restricted by translational springs and revolute joints restricted by torsional springs. Such a coupling should be configured with other unrestricted joints so that when all of the springs are removed from their joints, the coupling transmits no forces or torques between the two bodies which it connects. (Three examples are given in this chapter.)

The word "simple" is used to denote that the stiffness mapping of such a coupling is readily obtained from simple geometrical constructions and simple scalar deflection relations (for example, $\delta f = k\ \delta x$, which relates the change of force δf in a translational spring with stiffness k to a spring displacement δx). The compliant couplings given in Figures 1.1, 1.2, 2.1, and 2.4 are considered simple, but on the other hand, the coupling used in the implementation (See Figure 2.6) is considered general.

The impetus for these investigations evolved from the recurrence of asymmetries in experimentally determined stiffness matrices. While Chapter 1 introduced the concept of replacing a general coupling with a 3-3 Stewart Platform (simple compliant coupling) model, it also restricted itself to symmetric mappings. In that chapter, the disclaimer was made that the coupling (as well as its model) should remain virtually near an unloaded configuration, and this implies a symmetric stiffness mapping. However, when stiffness mappings of real couplings were obtained by direct measurement (See Chapter 2.), they were asymmetric. (In Chapter 2, the spatial spring of the experimental apparatus was nearly unloaded, and [K] was experimentally determined to be asymmetric in many entries.)

These asymmetries require the theory of Kinestatic Control (See Chapter 1.) to use asymmetric stiffness matrices. Chapter 1 established the theme of this

dissertation: "A knowledge of the mapping of spatial stiffness is an essential ingredient in establishing the control of both the force and the displacement of a partially constrained rigid body." That the mapping is asymmetric does not in any way detract from the proposed theory, and the work detailed here is meant to extend it. Noteworthy achievements presented in this chapter include what is believed to be the clearest and simplest possible expressions for the global stiffnesses of three simple compliant couplings as well as a clear indication of how and where such mappings lose their symmetry.

3.1 Planar Two-Dimensional Spring

Figure 3.1 illustrates two translational springs[1] acting in-parallel, one grounded at pivot point A and the other grounded at pivot point B. The other ends of the two springs are connected and pivoted at point P, which is located with Cartesian coordinates x and y. The two springs taken together as a single unit define a *planar two-dimensional spring.* The spring is two-dimensional because two independent forces act in its translational springs, and it is planar since the forces remain in a plane.

An external force $\vec{f} = f_x \vec{i} + f_y \vec{j}$ is applied to the two-dimensional spring at P. The external force is in static equilibrium with the forces acting in the springs, and this system remains in static equilibrium as the point P displaces. To accommodate this, the external force changes as point P moves. It is now desired to find the mapping of stiffness,

[1]Either of the springs can be thought of as acting in the prismatic joint of a revolute-prismatic-revolute serial chain. Two such serial chains act in-parallel to define the simple compliant coupling shown in Figure 3.1.

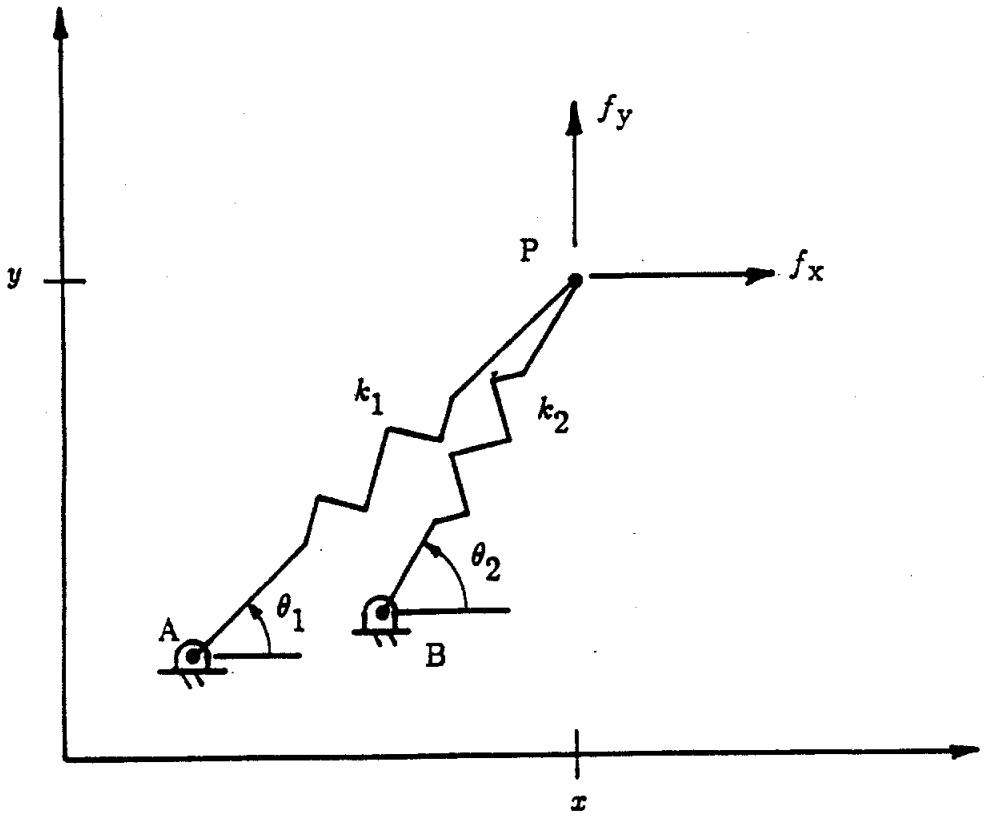

Figure 3.1

$$\begin{bmatrix} \delta f_x \\ \delta f_y \end{bmatrix} = \begin{bmatrix} k_{11} & k_{12} \\ k_{21} & k_{22} \end{bmatrix} \begin{bmatrix} \delta x \\ \delta y \end{bmatrix}, \tag{3.1}$$

where $\delta\vec{f} = \delta f_x \vec{i} + \delta f_y \vec{j}$ is a small increment in $\vec{f}$ that is related via k_{ij} to the small displacement $\delta\vec{d} = \delta x \vec{i} + \delta y \vec{j}$ of point P. Based on the locations of points A, B, and P, the lengths l_1 and l_2 and angles θ_1 and θ_2 can be computed. The spring constants k_1 and k_2 and free lengths l_{o1} and l_{o2} are considered known.

In order to obtain (3.1), it is necessary first to express the finite forces that are applied to the springs by the external force:

$$\begin{bmatrix} f_x \\ f_y \end{bmatrix} = \begin{bmatrix} c_1 & c_2 \\ s_1 & s_2 \end{bmatrix} \begin{bmatrix} k_1 (l_1 - l_{o1}) \\ k_2 (l_2 - l_{o2}) \end{bmatrix}, \tag{3.2}$$

where $c_i = \cos(\theta_i)$ and $s_i = \sin(\theta_i)$, and where k_i and $(l_i - l_{oi})$ are respectively the positive non-zero spring constant and the difference between the current and free lengths of the i^{th} spring. A complete differential of (3.2) gives

$$\begin{bmatrix} \delta f_x \\ \delta f_y \end{bmatrix} = \begin{bmatrix} c_1 & c_2 \\ s_1 & s_2 \end{bmatrix} \begin{bmatrix} k_1\, \delta l_1 \\ k_2\, \delta l_2 \end{bmatrix} + \begin{bmatrix} -s_1 & -s_2 \\ c_1 & c_2 \end{bmatrix} \begin{bmatrix} k_1 (l_1 - l_{o1})\, \delta\theta_1 \\ k_2 (l_2 - l_{o2})\, \delta\theta_2 \end{bmatrix}, \tag{3.3}$$

where δf_x and δf_y are deviations away from f_x and f_y, where δl_i is a deviation of the i^{th} spring extending from its current length, and where $\delta\theta_i$ is a deviation of θ_i.

The dimensionless parameters $\rho_1 = l_{o1}/l_1$ and $\rho_2 = l_{o2}/l_2$ are now introduced, whose respective deviations from unity give indications of how far the two-dimensional spring is away from an unloaded configuration. The scalar ρ_i is positive; when $\rho_i < 1$, the i^{th} spring is extended, and when $\rho_i > 1$, the i^{th} spring is compressed. Substituting ρ_i into (3.3) yields

$$\begin{bmatrix} \delta f_x \\ \delta f_y \end{bmatrix} = \begin{bmatrix} c_1 & c_2 \\ s_1 & s_2 \end{bmatrix} \begin{bmatrix} k_1\, \delta l_1 \\ k_2\, \delta l_2 \end{bmatrix} + \begin{bmatrix} -s_1 & -s_2 \\ c_1 & c_2 \end{bmatrix} \begin{bmatrix} k_1\,(1-\rho_1)\, l_1\, \delta\theta_1 \\ k_2\,(1-\rho_2)\, l_2\, \delta\theta_2 \end{bmatrix}. \tag{3.4}$$

In order to determine (3.1), it is necessary to make substitutions of δx and δy for δl_i and $l_i\ \delta\theta_i$. (Such a substitution ensures a compatible set of the four differentials, δl_i and $l_i \delta\theta_i$, i = 1, 2.) Prior to the substitution, (3.4) is rearranged into the form,

$$\begin{bmatrix} \delta f_x \\ \delta f_y \end{bmatrix} = \begin{bmatrix} c_1 & c_2 \\ s_1 & s_2 \end{bmatrix} \begin{bmatrix} k_1 & 0 \\ 0 & k_2 \end{bmatrix} \begin{bmatrix} \delta l_1 \\ \delta l_2 \end{bmatrix}$$
$$+ \begin{bmatrix} -s_1 & -s_2 \\ c_1 & c_2 \end{bmatrix} \begin{bmatrix} k_1\,(1-\rho_1) & 0 \\ 0 & k_2\,(1-\rho_2) \end{bmatrix} \begin{bmatrix} l_1\, \delta\theta_1 \\ l_2\, \delta\theta_2 \end{bmatrix}, \tag{3.5}$$

which facilitates the substitutions that are necessary.

Figure 3.2 illustrates how the connection point may displace $\delta\vec{d}$. This is projected onto two normalized directions for the first spring, which are the direction of the spring ($\vec{s}_1 = c_1\,\vec{i} + s_1\,\vec{j}$) and the direction of its derivative with respect to θ_1 ($\delta\vec{s}_1 = -s_1\,\vec{i} + c_1\,\vec{j}$). The results of these projections yield respectively the desired translations: δl_1 and $l_1\ \delta\theta_1$. Repeating for the second spring and incorporating the overall results into (3.5) provides the desired (3.1) where

$$\begin{bmatrix} k_{11} & k_{12} \\ k_{21} & k_{22} \end{bmatrix} = \begin{bmatrix} c_1 & c_2 \\ s_1 & s_2 \end{bmatrix} \begin{bmatrix} k_1 & 0 \\ 0 & k_2 \end{bmatrix} \begin{bmatrix} c_1 & s_1 \\ c_2 & s_2 \end{bmatrix} +$$
$$+ \begin{bmatrix} -s_1 & -s_2 \\ c_1 & c_2 \end{bmatrix} \begin{bmatrix} k_1\,(1-\rho_1) & 0 \\ 0 & k_2\,(1-\rho_2) \end{bmatrix} \begin{bmatrix} -s_1 & c_1 \\ -s_2 & c_2 \end{bmatrix}. \tag{3.6}$$

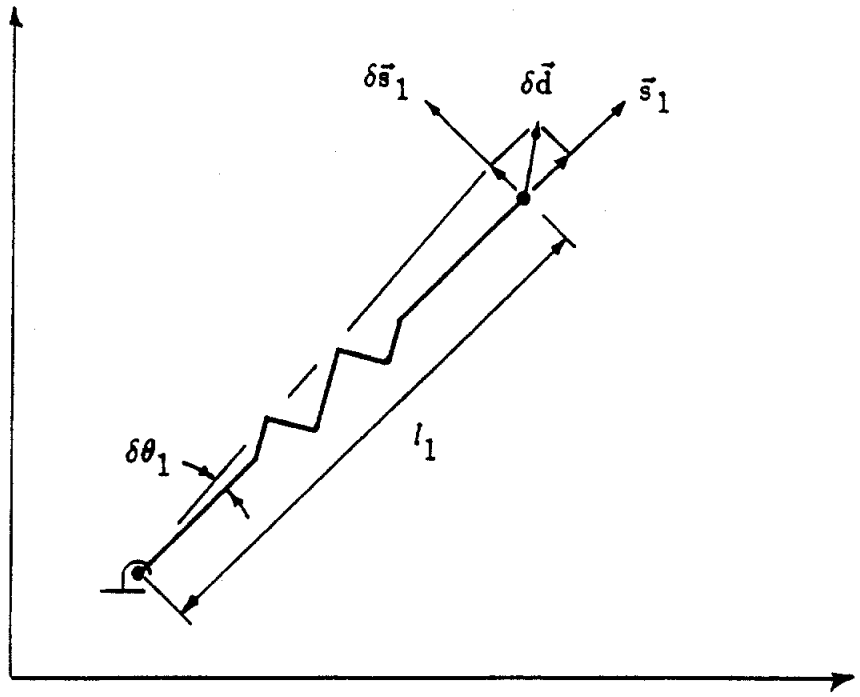

Figure 3.2

Equation (3.1) may be more compactly written in the form,

$$\delta\vec{f} = [K]\ \delta\vec{d}, \tag{3.7}$$

where from (3.6),

$$[K] = [j]\ [k_i]\ [j]^T + [\delta j]\ [k_i(1-\rho_i)]\ [\delta j]^T, \tag{3.8}$$

where [j] is the formal instantaneous static Jacobian relating the differential change in the scalar spring forces to $\delta\vec{f}$, where $[\delta j]$ is its derivative with respect to θ_1 and θ_2, and where $[k_i]$ and $[k_i(1-\rho_i)]$ are the 2x2 diagonal matrices. (When $\rho_1 = \rho_2 = 1$, the (3.8) spring matrix [K] reduces to the Chapter 2 [K], which was determined for the wheel-spring-platform arrangement in the unloaded configuration.)

It is useful to make the following observations on the 2x2 spring matrix [K] defined by (3.8):

i) The matrix [K] is the sum of two symmetric matrices and therefore is always symmetric.

ii) In general, the matrix [K] is not positive-definite. It is positive definite whenever the springs are both extended ($\rho_i \leq 1,\ i = 1,\ 2$). Otherwise, it may be indefinite.

iii) The three independent elements of [K] are specified by ten parameters. (Three points, two spring constants, and two free lengths.) Therefore, an ∞^7 of two-dimensional springs have the same [K].

iv) For an unloaded two-dimensional spring, $[K] = [j]\ [k_i]\ [j]^T$, since $\rho_i = 1$ in (3.8). Because [K] is, in general, the sum of two matrices of this form (See (3.8).), the initially loaded two-dimensional spring shown in Figure 3.1 is equivalent to a *pair of unloaded two-dimensional springs*

acting in-parallel, one having the stiffness matrix $[j]\,[k_i]\,[j]^T$ and the other having the stiffness matrix $[\delta j]\,[k_i(1-\rho_i)]\,[\delta j]^T$. Figure 3.3 shows such a pair of unloaded two-dimensional springs acting in-parallel – four translational springs with constants k_1, k_2, $k_1(1-\rho_1)$, and $k_2(1-\rho_2)$.

v) The matrix [K] may be non-singular even though [j] is singular. (Consider the example illustrated in Figure 3.4.)

vi) The matrix [K] may be singular when [j] is non-singular. (Consider the example illustrated in Figure 3.5 with either $k_1 + k_2(1-\rho_2) = 0$ or $k_2 + k_1(1-\rho_1) = 0$.)

vii) The matrix [K] may be negative-definite. (Consider Figure 3.5 with both $k_1 + k_2(1-\rho_2)<0$ and $k_2 + k_1(1-\rho_1)<0$.)

3.2 Planar Three-Dimensional Spring

Figure 3.6 illustrates a moveable platform connected to ground by three translational springs[2] acting in-parallel. The three springs taken together as a single unit define a *planar three-dimensional spring.* The spring is three-dimensional since three independent forces act in its translational springs, and it is planar because these forces remain in the same plane.

A resultant external force f with coordinates $\hat{w}_o = [f_x, f_y; m_o]^T$ acts on the moveable platform along line $\$_o$. The external force is in static equilibrium with the three spring forces, and the system remains in static equilibrium as the moveable platform rotates $\delta\phi$ about point R. To accommodate this, the external force changes as the moveable platform moves, and its change is defined as a *force increment.* (The force increment δf has coordinates $\hat{w} = [\delta f_x, \delta f_y; \delta m_o]^T$ and acts

[2]Each of the springs can be thought of as acting in the prismatic joint of a revolute-prismatic-revolute serial chain. Three such serial chains act in-parallel to define the simple compliant coupling shown in Figure 3.6.

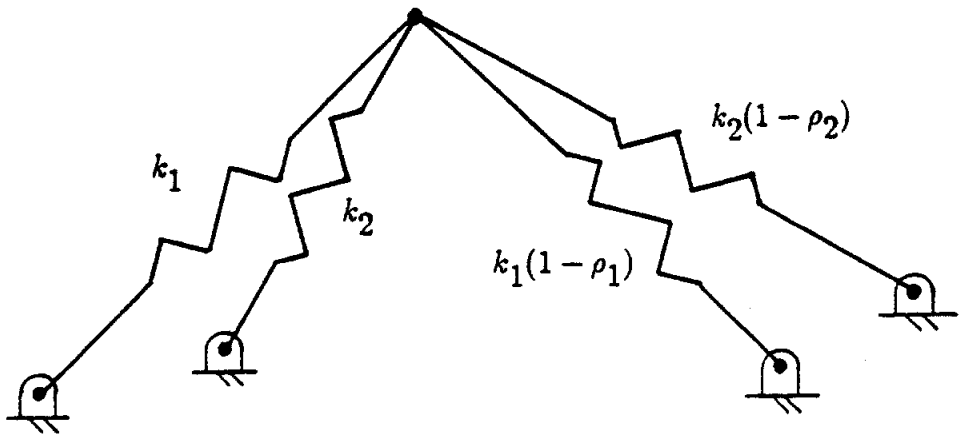

Figure 3.3

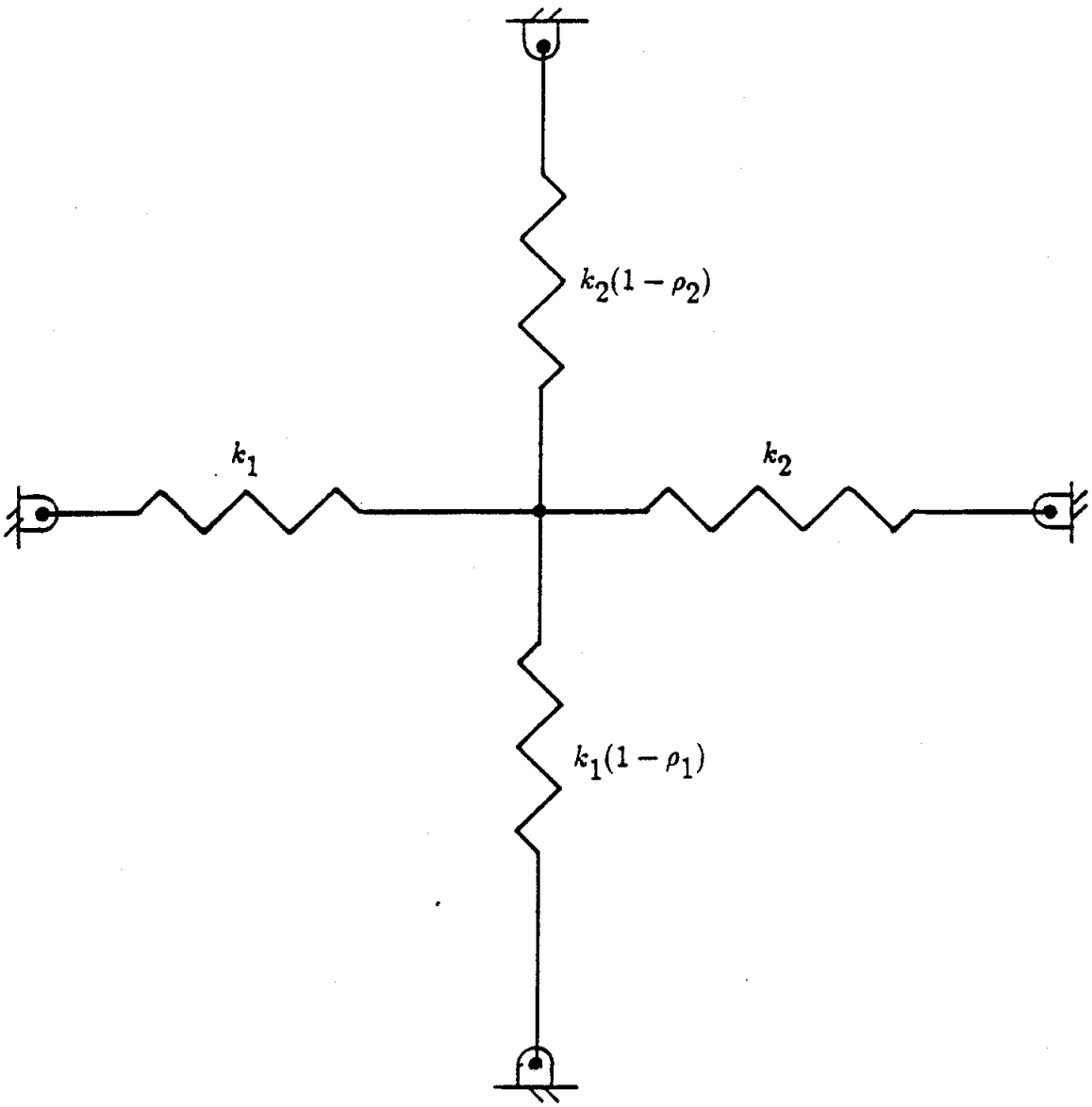

Figure 3.4

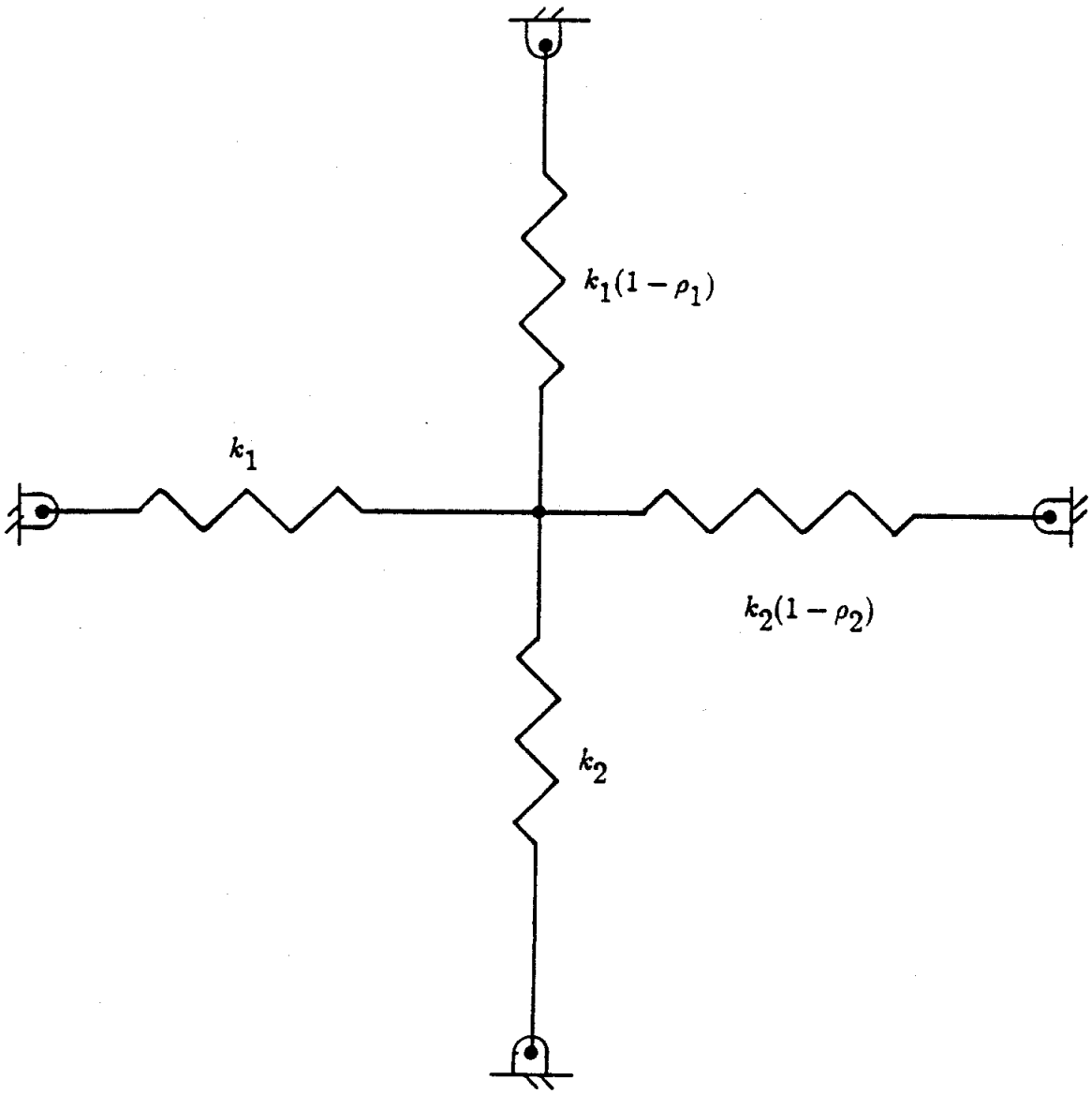

Figure 3.5

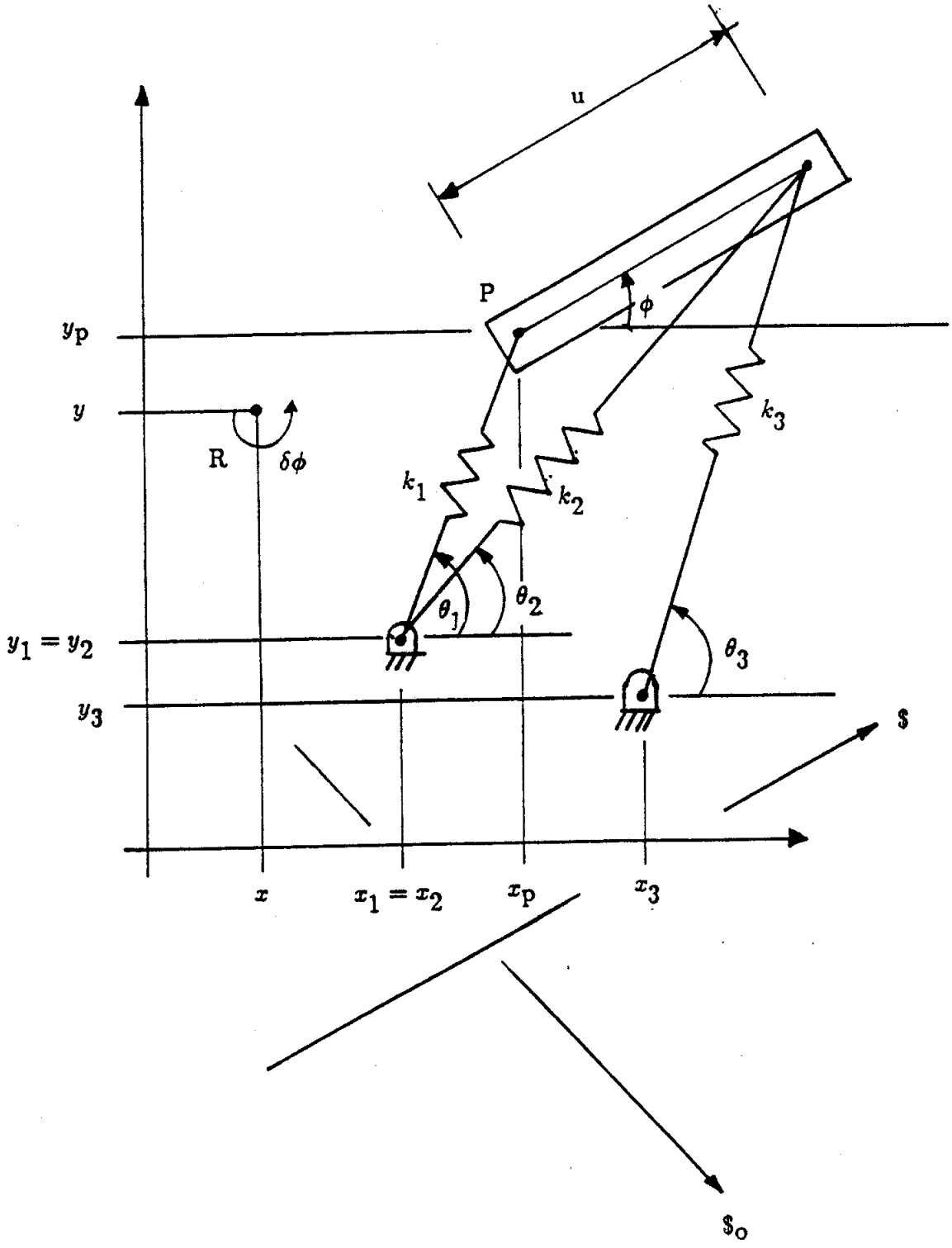
u
P
ϕ
y_p
y
R
$\delta\phi$
k_1
k_2
k_3
θ_1
θ_2
θ_3
$y_1 = y_2$
y_3
x
$x_1 = x_2$
x_p
x_3
$
$_o

Figure 3.6

along a line \$.) The coordinates of a force are scalar multiples of normalized line coordinates: $f\ \hat{\mathrm{s}}$, where f is the magnitude of the force (δf for a force increment), and where coordinates $\hat{\mathrm{s}} = [c,\ s;\ r]^{\mathrm{T}}$ are normalized coordinates of the line of the force (c and s are the direction cosines of the line, and r is the signed perpendicular distance of the line from the origin).

The moveable platform is located by the Cartesian coordinates x_{p} and y_{p} of point P together with an orientation angle ϕ. A differential rotation $\delta\phi$ of the moveable platform about point R is represented with twist coordinates,

$$\hat{\mathrm{D}} = [\delta x,\ \delta y;\ \delta\phi]^{\mathrm{T}} = [\delta\phi\ y,\ -\delta\phi\ x;\ \delta\phi]^{\mathrm{T}} = \delta\phi[\ y, -x;\ 1]^{\mathrm{T}} = \delta\phi\ \hat{\mathrm{S}}, \qquad [(2.14)]$$

where x, y are the Cartesian coordinates of the instant center R, and where coordinates $\hat{\mathrm{S}}$ are defined as the normalized coordinates of point R. (The coordinates $\hat{\mathrm{S}}$ can also be thought of as the coordinates of the line perpendicular to the plane of motion at point R, and accordingly, the platform can be thought to rotate $\delta\phi$ about this line.)

It is instructive to consider that the two twist coordinates δx and δy also specify the displacement of a point in the moveable platform which is coincident with the origin. Consider that such a point displaces

$$\delta\vec{\mathrm{d}}_{\mathrm{o}} = \delta x\ \vec{\mathrm{i}} + \delta y\ \vec{\mathrm{j}}\ = \delta\phi\ y\ \vec{\mathrm{i}} - \delta\phi\ x\ \vec{\mathrm{j}}.$$

For completeness, also consider that point P displaces

$$\delta\vec{\mathrm{d}}_{\mathrm{p}} = (\delta x - \delta\phi\ y_{\mathrm{p}})\ \vec{\mathrm{i}} + (\delta y + \delta\phi\ x_{\mathrm{p}})\ \vec{\mathrm{j}} = \delta\phi(y - y_{\mathrm{p}})\ \vec{\mathrm{i}} - \delta\phi(x - x_{\mathrm{p}})\ \vec{\mathrm{j}}. \qquad (3.9)$$

Now, given that the moveable platform rotates $\delta\phi$ about point R, it is required to determine the stiffness mapping,

$$\begin{bmatrix} \delta f_{\mathrm{x}} \\ \delta f_{\mathrm{y}} \\ \delta m_{\mathrm{o}} \end{bmatrix} = \begin{bmatrix} k_{11} & k_{12} & k_{13} \\ k_{21} & k_{22} & k_{23} \\ k_{31} & k_{32} & k_{33} \end{bmatrix} \begin{bmatrix} \delta x \\ \delta y \\ \delta\phi \end{bmatrix}, \qquad (3.10)$$

where $\hat{w} = [\delta f_x,\ \delta f_y;\ \delta m_o]^T$ denotes the change in resultant force that is related via k_{ij} to the changes $\hat{D} = [\delta x,\ \delta y;\ \delta\phi]^T$. Based on x_p, y_p, and ϕ and the locations of the fixed pivots, the lengths l_1, l_2, and l_3 and angles θ_1, θ_2, and θ_3 can be calculated. The spring constants k_1, k_2, and k_3 and free lengths l_{o1}, l_{o2}, and l_{o3} are considered known.

The mapping of stiffness (3.10) is global. The simple compliant coupling of Figure 3.6 is not restricted to being near an unloaded configuration as it was in Section 2.2.1. (The platform of Section 2.2.1 is replaced here by ground, while the gripper is replaced by the moveable platform.) Nevertheless, (3.10) represents the same kind of mapping as did (2.17), i. e. one which relates a point R of rotation to a line $ of an increment of force.

In order to determine the mapping of stiffness (3.10), it is necessary to first express the finite forces that the resultant $\hat{w}_o$ applies to the springs:

$$\begin{bmatrix} f_x \\ f_y \\ m_o \end{bmatrix} = \begin{bmatrix} c_1 & c_2 & c_3 \\ s_1 & s_2 & s_3 \\ r_1 & r_2 & r_3 \end{bmatrix} \begin{bmatrix} k_1\,(l_1 - l_{o1}) \\ k_2\,(l_2 - l_{o2}) \\ k_3\,(l_3 - l_{o3}) \end{bmatrix}, \tag{3.11}$$

where the columns of the 3x3 matrix contain the normalized homogeneous line coordinates ($\hat{s}_1$, $\hat{s}_2$, and $\hat{s}_3$) of the lines ($\$_1$, $\$_2$, and $\$_3$) of the three extensible legs shown in Figure 3.6, and where $k_i\,(l_i - l_{oi})$ is the leg force due to the extension of the i^{th} spring. For the line coordinates r_i, i = 1, 2, and 3,

$$r_i = x_i\, s_i - y_i\, c_i, \tag{3.12}$$

where $s_i = \sin(\theta_i)$, $c_i = \cos(\theta_i)$, and where x_i and y_i are the Cartesian coordinates of the fixed pivot point of the i^{th} spring. For Figure 3.6, all x_i and y_i are constants, and $x_1 = x_2$ and $y_1 = y_2$.

A complete differential of (3.11) is an extension of (3.3) that assumes the form,

$$\begin{bmatrix} \delta f_x \\ \delta f_y \\ \delta m_o \end{bmatrix} = \begin{bmatrix} c_1 & c_2 & c_3 \\ s_1 & s_2 & s_3 \\ r_1 & r_2 & r_3 \end{bmatrix} \begin{bmatrix} k_1\,\delta l_1 \\ k_2\,\delta l_2 \\ k_3\,\delta l_3 \end{bmatrix} + \begin{bmatrix} -s_1 & -s_2 & -s_3 \\ c_1 & c_2 & c_3 \\ \delta r_1 & \delta r_2 & \delta r_3 \end{bmatrix} \begin{bmatrix} k_1\,(l_1 - l_{o1})\,\delta\theta_1 \\ k_2\,(l_2 - l_{o2})\,\delta\theta_2 \\ k_3\,(l_3 - l_{o3})\,\delta\theta_3 \end{bmatrix}, \tag{3.13}$$

where in the 3x3 differential matrix, for i = 1, 2, and 3,

$$\delta r_i = x_i\, c_i + y_i\, s_i. \tag{3.14}$$

While the i^{th} column of the first 3x3 matrix in (3.13) corresponds to the normalized line coordinates $\hat{s}_i$ of the line $\$_i$ of the i^{th} spring, it is of the utmost importance to consider the i^{th} column of the second 3x3 differential matrix as the normalized line coordinates $\delta\hat{s}_i$ of the line $\delta\$_i$, which is the derivative of $\$_i$ with respect to θ_i. See Figure 3.7, which clearly shows that $\delta\$_1$ is perpendicular to $\$_1$ and that both pass through the first fixed pivot point. ($\delta\$_2$ and $\delta\$_3$ are also perpendicular to $\$_2$ and $\$_3$ respectively, and they also pass through their respective fixed pivot points.) Therefore, an increment of $\delta\theta_i$ from θ_i gives the $\theta_i + \delta\theta_i$ line coordinates of the i^{th} spring line:

$$\hat{s}_i(\theta_i + \delta\theta_i) = \hat{s}_i(\theta_i) + \delta\hat{s}_i(\theta_i)\,\delta\theta_i, \tag{3.15}$$

in the limit as $\delta\theta_i \to 0$.

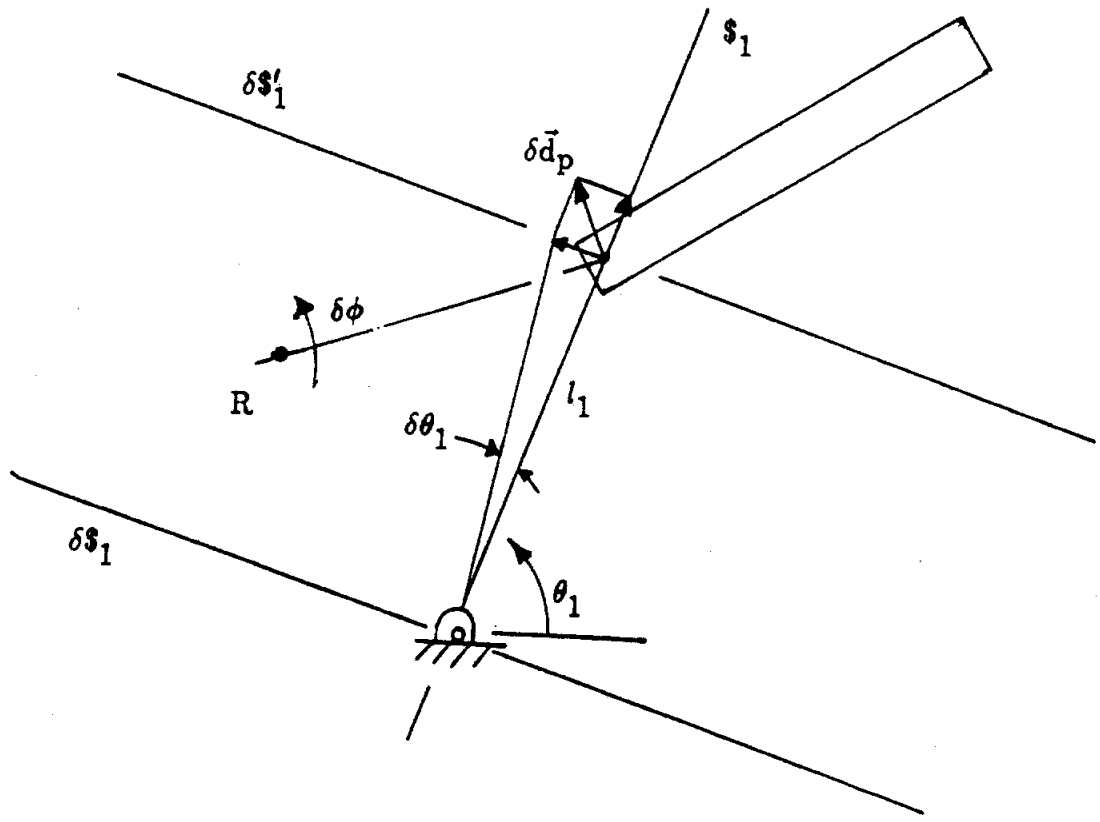
$\delta\$_1'$
$\$_1$
$\delta\vec{d}_p$
$\delta\phi$
R
$\delta\theta_1$
l_1
$\delta\$_1$
θ_1

Figure 3.7

Making the substitutions of $\rho_i = l_{oi}/l_i$ into (3.13) and rearranging yields

$$\begin{bmatrix} \delta f_x \\ \delta f_y \\ \delta m_o \end{bmatrix} = \begin{bmatrix} c_1 & c_2 & c_3 \\ s_1 & s_2 & s_3 \\ r_1 & r_2 & r_3 \end{bmatrix} \begin{bmatrix} k_1 & 0 & 0 \\ 0 & k_2 & 0 \\ 0 & 0 & k_3 \end{bmatrix} \begin{bmatrix} \delta l_1 \\ \delta l_2 \\ \delta l_3 \end{bmatrix} +$$

$$\begin{bmatrix} -s_1 & -s_2 & -s_3 \\ c_1 & c_2 & c_3 \\ \delta r_1 & \delta r_2 & \delta r_3 \end{bmatrix} \begin{bmatrix} k_1(1-\rho_1) & 0 & 0 \\ 0 & k_2(1-\rho_2) & 0 \\ 0 & 0 & k_3(1-\rho_3) \end{bmatrix} \begin{bmatrix} l_1\, \delta\theta_1 \\ l_2\, \delta\theta_2 \\ l_3\, \delta\theta_3 \end{bmatrix}, \qquad (3.16)$$

which could be considered a more general form of (3.5). It remains to replace the displacements δl_i and $l_i\ \delta\theta_i$ by δx, δy, and $\delta\phi$. (Such a substitution ensures a compatible set of the six differentials, δl_i and $l_i\ \delta\theta_i$, i = 1, 2, and 3.)

Prior to this substitution, consider first that points in the moveable platform that lie on a given line must displace relative to ground so that their components along the line are the same (in other words, the requirement of moveable platform being a rigid body). This component is $\delta\phi\ d$, where d is the signed perpendicular distance of the line from point R of rotation. Analogous to (2.15), the perpendicular distance is given by

$$d = \hat{s}^T \hat{S} = c\, y - s\, x + r, \qquad (3.17)$$

where $\hat{s} = [c,\ s;\ r]^T$ are the normalized coordinates of the line. Multiplying (3.17) by $\delta\phi$ and substituting (2.14) yields

$$\delta\phi\ d = \hat{s}^T\ \delta\phi\ \hat{S} = \hat{s}^T\ \hat{D}, \qquad (3.18)$$

and accordingly, all points that lie on the line with coordinates $\hat{s}$ will displace with a component $\delta\phi\ d$ along that line. (The expression $\hat{s}^T\ \hat{D}$ also yields the correct displacement component whenever $\hat{D}$ describes a pure translation, e. g. $\hat{D} = [\delta x,\ 0;\ 0]^T$.)

Now, consider the line $\$_1$ of the first leg spring. Its coordinates are $\hat{s}_1$, and via (3.18), points on that line in the moveable platform must displace with a component $\hat{s}_1^T \hat{D}$ along that line. Because the first moveable pivot point is on that line, the component $\hat{s}_1^T \hat{D}$ defines the extension of the first leg, and consequently, $\delta l_1 = \hat{s}_1^T \hat{D}$. Repeating for the other two legs gives

$$\begin{bmatrix} \delta l_1 \\ \delta l_2 \\ \delta l_3 \end{bmatrix} = \begin{bmatrix} c_1 & s_1 & r_1 \\ c_2 & s_2 & r_2 \\ c_3 & s_3 & r_3 \end{bmatrix} \begin{bmatrix} \delta x \\ \delta y \\ \delta \phi \end{bmatrix}, \tag{3.19}$$

which is the same as (2.16). Consider the line $\delta\$'_1$ with coordinates $\hat{s}'_1$. (See Figure 3.7.) Because this line is perpendicular to $\$_1$ (and parallel to $\delta\$_1$) and passes through the first moveable pivot point, then $l_1\, \delta\theta_1 = \hat{s}'^{\,T}_1 \hat{D}$. Repeating for the other two legs and combining the results yields,

$$\begin{bmatrix} l_1\, \delta\theta_1 \\ l_2\, \delta\theta_2 \\ l_3\, \delta\theta_3 \end{bmatrix} = \begin{bmatrix} -s_1 & c_1 & \delta r'_1 \\ -s_2 & c_2 & \delta r'_2 \\ -s_3 & c_3 & \delta r'_3 \end{bmatrix} \begin{bmatrix} \delta x \\ \delta y \\ \delta \phi \end{bmatrix}, \tag{3.20}$$

where

$$\delta r'_i = \delta r_i + l_i. \tag{3.21}$$

Substituting (3.20) and (3.19) into (3.16) determines the mapping of stiffness (3.10), and the spring matrix assumes the form,

$$\begin{bmatrix} k_{11} & k_{12} & k_{13} \\ k_{21} & k_{22} & k_{23} \\ k_{31} & k_{32} & k_{33} \end{bmatrix} = \begin{bmatrix} c_1 & c_2 & c_3 \\ s_1 & s_2 & s_3 \\ r_1 & r_2 & r_3 \end{bmatrix} \begin{bmatrix} k_1 & 0 & 0 \\ 0 & k_2 & 0 \\ 0 & 0 & k_3 \end{bmatrix} \begin{bmatrix} c_1 & s_1 & r_1 \\ c_2 & s_2 & r_2 \\ c_3 & s_3 & r_3 \end{bmatrix} +$$

$$\begin{bmatrix} -s_1 & -s_2 & -s_3 \\ c_1 & c_2 & c_3 \\ \delta r_1 & \delta r_2 & \delta r_3 \end{bmatrix} \begin{bmatrix} k_1(1-\rho_1) & 0 & 0 \\ 0 & k_2(1-\rho_2) & 0 \\ 0 & 0 & k_3(1-\rho_3) \end{bmatrix} \begin{bmatrix} -s_1 & c_1 & \delta r'_1 \\ -s_2 & c_2 & \delta r'_2 \\ -s_3 & c_3 & \delta r'_3 \end{bmatrix}. \tag{3.22}$$

A more compact expression for (3.10) assumes the form,

$$\hat{w} = [K]\ \hat{D}, \tag{3.23}$$

where from (3.22), the 3x3 stiffness matrix is

$$[K] = [j]\ [k_i]\ [j]^T\ +\ [\delta j]\ [k_i(1-\rho_i)]\ [\delta j']^T, \tag{3.24}$$

where

the i^{th} column of [j] is $\hat{s}_i$ ([j] is the formal instantaneous static Jacobian relating the differential change in the scalar spring forces to $\hat{w}$),

the i^{th} column of $[\delta j]$ is $\delta\hat{s}_i$ ($[\delta j]$ is derivative of [j] with respect to θ_1, θ_2, and θ_3),

the i^{th} column of $[\delta j']$ is $\delta\hat{s}_i'$,

and where

$[k_i]$ is a 3x3 diagonal matrix whose ii^{th}.element is k_i and

$[k_i(1-\rho_i)]$ is a 3x3 diagonal matrix whose ii^{th} element is $k_i(1-\rho_i)$.

(The spring matrix (3.24) can be considered an extension of the spring matrix [K] of (3.8).) Comparing (3.21) and (3.22) with (3.24) yields

$$[\delta j']^T = [\delta j]^T + [l_i]^T, \tag{3.25}$$

where $[l_i]$ is the 3x3 matrix of moments:

$$[l_i] = \begin{bmatrix} 0 & 0 & 0 \\ 0 & 0 & 0 \\ l_1 & l_2 & l_3 \end{bmatrix}. \tag{3.26}$$

Substituting (3.25) into (3.24), [K] can be expressed in the form,

$$[K] = [j]\ [k_i]\ [j]^T + [\delta j]\ [k_i(1-\rho_i)]\ [\delta j]^T + [\delta j]\ [k_i(1-\rho_i)]\ [l_i]^T, \tag{3.27}$$

for which the following observations can be made:

i) The spring matrix [K] is not symmetric. It is the sum of three matrices. Only the first two are symmetric. Specifically, the last matrix causes the asymmetry, and it is of the form:

$$[\delta j]\ [k_i(1-\rho_i)]\ [l_i]^T = \begin{bmatrix} 0 & 0 & \sum -k_i(1-\rho_i)l_i s_i \\ 0 & 0 & \sum k_i(1-\rho_i)l_i c_i \\ 0 & 0 & \sum k_i(1-\rho_i)l_i \delta r_i \end{bmatrix}. \tag{3.28}$$

It is clear that this 3x3 matrix provides elements in the third column of [K], and therefore, the upper 2x2 of [K] is globally symmetric. For small $(1-\rho_i)$, [K] remains nearly symmetric. ([K] cannot be made symmetric by a change of coordinate system, because a change in representation assumes the form, $[K'] = [E]^T[K][E]$, where [E] defines the transformation of twist coordinates.)

ii) There are eight independent elements in [K], which are specified by 14 parameters. (4 points, three spring constants, and three free lengths.) Therefore, there are an ∞^6 of three-dimensional springs of this type having the same [K].

iii) It is unclear exactly under what conditions the symmetric part of [K] will be positive definite.[3] (It may be recalled that for the two-dimensional spring, the 2x2 [K] is positive-definite when $\rho_i \leq 1$.) For a given planar three-dimensional compliant coupling, ranges for the ρ_i's can be established that will ensure positive definiteness. But when a ρ_i deviates significantly away from these ranges, ad hoc calculations of the signs of eigenvalues of $([K]+[K]^T)/2$ are required to determine its definiteness (signature).

[3] A matrix [K] can be expressed uniquely as the sum of a symmetric matrix $([K]+[K]^T)/2$ and a skew-symmetric matrix $([K]-[K]^T)/2$.

iv) The matrix [K] can be non-singular even though [j] is singular, or it can be singular even when [j] is non-singular. (This is analogous to the planar two-dimensional case.)

It is instructive to consider a numerical determination of [K]. This is accomplished by the development and the repeated application of an algorithm that determines the nominal wrench $\hat{w}_o$ that must be applied to the coupling when the position and orientation of the coupling is specified. In other words, numerical values for the right side of (3.11) are inserted to determine $\hat{w}_o$. For example, consider that

$k_1 = k_2 = k_3 = 10$ N/cm.,

$l_{o1} = l_{o2} = l_{o3} = 12$ cm.,

$x_1 = x_2 = y_1 = y_2 = y_3 = 0.$,

$x_3 = 15$ cm.,

$u = 10$ cm. (length of moveable platform),

$x_p = 30$ cm., $y_p = 40$ cm., $\phi = 45^\circ$,

$\theta_1 = 53.130^\circ$, $\theta_2 = 51.778^\circ$, $\theta_3 = 64.879^\circ$,

$l_1 = 50.0$ cm., $l_2 = 59.916$ cm., $l_3 = 51.989$ cm.,

$\rho_1 = 0.240$, $\rho_2 = 0.200$, $\rho_3 = 0.231$.

Substituting these values into the right side of (3.11) gives $\hat{w}_o =$ [694.23 N, 1042.50 N; 5430.92 Ncm]^T.

Now increment x_p by $\delta x_p = 5(10)^{-6}$ cm (keeping y_p and ϕ the same). This specifies the twist $\hat{D} = [\delta x_p, 0; 0]^T$. Make the appropriate substitutions in right side of (3.11), which yields $\hat{w}'_o$. Dividing the increment of force, $\hat{w}'_o - \hat{w}_o$, by δx_p yields the first column of the numerically obtained [K].

Repeating the same calculation for a $\delta y_p = 5(10)^{-6}$ cm specifies a twist $\hat{D} = [0,\ \delta y_p;\ 0]^T$. This is used to determine the second column of [K].

Finally, repeating the calculation for a small rotation $\delta\phi = 5(10)^{-6}$ radians of the moveable platform about the origin yields the third column of [K]. For a twist $\hat{D} = [0,\ 0;\ \delta\phi]^T$, the point P displaces, and $\delta x_p = -\delta\phi\ y_p$ and $\delta y_p = \delta\phi\ x_p$ (obtained from (3.9) with $x = y = 0$). The numerical value for the [K] matrix thus obtained is

$$\begin{bmatrix} 25.336\ \text{N/cm} & 3.0127\ \text{N/cm} & -1029.190\ \text{N} \\ 3.0127\ \text{N/cm} & 27.953\ \text{N/cm} & 837.992\ \text{N} \\ 13.308\ \text{N} & 143.760\ \text{N} & 4702.896\ \text{Ncm} \end{bmatrix}.$$

This matrix is asymmetric and has a positive-definite symmetric part. This is the same result that was obtained analytically using (3.27).

3.3 Spatial Six-Dimensional Spring

Figure 3.8 illustrates a plan view of a moveable platform connected to ground by six translational springs[4] acting in-parallel. The six springs taken together as a single unit define a *spatial six-dimensional spring.* The spring is spatial and six-dimensional since, in general, six independent forces act in its translational springs.

The moveable platform is defined by its spherical pivot points r, s, and t, while the grounded spherical pivots are points o, p, and q. The six springs are connected pair-wise to these pivots. A coordinate system is considered fixed to ground, with its origin at o. Point p is on the x-axis, while point q lies in the xy plane. Points p, q, r, s, and t are located relative to o with position vectors $\vec{op}$, $\vec{oq}$, $\vec{or}$, $\vec{os}$, and $\vec{ot}$, respectively.

[4]Each of the springs can be thought of as acting in the prismatic joint of a spherical-prismatic-spherical serial chain. Six such serial chains act in-parallel to define the simple compliant coupling delineated in Figure 3.8.

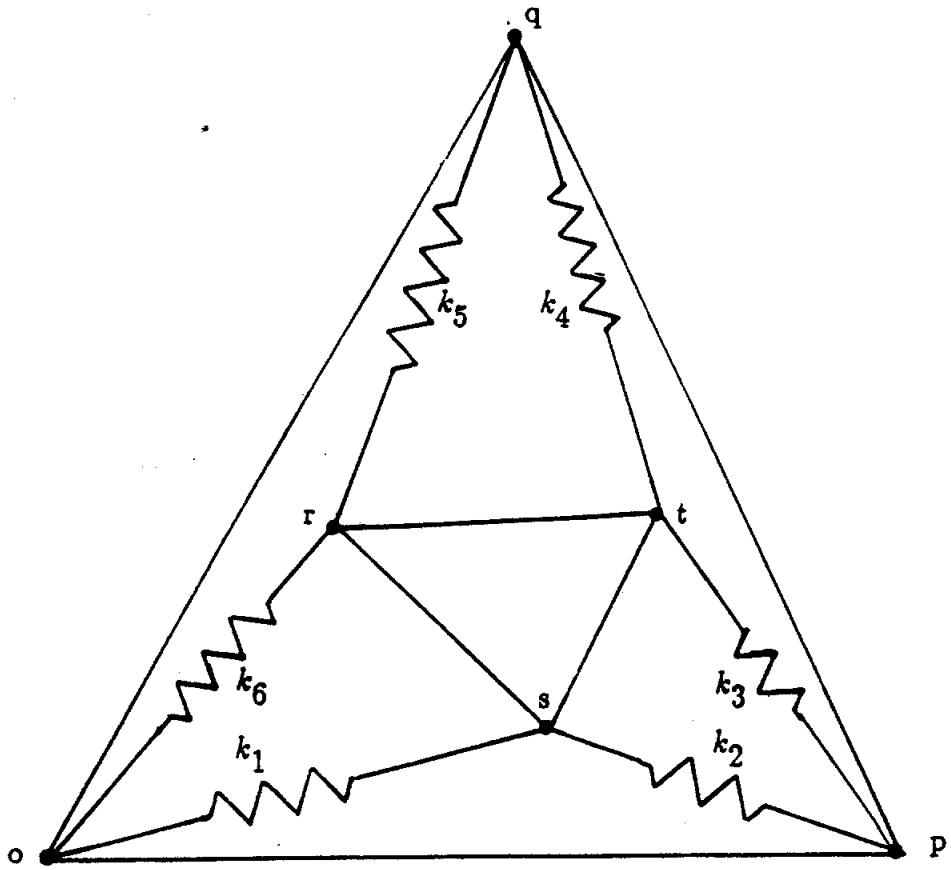

Figure 3.8

A resultant external wrench with six coordinates $\hat{w}_O = [\vec{f}; \vec{m}_O]$ is applied to the moveable platform.[5] The external wrench is in static equilibrium with the six spring forces, and the system remains in static equilibrium as the moveable platform twists relative to ground. To accommodate this, the external wrench changes as the moveable platform moves, and its change is defined as a *wrench increment.* (The wrench increment has the six coordinates $\hat{w} = [\delta\vec{f}; \delta\vec{m}_O]$.)

It is required to determine the mapping

$$\hat{w} = [K]\,\hat{D}, \tag{3.29}$$

where the wrench increment is given by $\hat{w} = [\delta\vec{f}; \delta\vec{m}_O]$ is related via a 6x6 stiffness matrix [K] to the twist of the moveable platform relative to ground, which is given by the six twist coordinates[6] $\hat{D} = [\delta\vec{x}_O; \delta\vec{\phi}]$. (This example is a more thorough investigation than the one given in Section 1.4. Here, the 3-3 is not restricted to being near an unloaded configuration, and the above mapping is not symmetric.)

To obtain (3.29), it is necessary to establish the geometry of the system. The following are position vectors that define the directions of the six legs, and their magnitudes define the lengths of the six legs:

$$l_1 = \|\overrightarrow{os}\|,\ l_2 = \|\overrightarrow{ps} = \overrightarrow{os} - \overrightarrow{op}\|,\ l_3 = \|\overrightarrow{pt} = \overrightarrow{ot} - \overrightarrow{op}\|,$$
$$l_4 = \|\overrightarrow{qt} = \overrightarrow{ot} - \overrightarrow{oq}\|,\ l_5 = \|\overrightarrow{qr} = \overrightarrow{or} - \overrightarrow{oq}\|,\ \text{and}\ l_6 = \|\overrightarrow{or}\|. \tag{3.30}$$

The lengths of nine of the twelve edges of the octahedron must be known. In

[5] A wrench can be thought of as a force (with coordinates $[\vec{f}; \vec{0}]$) acting though the origin together with a general couple (with coordinates $[\vec{0}; \vec{m}_O]$). Adding these sets of coordinates together reproduces the original six wrench coordinates: $\hat{w} = [\vec{f}; \vec{m}_O]$.

[6] A twist can be thought of as a rotation (with coordinates $[\vec{0}; \delta\vec{\phi}]$) about a line through the origin together with a general translation (with coordinates $[\delta\vec{x}; \vec{0}]$). Adding these sets of coordinates together reproduces the original six twist coordinates: $\hat{D} = [\delta\vec{x}; \delta\vec{\phi}]$.

addition to the six l_i, the following three distances between grounded pivots must be known:

$$d_1 = \|\vec{op}\|,\ d_2 = \|\vec{pq} = \vec{oq} - \vec{op}\|, \text{ and } d_3 = \|\vec{oq}\|. \tag{3.31}$$

In order to determine (3.29), two orientation angles must be defined for each leg. Figure 3.9 (See Griffis and Duffy [1989].) illustrates this geometry. An α_i angle defines how the i^{th} leg is oriented within a side face of the octahedron, while θ_x, θ_y, and θ_z define the elevation angles of the three side faces from the xy plane. The six α_i are defined as follows:

α	$\angle$
α_1	$\angle$sop
α_2	$\angle$ops
α_3	$\angle$tpq
α_4	$\angle$pqt
α_5	$\angle$rqo
α_6	$\angle$qor.

The determination of (3.29) begins with an expression of the finite forces that the resultant wrench applies to the springs. Direct extensions of (3.2) and (3.11) yields the expression,

$$\begin{bmatrix} \vec{f} \\ \vec{m}_o \end{bmatrix} = \begin{bmatrix} \vec{s}_1 & \vec{s}_2 & \vec{s}_3 & \vec{s}_4 & \vec{s}_5 & \vec{s}_6 \\ \vec{0} & \vec{op}\times\vec{s}_2 & \vec{op}\times\vec{s}_3 & \vec{oq}\times\vec{s}_4 & \vec{oq}\times\vec{s}_5 & \vec{0} \end{bmatrix} \begin{bmatrix} k_1\,(l_1 - l_{o1}) \\ k_2\,(l_2 - l_{o2}) \\ k_3\,(l_3 - l_{o3}) \\ k_4\,(l_4 - l_{o4}) \\ k_5\,(l_5 - l_{o5}) \\ k_6\,(l_6 - l_{o6}) \end{bmatrix}, \tag{3.32}$$

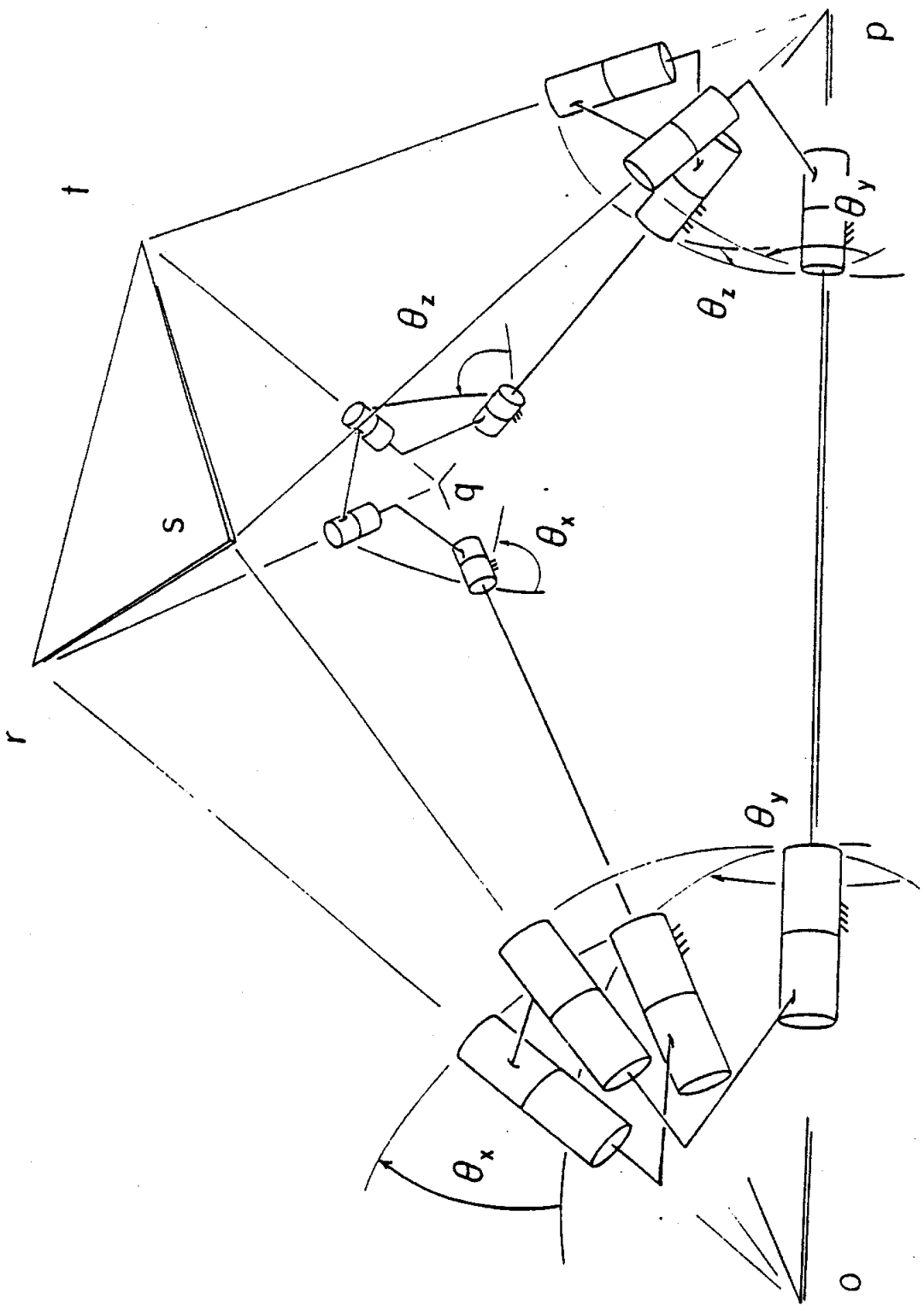

Figure 3.9

where $k_i\ (l_i - l_{oi})$ is the force in the i^{th} leg due to the extension of the i^{th} spring, where $\vec{s}_i$ is the direction cosines of the line of the i^{th} leg, and where $\vec{0}$ is a zero vector. The direction cosines can be obtained from the position vectors aligned along a given leg, and these six sets are given by

$$\vec{s}_1 = \frac{\overrightarrow{os}}{l_1}\ ,\ \vec{s}_2 = \frac{\overrightarrow{ps}}{l_2}\ ,\ \vec{s}_3 = \frac{\overrightarrow{pt}}{l_3}\ ,\ \vec{s}_4 = \frac{\overrightarrow{qt}}{l_4}\ ,\ \vec{s}_5 = \frac{\overrightarrow{qr}}{l_5}\ ,\ \text{and}\ \vec{s}_6 = \frac{\overrightarrow{or}}{l_6}\ . \tag{3.33}$$

The lower three rows of the 6x6 matrix in (3.32) contain the moments of the six lines. Because locations of the grounded pivots $\overrightarrow{op}$ and $\overrightarrow{oq}$ are known constants, this matrix is solely a function of the direction cosines of the six legs.

A differential of (3.32) is an extension of (3.3) and (3.13) is expressed here in the form,

$$\begin{bmatrix} \delta\vec{f} \\ \delta\vec{m}_o \end{bmatrix} = \begin{bmatrix} \vec{s}_1 & \vec{s}_2 & \vec{s}_3 & \vec{s}_4 & \vec{s}_5 & \vec{s}_6 \\ \vec{0} & \overrightarrow{op}\times\vec{s}_2 & \overrightarrow{op}\times\vec{s}_3 & \overrightarrow{oq}\times\vec{s}_4 & \overrightarrow{oq}\times\vec{s}_5 & \vec{0} \end{bmatrix} \begin{bmatrix} k_1\,\delta l_1 \\ k_2\,\delta l_2 \\ k_3\,\delta l_3 \\ k_4\,\delta l_4 \\ k_5\,\delta l_5 \\ k_6\,\delta l_6 \end{bmatrix}$$

$$+ \begin{bmatrix} \delta\vec{s}_1 & \delta\vec{s}_2 & \delta\vec{s}_3 & \delta\vec{s}_4 & \delta\vec{s}_5 & \delta\vec{s}_6 \\ \vec{0} & \overrightarrow{op}\times\delta\vec{s}_2 & \overrightarrow{op}\times\delta\vec{s}_3 & \overrightarrow{oq}\times\delta\vec{s}_4 & \overrightarrow{oq}\times\delta\vec{s}_5 & \vec{0} \end{bmatrix} \begin{bmatrix} k_1(1-\rho_1)l_1 \\ k_2(1-\rho_2)l_2 \\ k_3(1-\rho_3)l_3 \\ k_4(1-\rho_4)l_4 \\ k_5(1-\rho_5)l_5 \\ k_6(1-\rho_6)l_6 \end{bmatrix}, \tag{3.34}$$

where only $\delta\vec{s}_i$ remain to be determined. (Note that in (3.34) the dimensionless ratios $\rho_i = l_{oi}/l_i$ have been incorporated.)

Figure 3.10 illustrates for a representative leg that $\delta\vec{s}_i$ may be written as a linear combination,

$$\delta\vec{s}_i = \delta\vec{s}_i^{\theta}\, s_i\, \delta\theta + \delta\vec{s}_i^{\alpha}\, \delta\alpha, \tag{3.35}$$

where

$$\delta\vec{s}_i^{\theta} = \vec{v}_i,\ s_i = \sin(\alpha_i),\ \text{and}\ \delta\vec{s}_i^{\alpha} = \vec{v}_i \times \vec{s}_i,$$

and where

$$\vec{v}_i = \frac{\vec{u}_i \times \vec{s}_i}{\left\| \vec{u}_i \times \vec{s}_i \right\|}.$$

Note that $\left\| \delta\vec{s}_i^{\theta} \right\| = 1$, and $\left\| \delta\vec{s}_i^{\alpha} \right\| = 1$. The six $\vec{u}_i$ are constants given by

$$\vec{u}_1 = \frac{\overrightarrow{op}}{d_1},\ \vec{u}_2 = \frac{-\overrightarrow{op}}{d_1},\ \vec{u}_3 = \frac{\overrightarrow{pq}}{d_2},\ \vec{u}_4 = \frac{-\overrightarrow{pq}}{d_2},\ \vec{u}_5 = \frac{-\overrightarrow{oq}}{d_3},\ \text{and}\ \vec{u}_6 = \frac{\overrightarrow{oq}}{d_3}. \tag{3.36}$$

Substituting these results into Equation (3.34) and distributing yields

$$\begin{bmatrix} \delta\vec{f} \\ \delta\vec{m}_o \end{bmatrix} = \begin{bmatrix} \vec{s}_1 & \vec{s}_2 & \vec{s}_3 & \vec{s}_4 & \vec{s}_5 & \vec{s}_6 \\ \vec{0} & \overrightarrow{op}\times\vec{s}_2 & \overrightarrow{op}\times\vec{s}_3 & \overrightarrow{oq}\times\vec{s}_4 & \overrightarrow{oq}\times\vec{s}_5 & \vec{0} \end{bmatrix} \begin{bmatrix} k_i \end{bmatrix} \begin{bmatrix} \delta l_1 \\ \delta l_2 \\ \delta l_3 \\ \delta l_4 \\ \delta l_5 \\ \delta l_6 \end{bmatrix}$$

$$+ \begin{bmatrix} \delta\vec{s}_1^{\theta} & \delta\vec{s}_2^{\theta} & \delta\vec{s}_3^{\theta} & \delta\vec{s}_4^{\theta} & \delta\vec{s}_5^{\theta} & \delta\vec{s}_6^{\theta} \\ \vec{0} & \overrightarrow{op}\times\delta\vec{s}_2^{\theta} & \overrightarrow{op}\times\delta\vec{s}_3^{\theta} & \overrightarrow{oq}\times\delta\vec{s}_4^{\theta} & \overrightarrow{oq}\times\delta\vec{s}_5^{\theta} & \vec{0} \end{bmatrix} \begin{bmatrix} k_i(1-\rho_i) \end{bmatrix} \begin{bmatrix} l_1 s_1\, \delta\theta_y \\ l_2 s_2\, \delta\theta_y \\ l_3 s_3\, \delta\theta_z \\ l_4 s_4\, \delta\theta_z \\ l_5 s_5\, \delta\theta_x \\ l_6 s_6\, \delta\theta_x \end{bmatrix}$$

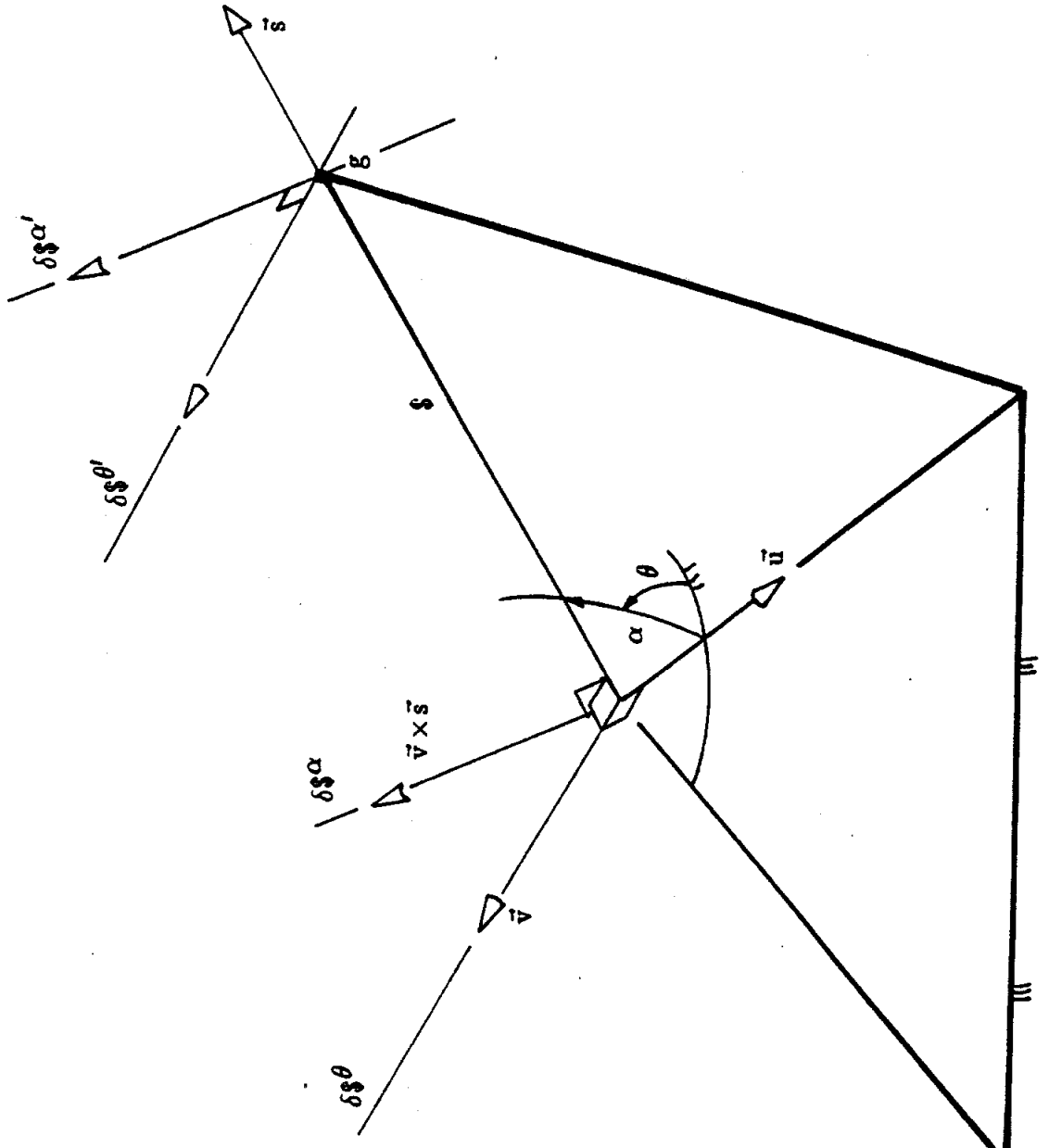
$\vec{s}$
g
$\delta\$\alpha'$
$\delta\$\theta'$
$\$$
θ
$\vec{u}$
α
$\vec{s}\times\vec{a}$
$\delta\$\alpha$
$\vec{a}$
$\delta\$\theta$

Figure 3.10

$$+\begin{bmatrix} \delta\vec{s}_1^{\alpha} & \delta\vec{s}_2^{\alpha} & \delta\vec{s}_3^{\alpha} & \delta\vec{s}_4^{\alpha} & \delta\vec{s}_5^{\alpha} & \delta\vec{s}_6^{\alpha} \\ \vec{0} & \overrightarrow{op}\times\delta\vec{s}_2^{\alpha} & \overrightarrow{op}\times\delta\vec{s}_3^{\alpha} & \overrightarrow{oq}\times\delta\vec{s}_4^{\alpha} & \overrightarrow{oq}\times\delta\vec{s}_5^{\alpha} & \vec{0} \end{bmatrix} \begin{bmatrix} k_i(1-\rho_i) \end{bmatrix} \begin{bmatrix} l_1\,\delta\alpha_1 \\ l_2\,\delta\alpha_2 \\ l_3\,\delta\alpha_3 \\ l_4\,\delta\alpha_4 \\ l_5\,\delta\alpha_5 \\ l_6\,\delta\alpha_6 \end{bmatrix}, \tag{3.37}$$

which in analogy with (3.16) contains the 6x6 diagonal matrices $[k_i]$ and $[k_i(1-\rho_i)]$.

Equation (3.37) can be alternatively expressed in the compact form,

$$\hat{w} = [j]\,[k_i]\,\delta\underline{l} + [\delta j_\theta]\,[k_i(1-\rho_i)]\,\delta\underline{\theta}^* + [\delta j_\alpha]\,[k_i(1-\rho_i)]\,\delta\underline{\alpha}^*, \tag{3.38}$$

where $\delta\underline{\theta}^* = [l_1 s_1\,\delta\theta_y, \ldots, l_6 s_6\,\delta\theta_x]^T$ and $\delta\underline{\alpha}^* = [l_1\,\delta\alpha_1, \ldots, l_6\,\delta\alpha_6]^T$. From (3.37), the columns of the 6x6 matrices [j], $[\delta j_\theta]$, and $[\delta j_\alpha]$ are line coordinates. While the i^{th} column of [j] is the line coordinates for the line $\$_i$ of the i^{th} leg, the i^{th} column of $[\delta j_\theta]$ is the line coordinates of the derivative $\delta\$_i^\theta$ with respect to the appropriate θ, and the i^{th} column of $[\delta j_\alpha]$ is the line coordinates of the derivative $\delta\$_i^\alpha$ with respect to α_i. Figure 3.10 illustrates that the two derivatives pass through the same grounded pivot as $\$_i$. Because the $\$_i$ always passes through the same grounded pivot, it is clear that its derivative must also pass through that point. (This can be considered to be an extension of (3.15).) The three lines \$, $\delta\$^\theta$, and $\delta\$^\alpha$ are mutually perpendicular.

While comparing (3.38) with (3.29), one sees that it remains to make substitutions for $\delta\underline{l}$, $\delta\underline{\alpha}^*$, and $\delta\underline{\theta}^*$ in terms of $\hat{D}$. This substitution inherently determines a compatible set of the 18 differentials $\delta\underline{l}$, $\delta\underline{\alpha}^*$, and $\delta\underline{\theta}^*$.

Equation (1.26) has already demonstrated that

$$\delta \underline{l} = [\mathrm{j}]^{\mathrm{T}}\, \hat{\mathrm{D}}, \qquad [(1.26)]$$

which is analogous to (3.19).

In order to obtain $\delta \underline{\alpha}^*$, consider that a derivative line $\delta \$_{\mathrm{i}}^{\alpha}$ has been given a self-parallel displacement along the i^{th} leg, until it contains the point at the end of the leg. (See Figure 3.10, which illustrates the resulting line as $\delta \$_{\mathrm{i}}^{\alpha'}$ and the end of the i^{th} leg is shown as g.) It remains to project the displacement of the end point of the leg onto $\delta \$_{\mathrm{i}}^{\alpha'}$.[7] Therefore, for the i^{th} leg,

$$l_{\mathrm{i}}\, \delta \alpha_{\mathrm{i}} = (\delta \hat{\mathrm{s}}_{\mathrm{i}}^{\alpha'})^{\mathrm{T}}\, \hat{\mathrm{D}} = \delta \vec{\mathrm{s}}_{\mathrm{i}}^{\alpha} \cdot \delta \vec{\mathrm{x}}_{\mathrm{o}} + (\overrightarrow{\mathrm{og}} \times \delta \vec{\mathrm{s}}_{\mathrm{i}}^{\alpha}) \cdot \delta \vec{\phi}, \qquad (3.39)$$

where the normalized line coordinates of $\delta \$_{\mathrm{i}}^{\alpha'}$ are given by $\delta \hat{\mathrm{s}}_{\mathrm{i}}^{\alpha'} = [\delta \vec{\mathrm{s}}_{\mathrm{i}}^{\alpha};\ \overrightarrow{\mathrm{og}} \times \delta \vec{\mathrm{s}}_{\mathrm{i}}^{\alpha}]$, where $\overrightarrow{\mathrm{og}}$ is a position vector from point o to point g (the end of the i^{th} leg). Equation (3.39) can be applied to all legs so that

$$\delta \underline{\alpha}^* = [\delta \mathrm{j}'_{\alpha}]^{\mathrm{T}}\, \hat{\mathrm{D}}, \qquad (3.40)$$

where the i^{th} column of the 6x6 matrix $[\delta \mathrm{j}'_{\alpha}]$ contains the normalized line coordinates of the line $\delta \$_{\mathrm{i}}^{\alpha'}$ resulting from a self-parallel translation of the i^{th} line $\delta \$_{\mathrm{i}}^{\alpha}$ a distance l_{i} along the i^{th} leg. In other words,

$$[\delta \mathrm{j}'_{\alpha}] = \begin{bmatrix} \delta \vec{\mathrm{s}}_1^{\alpha} & \delta \vec{\mathrm{s}}_2^{\alpha} & \delta \vec{\mathrm{s}}_3^{\alpha} & \delta \vec{\mathrm{s}}_4^{\alpha} & \delta \vec{\mathrm{s}}_5^{\alpha} & \delta \vec{\mathrm{s}}_6^{\alpha} \\ \overrightarrow{\mathrm{os}} \times \delta \vec{\mathrm{s}}_1^{\alpha} & \overrightarrow{\mathrm{os}} \times \delta \vec{\mathrm{s}}_2^{\alpha} & \overrightarrow{\mathrm{ot}} \times \delta \vec{\mathrm{s}}_3^{\alpha} & \overrightarrow{\mathrm{ot}} \times \delta \vec{\mathrm{s}}_4^{\alpha} & \overrightarrow{\mathrm{or}} \times \delta \vec{\mathrm{s}}_5^{\alpha} & \overrightarrow{\mathrm{or}} \times \delta \vec{\mathrm{s}}_6^{\alpha} \end{bmatrix}. \qquad (3.41)$$

A comparison of (3.38) with (3.37) and (3.35) yields that $[\delta \mathrm{j}'_{\alpha}]$ may be expressed in terms of $[\delta \mathrm{j}_{\alpha}]$. In other words,

$$[\delta \mathrm{j}'_{\alpha}] = [\delta \mathrm{j}_{\alpha}] + [\mathrm{v}_{\alpha}], \qquad (3.42)$$

where $[\mathrm{v}_{\alpha}]$ is a 6x6 matrix of moment vectors:

[7] This is analogous to the determination of $l_{\mathrm{i}}\, \delta \theta_{\mathrm{i}}$ in Section 3.2.

$$[v_\alpha] = \begin{bmatrix} \vec{0} & \vec{0} & \vec{0} & \vec{0} & \vec{0} & \vec{0} \\ l_1\vec{v}_1 & l_2\vec{v}_2 & l_3\vec{v}_3 & l_4\vec{v}_4 & l_5\vec{v}_5 & l_6\vec{v}_6 \end{bmatrix}. \tag{3.43}$$

In order to obtain $\delta\underline{\theta}^*$, consider that a derivative line $\delta\$_i^\theta$ has been given a self-parallel displacement along the i^{th} leg, until it contains the point at the end of the leg. (See Figure 3.10, which illustrates the resulting line as $\delta\$_i^{\theta'}$ and the end of the i^{th} leg is shown as g.) It remains to project the displacement of the end point of the leg onto $\delta\$_i^{\theta'}$. Therefore, for the i^{th} leg,

$$l_i\, s_i\, \delta\theta_i = (\delta\hat{s}_i^{\theta'})^T\, \hat{D} = \delta\vec{s}_i^{\theta} \cdot \delta\vec{x}_o + (\vec{og} \times \delta\vec{s}_i^{\theta}) \cdot \delta\vec{\phi}, \tag{3.44}$$

where the normalized line coordinates of $\delta\$_i^{\theta'}$ are given by $\delta\hat{s}_i^{\theta'} = [\delta\vec{s}_i^{\theta};\ \vec{og} \times \delta\vec{s}_i^{\theta}]$, where $\vec{og}$ is a position vector from point o to point g (the end of the i^{th} leg). Equation (3.44) can be applied to all legs so that

$$\delta\underline{\theta}^* = [\delta j'_\theta]^T\, \hat{D}, \tag{3.45}$$

where the i^{th} column of the 6x6 matrix $[\delta j'_\theta]$ contains the normalized line coordinates of the line $\delta\$_i^{\theta'}$ resulting from a self-parallel translation of the i^{th} line $\delta\$_i^{\theta}$ a distance l_i along the i^{th} leg. In other words, similar to (3.41),

$$[\delta j'_\theta] = \begin{bmatrix} \delta\vec{s}_1^{\theta} & \delta\vec{s}_2^{\theta} & \delta\vec{s}_3^{\theta} & \delta\vec{s}_4^{\theta} & \delta\vec{s}_5^{\theta} & \delta\vec{s}_6^{\theta} \\ \vec{os} \times \delta\vec{s}_1^{\theta} & \vec{os} \times \delta\vec{s}_2^{\theta} & \vec{ot} \times \delta\vec{s}_3^{\theta} & \vec{ot} \times \delta\vec{s}_4^{\theta} & \vec{or} \times \delta\vec{s}_5^{\theta} & \vec{or} \times \delta\vec{s}_6^{\theta} \end{bmatrix}. \tag{3.46}$$

A comparison of (3.38) with (3.37) and (3.35) yields that $[\delta j'_\theta]$ may be expressed in terms of $[\delta j_\theta]$. In other words, analogous to (3.42),

$$[\delta j'_\theta] = [\delta j_\theta] + [v_\theta], \tag{3.47}$$

where $[v_\theta]$ is a 6x6 matrix of moment vectors:

$$[\mathrm{v}_\theta] = \begin{bmatrix} \vec{0} & \vec{0} & \vec{0} & \vec{0} & \vec{0} & \vec{0} \\ l_1\,\vec{s}_1 \times \vec{v}_1 & l_2\,\vec{s}_2 \times \vec{v}_2 & l_3\,\vec{s}_3 \times \vec{v}_3 & l_4\,\vec{s}_4 \times \vec{v}_4 & l_5\,\vec{s}_5 \times \vec{v}_5 & l_6\,\vec{s}_6 \times \vec{v}_6 \end{bmatrix}. \tag{3.48}$$

Substitutions of the above equations into (3.38) yields the mapping (3.29), where the global stiffness matrix is written as the sum of five matrices:

$$[\mathrm{K}] = [\mathrm{j}][k_\mathrm{i}][\mathrm{j}]^\mathrm{T} + [\delta \mathrm{j}_\theta][k_\mathrm{i}(1-\rho_\mathrm{i})][\delta \mathrm{j}_\theta]^\mathrm{T} + [\delta \mathrm{j}_\alpha][k_\mathrm{i}(1-\rho_\mathrm{i})][\delta \mathrm{j}_\alpha]^\mathrm{T} + [\delta \mathrm{j}_\theta][k_\mathrm{i}(1-\rho_\mathrm{i})][\mathrm{v}_\theta]^\mathrm{T} + [\delta \mathrm{j}_\alpha][k_\mathrm{i}(1-\rho_\mathrm{i})][\mathrm{v}_\alpha]^\mathrm{T}. \tag{3.49}$$

The following observations can be made about the 3-3 Stewart Platform compliant coupling:

i) The asymmetries are due to the last two matrices. (The first three are symmetric.) Specifically, the last 6x6 two matrices have elements in the last three columns only. Therefore, the upper-left 3x3 of [K] remains globally symmetric. (The matrix [K] cannot be made symmetric by a change of coordinate system, because from (1.12), $[\mathrm{K}'] = [\mathrm{E}]^\mathrm{T}[\mathrm{K}][\mathrm{E}]$.)

ii) Twenty-one independent parameters exist in a symmetric [K]. (See Section 1.4.) It is clear that this number will increase for the global [K]. That the upper-left 3x3 is symmetric may lead one to believe that there are 33 independent elements. But, the upper bound is 30, since the matrix was determined by 30 parameters (six points, six spring constants, and six free lengths), which would result in a finite number of 3-3 Stewart Platforms having the same [K]. However, numerical examples indicate 27 to be the maximum. (The upper-right 3x3 matrix of the sum of the last two matrices of (3.49) is repeatedly skew-

symmetric, which introduces three independent parameters to the 21 of a symmetric 6x6 matrix. These three together with the three due to lower-right 3x3 of the same matrix introduces the six additional parameters to an otherwise symmetric matrix.)

iii) It is difficult to predict (as it was for the planar three-dimensional spring) the conditions that [K] has a positive-definite symmetric part $([K]+[K]^T)/2$. Specifying for all ρ_i close to or less than unity will presumably keep it positive-definite. However, setting exact limits on all six ρ_i to ensure positive-definiteness would be a monumental task. This is because the geometry must be expressed in terms of the displacement of the six legs, which is known to be dependent on an eighth degree polynomial. (Griffis and Duffy, [1989].)

iv) Similar to the previous two examples, it is clear that singularities in [j] do not necessitate singularities in [K]. (A singularity in [j] denotes a statically unstable region.)

v) Singularities in [K] also do not necessitate singularities in [j]. (A singularity in [K] denotes that some twists will not generate a change of wrench.)

A numerical exercise convinces one that (3.49) is correct. Consider that [K] may alternatively be calculated numerically by repeated applications of (3.32) around a given operating position. (This constitutes a natural extension of how applications of (3.11) performed the same exercise in Section 3.2, and therefore, such a procedure need not be detailed here.) Consider the following numerical example, where for $i = 1, \ldots, 6$, the spring constants and free lengths are

$k_i = 10, 20, 30, 40, 50, 60$ N/cm. and $l_{oi} = 11, 12, 13, 14, 15, 16$ cm.

The five position vectors are

$\overrightarrow{op} = [7, 0, 0]^T$, $\overrightarrow{oq} = [3.5, 6.062, 0]^T$, $\overrightarrow{or} = [10, 4, 12]$,

$\overrightarrow{os} = [14.041, 8.041, 16.041]^T$, $\overrightarrow{ot} = [14.496, 1.071, 16.496]^T$ cm.

For this example, the following stiffness matrix was determined both numerically and analytically (by (3.49)):

$$[K] = \begin{bmatrix} 80.0 & 5.2 & 75.6 & 206.9 & 303.5 & -239.5 \\ 5.2 & 39.3 & 5.2 & -581.5 & 5.3 & 516.7 \\ 75.6 & 5.2 & 150.6 & 466.5 & -836.8 & -212.2 \\ 206.9 & -75.5 & 407.2 & 2141.6 & -2094.7 & -1518.8 \\ -202.4 & 5.2 & -532.2 & -1725.2 & 4107.4 & 608.6 \\ -180.2 & 212.0 & -212.2 & -3895.1 & -336.4 & 3263.9 \end{bmatrix},$$

where the 3x3 sub-matrices have the following units –

upper-left: N/cm upper-right: N

lower-left: N lower-right: Ncm.

CHAPTER 4
THE NEW ROLE OF COMPLIANCE IN THE CONTROL OF FORCE

Kinestatic Control has established a new method and philosophy for the simultaneous control of wrench and twist.[1] Essentially, the theory depends upon the *knowledge* of the mapping of stiffness to establish a geometrically meaningful, potential-energy-based, positive-definite inner product that decomposes a general twist into a twist of freedom and a twist of compliance.

An important experiment was successfully performed on an apparatus consisting of a robot, a force/torque sensor, a compliant device, and a gripper that was partially constrained to its environment. The constraint wrenches and twist freedoms of the gripper were simultaneously controlled by commanding the twist of the end-effector that was connected to the gripper by the force/torque sensor and the compliant device. This commanded twist was generated by the simultaneous control of *all six independent actuators of the robot.* The inner product established by the stiffness of the compliant device decomposed the commanded twist of the end-effector into a twist of freedom for the gripper and a wrench-corrective twist of compliance. This implementation employed an empirically determined stiffness mapping that was asymmetric.

[1] "Twist" is used here as a generic word to denote the infinitesimal displacement/rotation of one rigid body relative to another, while "wrench" is a similar generic word for the forces/torques that interact between two rigid bodies.

In general, the methodology necessary to apply Kinestatic Control can be summarized as follows.

i) A gripper is connected to ground by a robot, and the robot is considered to be a spatially deflecting spring. At the outset, it is necessary to determine the mapping of stiffness for the robot. This mapping relates a twist of the gripper relative to ground to a change in the wrench (a wrench increment) that acts on the gripper, and it is independent of the task required of the gripper. In the spatial case, the mapping can be represented by

$$\hat{w} = [K]\ \hat{D}, \tag{4.1}$$

where $\hat{w} = [\delta\vec{f};\ \delta\vec{m}]$ are the six wrench-increment coordinates, where $\hat{D} = [\delta\vec{x};\ \delta\vec{\phi}]$ are the six twist coordinates[2], and where [K] is a 6x6 stiffness matrix. The matrix [K] is not symmetric, and when it is not symmetric, it is said to be *asymmetric*. In general, [K] may be written uniquely as the sum of a symmetric matrix $([K]+[K]^T)/2$ and a skew-symmetric matrix $([K]-[K]^T)/2$. General Kinestatic Control of the gripper requires the symmetric part of [K] to be positive-definite.

---

[2]In the spatial case, a wrench increment is a (small) force acting along a unique line together with a (small) couple in the same direction. It can also be thought of as a force acting through the origin together with a general couple. (The coordinates of the force through the origin are $[\delta\vec{f};\ \vec{0}]$, while the coordinates of the general couple are $[\vec{0};\ \delta\vec{m}]$, where $\vec{0}$ is a zero vector. Adding these two sets of coordinates together reproduce the coordinates of the original wrench increment.)

Similarly in the spatial case, a twist is a (small) rotation about a general line together with a (small) translation in the same direction. It can also be thought of as a rotation about a line through the origin together with a general translation. (The coordinates of the rotation about a line through the origin are $[\vec{0};\ \delta\vec{\phi}]$, while the coordinates of the general translation are $[\delta\vec{x};\ \vec{0}]$. Adding these two sets of coordinates together reproduce the coordinates of the original twist.)

Figure 2.1 illustrates a simplified example of this theory – a wheel is connected to a platform via two translational springs which are capable of compression as well as tension. The platform is subsequently connected to ground via two actuated prismatic (slider) joints that are tuned for fine-position control. (They are stiff and non-back-drivable.) The mapping of stiffness for this mechanism assumes the form, $\delta\vec{f} = [K]\ \delta\vec{x}$, where $\delta\vec{f} = [\delta f_x, \delta f_y]^T$ denotes a change in the force that is applied to the wheel and where $\delta\vec{x} = [\delta x, \delta y]^T$ denotes an infinitesimal displacement of the center point of the wheel relative to ground. For the numerical example given in Chapter 2, the 2x2 stiffness matrix was $[K] = \begin{bmatrix} 5. & 5. \\ 5. & 15. \end{bmatrix}$ N/cm.

ii) It is necessary to determine how the gripper is constrained relative to its environment. This establishes a subspace of wrenches, any one of which may be applied to the gripper by the environment. This subspace (called the wrenches of constraint) is in the spatial case described by the column space of a 6xm matrix [a], where m denotes the number of constraints. In other words, the columns of [a] are the coordinates of the basis elements of the wrenches of constraint. (For the example in Figure 2.1, there is a single constraint, and this is a force $\vec{f}_n = f_n\ \vec{u}_n$, where $\vec{u}_n = [.707, .707]^T$ and where f_n is the magnitude of the normal force.)

When the subspace of constraints is established, the subspace of freedoms is simultaneously established. This unique subspace (called the twists of freedom) is in the spatial case described by the column space of a 6xn matrix [B], where n denotes the number of freedoms. In other words, the columns of [B] are the coordinates of the basis elements of the twists of

freedom. (For the example in Figure 2.1, there is a single twist of freedom, and this is a displacement in the $\vec{u}_t = [-.707, .707]^T$ direction.)

The twists of freedom share the following relationship with the wrenches of constraint:

$$[B]^T [a] = [0]_{nxm}, \tag{4.2}$$

where $[0]_{nxm}$ is an nxm matrix of zeros and where in the spatial case $n + m = 6$. This is the result of the statement that a wrench of constraint can do no work. For the example in Figure 2.1, $\vec{u}_t \cdot \vec{u}_n = \vec{u}_t^T \vec{u}_n = 0$.

iii) It is necessary to determine the subspace of the twists of compliance that constitute the twists that are necessary to change the wrenches of constraint. Therefore, a corrective twist must be an element of this space in order to null a constraint wrench error. This subspace is described in the spatial case by the column space of a 6xm matrix [C], where the columns of [C] are the coordinates of the basis elements of the twists of compliance. Through the mapping of stiffness of the robot, these basis elements have a one-to-one relationship with the basis elements of the wrenches of constraint, and

$$[a] = [K] [C]. \tag{4.3}$$

The subspace [C] can thus be obtained by inverting the mapping of stiffness (which is a mapping of compliance):

$$[C] = [K]^{-1} [a]. \tag{4.4}$$

(For Figure 2.1 and the 2x2 [K] given above, the twist of compliance is to a scalar multiple the displacement $\vec{u}_C = [-1, 0]^T$.)

iv) Once both twist spaces are established, it becomes clear that they are [K]-orthogonal complements. Substituting (4.3) into (4.2) yields

$$[B]^T\,[K]\,[C] = [0]_{nxm}, \tag{4.5}$$

where the inner product[3] is a meaningful physical quantity. It is based on potential energy and is specified by the stiffness of the robot:

$$\langle \hat{D}_b, \hat{D}_c \rangle = \hat{D}_b^T\,[K]\,\hat{D}_c = 0, \tag{4.6}$$

where $\hat{D}_b \in [B]$ and $\hat{D}_c \in [C]$. (For the example in Figure 2.1, $\vec{u}_t^T\,[K]\,\vec{u}_c = 0$.)

Because the two subspaces are [K]-orthogonal complements, and because the symmetric part of [K] is positive-definite, it follows that the subspaces [B] and [C] have no intersection and together span all twists. In other words, the coordinates $\hat{D}$ of a general twist is written as

$$\hat{D} = G_1\,\hat{D}_b + G_2\,\hat{D}_c, \tag{4.7}$$

where $\hat{D}_b$ are the coordinates of a unique twist of freedom and where $\hat{D}_c$ are the coordinates of a unique wrench-corrective twist of compliance. Equation (4.7) defines a new law that governs Kinestatic Control, and the dimensionless scalars G_1 and G_2 represent respectively twist and wrench gains.

New research and development must take advantage of this new role of compliance in the control of force. It should extend the theoretical and

---

[3]This meaningful inner product supersedes the widely accepted technique of selecting a "compliant frame" and defining a task-dependent inner product (for homogeneous twist coordinates $\hat{D} = [\delta\vec{x};\ \delta\vec{\phi}]$) that assumes the non-Euclidean form,

$$\langle \hat{D}_1, \hat{D}_2 \rangle = \delta\vec{x}_1 \cdot \delta\vec{x}_2 + \delta\vec{\phi}_1 \cdot \delta\vec{\phi}_2.$$

See Duffy [1990]. For the example in Figure 2.1, this results in the erroneous notion that the best displacement to null an error in the normal force is a displacement in the normal direction. (See Chapter 2.)

experimental foundation of Kinestatic Control by developing new advanced supplementary theories, which themselves must be experimentally verified. In other words, any new work should itself on further developing the technology of Kinestatic Control, so that it is easily implemented in the next few years on the shop floor of a manufacturing facility. The following summarizes three necessities that facilitate such a goal.

4.1 The Need for Better Stiffness Models

Whitney [1977] is credited for significant work in multi-dimensional force control when he recognized the force feedback gain matrix $[K_f]$. (See Figure 2.3, which illustrates a control diagram that has been adapted from the literature.) From an analytical point of view, this is usually regarded as a matrix that operates on errors in solely the coordinates of force. However, it is the considered opinion of the investigator that $[K_f]$ be recognized as far more than a gain matrix. It is in fact a matrix that describes an important geometric mapping. This mapping cannot be considered as an extension of a one-dimensional example.[4] It is further important to recognize now that the two-dimensional wheel example is the simplest example of force control. This is because the mapping in the example changes both the *magnitude* and the *direction* of an error in force simultaneously, and this is an essential requirement.

Whenever back-drivable effects are minimal (shown as dotted lines in Figure 2.3), the mapping described by $[K_f]$ must be regarded as one of compliance that

[4]Consider the one-dimensional force control algorithms that exist today in the literature. Such a scalar control law operates to essentially scale (in a time varying way) an error in scalar force. This is so simplified a version of force control that it is difficult to extend it to more than a single dimension. In other words, the synthesis of a force controller for a two-dimensional application (such as that shown in Figure 2.1) is not readily obtained from an extension of a one-dimensional application.

maps a wrench error into a corrective twist (or a force error into a corrective displacement for the example of Figure 2.1). This mapping changes the errors in the magnitude, direction, location, and pitch of a wrench into the corresponding magnitude, direction, location, and pitch of a corrective twist. (For the example in Figure 2.1, the mapping changes errors in the magnitude and direction of a force into the corresponding magnitude and direction of a corrective displacement.) In other words, Kinestatic Control establishes the $[K_f]$ matrix as being independent of the task of the gripper:

$$[K_f] = -G_2 [K]^{-1}, \tag{4.8}$$

where [K] is the stiffness of the robot and where G_2 is a dimensionless scalar wrench gain. (See Chapter 2.)

The desire for non-back-drivable actuators is apparently on the increase, especially when compliance is incorporated into the limbs of a robot. (See Andeen and Kornbluh [1988].) For such a system, it is important to focus efforts on the *analysis* of the mapping of stiffness of the robot, rather than on the *synthesis* of it. While work has appeared in the literature in the area of the synthesis of stiffness – Cutkosky and Kao [1989], Goswami, Peshkin, and Colgate [1990], Peshkin [1990], and Yi, Freeman, and Tesar [1989] – no detailed analysis of it has been reported. The state-of-the-art continues to recognize stiffness matrices as symmetric, and the work of Dimentberg [1965] has remained the standard. However, his analysis pertains only to compliant couplings that remain near unloaded configurations.

The author believes that Chapter 3 documents significant advancements in stiffness modeling where the *global* mappings of stiffness are derived for a class of simple compliant couplings which are not restricted to being near unloaded

configurations. Such mappings are asymmetric, as were experimentally determined stiffness matrices given in Chapter 2. These results clearly indicate that in practice, it is necessary to employ asymmetric stiffness matrices.

The dependence of Kinestatic Control on the knowledge of actual robot stiffness necessitates better and more accurate means of modeling stiffness, which is in general asymmetric. Typically, robot stiffness is dependent on the configuration of the entire robot system, which in addition to the robot (that is made up of links, drivetrains, actuators & a servo system), consists of a gripper, a force/torque sensor, and any permanently attached compliant devices. It is clear that a stiffness model of the robot becomes more accurate as deflections in these elements are considered. It also becomes more accurate globally as the system deviates from its unloaded configuration. In other words, the ability to control force and displacement improves as the stiffness model becomes more accurate.

In modeling stiffness, the definition of accuracy has not been formalized. In order to extend the work in this thesis, a meaningful means of comparison must exist to quantify the differences between an actual stiffness and a modeled one. In other words, given a compliant coupling with its mapping of stiffness and given some simplified model with its own slightly different mapping of stiffness, how can the two be compared? It is proposed that the comparison can only be meaningfully done using the invariant properties of stiffness defined by the eigen-screws together with their corresponding eigenvalues. (See Section 1.3 and Patterson and Lipkin [1990a and 1990b].)

Then, the query is the same as that of a hundred years ago, i. e. how does a rigid body move when it is connected to ground by a complicated network of springs? (See "The Dynamical Parable," by Ball [1900].)

4.2 The Need for Constraint Recognition

The current state-of-the-art in force control does not provide for a comprehensive theory that determines the wrenches of constraint for a partially constrained gripper. It is important that this subspace (denoted by [a]) be known, because this establishes those wrenches that may be commanded to the kinestatic controller. (See Figure 2.3, where $\hat{w}_i \in [a]$.) Via Eq. (4.2), the constraints simultaneously establish the twists of freedom whose subspace is denoted by [B]. (Figure 2.3 shows $\hat{D}_i \in [B]$.)

Consider that some differences exist between the modeled constraints (denoted by [a]) and the actual constraints (denoted by $[a_o]$, which by (4.2) establishes the actual twists of freedom $[B_o]$). Then, it is desirable to avoid a situation where the kinestatic controller is commanded a wrench $\hat{w}_i \in [a]$ that would perform work as the gripper moves on an actual twist of freedom $\hat{D}_o \in [B_o]$. Clearly, such a wrench cannot be controlled in general.

For the implementation reported in Chapter 2, the constraints were known a priori, and they remained constant. (In other words, $[a] = [a_o]$ was a constant matrix). However, in a general application, the constraints of the gripper and its workpiece vary as the robot displaces and orients the palm of the gripper. They also vary as the gripper changes configuration to manipulate the partially constrained workpiece. Not only do the constraints themselves move, but they also change form as well as number.

A priori knowledge of [a] as a function of gripper position/orientation and configuration is not realistic in a general scenario. The main reason is that an enormous overhead (of [a] being stored as a function of gripper position/orientation

and configuration) would accompany each and every force controlled operation. Therefore, it is desirable that a robotic system have the capability to determine [a] on line in real time from information obtained from all available sensors (e. g. force/torque sensor, gripper sensors, and robot encoders). When successfully implemented, this will considerably improve the force controlled robot by making it more easily adapted to new tasks. (The turn-around-time for a change in task is considerably reduced, and this constitutes a substantial cost benefit to the user and the consumer.)

4.3 The Need to Filter Working Wrenches from Sensed Wrenches

Figure 2.3 assigns $\hat{w}_O$ to denote the actual non-working constraint wrench that is applied to the partially constrained gripper. *However, at this time, there is no known geometrically meaningful way to extract this wrench from the sensed wrench (provided by a force/torque sensor) denoted here by* $\hat{w}_S$. For example, this is due mainly to the fact that a working wrench of friction acts as a general wrench. (In other words, there is not a one-to-one correspondence between a twist of freedom and a wrench that performs work.)

This filtering problem is a formidable one that must be addressed in order to accomplish the general control of a constraint wrench. The filtering of working wrenches from sensed ones must be accomplished by analyzing all physical parameters constraining the gripper in its environment as well as all available sensory information. An integral part of this investigation must include friction, which remains a constraint until the instant that motion commences.

REFERENCES

An, C., and Hollerbach, J., 1989, "The Role of Dynamic Models in Cartesian Force Control of Manipulators," International Journal of Robotics Research, Vol. 8, No. 4, MIT Press, Cambridge, MA.

An, C., Atkeson, C., and Hollerbach, J., 1988, *Model-Based Control of a Robot Manipulator*, MIT Press, Cambridge, MA.

Andeen, G., and Kornbluh, R., 1988, "Design of Compliance in Robotics," Proc. IEEE International Conference on Robotics and Automation, Proc. IEEE International Conference on Robotics and Automation, Philadelphia, PA.

Ball, R., 1900, *A Treatise on the Theory of Screws*, Cambridge University Press, Cambridge, Eng.

Brockett, R., and Loncaric, J., 1986, "The Geometry of Compliance Programming," in *Theory and Applications of Nonlinear Control Systems*, eds. Byrnes and Lindquist, Elsevier Science Publishers, North-Holland.

Cutkosky, M., and Kao, I., 1989, "Computing and Controlling the Compliance of a Robotic Hand," IEEE Transactions on Robotics and Automation, Vol. 5, No. 2.

Dimentberg, F., 1965, "The Screw Calculus and Its Applications in Mechanics," US Dept. of Commerce Translation No. AD680993.

Duffy, J., 1990, "Editorial: The Fallacy of Modern Hybrid Control Theory That is Based on Orthogonal Complements of Twists and Wrench Spaces," Journal of Robotic Systems, Vol. 7, No. 2, John Wiley, New York.

Goswami, A., Peshkin, M., and Colgate, E., 1990, "Passive Robotics: An Exploration of Mechanical Computation," Proc. IEEE International Conference on Robotics and Automation, Cincinnati, OH.

Griffis, M., 1988, "Kinetic Considerations in the Hybrid Control of Robotic Manipulators," M. S. Thesis, University of Florida.

Griffis, M., and Duffy, J., 1989, "A Forward Displacement Analysis of a Class of Stewart Platforms," Journal of Robotic Systems, Vol. 6, No. 6, John Wiley, New York.

Haefner, K., Houpt, P., Baker, T., and Dausch, M., 1986, "Real-Time Robotic Position/Force Control for Deburring," Proc. of the Winter ASME Annual Meeting, Anahiem CA, DSC-Vol. 3.

Hennessey, M., 1986, "Robotic Force Tracking Using an IRCC," Proc. of the Winter ASME Annual Meeting, Anahiem CA, DSC-Vol. 3.

Hogan, N., 1985, "Impendence Control: An Approach to Manipulation, Parts I, II, and III," ASME Journal of Dynamic Systems, Measurement, and Control, Vol. 107.

Kazerooni, H., Sheridan, T., and Houpt, P., 1986, "Robust Compliant Motion for Manipulators, Part I: The Fundamental Concepts of Compliant Motion and Part II: Design Method," IEEE Journal of Robotics and Automation, Vol. RA-2, No. 2.

Korn, G., and Korn, T., 1968, *Mathematical Handbook for Scientists and Engineers*, McGraw Hill, New York.

Lipkin, H., and Duffy, J., 1985, "The Elliptic Polarity of Screws," ASME Journal of Mechanisms, Transmissions, and Automation in Design, Vol. 107.

Lipkin, H., and Duffy, J., 1988, "Hybrid Twist and Wrench Control of a Robotic Manipulator," ASME Journal of of Mechanisms, Transmissions, and Automation in Design, Vol. 110.

Loncaric, J., 1985, "Geometrical Analysis of Compliant Mechanisms in Robotics," Ph.D. Dissertation Harvard University.

Mason, M., 1981, "Compliance and Force Control for Computer-Controlled Manipulators," IEEE Transactions on Systems, Man, and Cybernetics, Vol. SMC-11, No. 6. (Also in *Robot Motion: Planning and Control*, eds. Brady, et. al.)

Mason, M., 1982, "Compliant Motion," in *Robot Motion: Planning and Control*, eds. Brady, et. al., MIT Press, Cambridge, MA.

Mason, M., and Salisbury, K., 1985, *Robot Hands and the Mechanics of Manipulation*, MIT Press, Cambridge, MA.

Patterson, T., and Lipkin, H., 1990a, "Structure of Robot Compliance," Proc. 21st ASME Mechanisms Conference, Chicago, IL.

Patterson, T., and Lipkin, H., 1990b, "A Classification of Robot Compliance," Proc. 21st ASME Mechanisms Conference, Chicago, IL.

Peshkin, M., 1990, "Programmed Compliance for Error Corrective Assembly," IEEE Transactions on Robotics and Automation, Vol. 6, No. 4.

Plücker, J., 1865, "On a New Geometry of Space," Phil. Trans. Royal Society of London, Vol. 155.

Plücker, J., 1866, "Fundamental Views Regarding Mechanics," Phil. Trans. Royal Society of London, Vol. 156.

Porteous, I., 1981, *Topological Geometry*, Cambridge University Press, Cambrige, Eng.

Raibert, M., and Craig, J., 1981, "Hybrid Position/Force Control of Manipulators," ASME Journal of Dynamic Systems, Measurement, and Control, Vol. 102.

Roberts, R., Paul, R., and Hillberry, B., 1985, "The Effect of Wrist Force Sensor Stiffness on the Control of Robot Manipulators," Proc. IEEE International Conference on Robotics and Automation, St Louis, MO.

Ryan, P., 1989, *Euclidean and Non-Euclidean An Analytic Approach*, Cambridge Unversity Press, Cambridge, Eng.

Salisbury, K., 1980, "Active Stiffness Control of a Manipulator in Cartesian Coordinates," Proc. IEEE Decision and Control Conference, Albuquerque, NM. (Also in *Robot Hands and the Mechanics of Manipulation*, Mason and Salisbury.)

Semple, J., and Kneebone, G., 1979, *Algebraic Projective Geometry*, Oxford Science Publications, Oxford, Eng.

Sommerville, D., 1929, *An Introduction to the Geometry of N Dimensions*, reprinted, Dover Pub. Co., New York, 1958.

Swinson, M., 1988, "Cross-Coordinated Control: An Experimentally Verified Technique for the Hybrid Twist and Wrench Control of a Voltage-Controlled Industrial Robot," Ph.D. Dissertation University of Florida.

Whitney, D., 1977, "Force Feedback Control of Manipulator Fine Motions," ASME Journal of Dynamic Systems, Measurement, and Control, Vol. 99.

Whitney, D., 1982, "Quasi-Static Assembly of Compliantly Supported Rigid Parts," ASME Journal of Dynamic Systems, Measurement, and Control, Vol 104.

Whitney, D., 1987, "Historical Perspective on the State of the Art in Robot Force Control," The International Journal of Robotics Research, Vol, 6, No. 1.

Xu, Y., and Paul, R., 1988, "On Position Compensation and Force Control Stability of a Robot with a Compliant Wrist," Proc. IEEE International Conference on Robotics and Automation, Philadelphia, PA.

Yi, B., Freeman, R., and Tesar, D., 1989, "Open-loop Stiffness Control of Overconstrained Mechanisms/Robotic Linkage Systems," Proc. IEEE International Conference on Robotics and Automation.

BIOGRAPHICAL SKETCH

Michael Griffis was born on March 31, 1963 in Stuttgart, West Germany. Michael, the eldest of four children, spent many of his days in Jacksonville, Florida, where he graduated as valedictorian of the 1981 class of Edward H. White Senior High School. His preoccupation with machines and what makes them move brought him 63 miles southwest to the University of Florida, where he was awarded a Bachelor of Science in Mechanical Engineering with Honors in 1985. A continued interest in mechanisms and the desire to teach others the subject convinced Michael to pursue advanced degrees.

Michael's plan for life includes happiness.